

## STRATEGIC CONSIDERATIONS OF COAL LIQUID REFINING

P.-Z. Zhou, J.J. Marano (Burns and Roe Services Corp.)  
R.A. Winschel (CONSOL, Inc.)

The development of the two-stage coal liquefaction process over the past decade has resulted in remarkable improvements in process efficiency, including increased liquid yield, better product quality, improved hydrogen efficiency, and dramatic reduction in production costs. At this stage in liquefaction development, serious consideration should be given to the refining of coal liquids into marketable transportation fuels.

### PROPERTIES OF COAL-DERIVED LIQUIDS

Properties of coal liquids representative of various single-stage and two-stage liquefaction (TSL) processes were compiled in a comprehensive review [Zhou and Rao, 1992]. The major differences between current two-stage liquefaction coal liquids and those from earlier processes are the higher hydrogen and lower heteroatom contents of the former. TSL liquids are usually richer in middle distillates than are single-stage liquids, probably due to the lower hydrogenation severity of the two-stage processes which leads to the lower hydrogen consumption and higher liquid yields.

Coal liquids produced from coals of the same rank under similar conditions are quite similar in properties. For coal liquids obtained from bituminous coals, the hydrogen content is high, in the range of 11.3-12.2 wt%; and heteroatom contents are low: 0.1- 0.3 wt% nitrogen, less than 0.1 wt% sulfur, and 1-2% oxygen [Lee et al. 1991]. Liquid products from lower-rank coals are characterized by more oxygen and higher paraffinicity than bituminous coal liquids. The subbituminous Black Thunder coal liquids have a greater concentration of normal paraffins, olefins, and phenols than Pittsburgh seam coal liquids [Robbins et al. 1992].

As complex mixtures of hydrocarbons and hetero-compounds, coal liquids and petroleum exhibit many fundamental similarities; therefore, coal liquids can be refined into liquid transportation fuels by current petroleum refining technologies. Extensive research on coal-liquid refining done by Chevron, UOP, and Exxon demonstrated that environmentally clean, quality liquid fuels, can be produced from coal liquids. Modern TSL liquids, however, have a lower boiling range than petroleum, with an end point around 427°C, and are free of residual materials and metals. The H/C ratio of TSL liquids falls within the H/C range of crude oils, although at the lower end, reflecting the cyclic nature of coal liquids. Coal liquids have very low sulfur contents, moderate nitrogen contents, and relatively high oxygen contents. These unique features of coal liquids require somewhat different refining strategies than those conventionally used for the refining of petroleum.

Oxygen compounds in coal liquids are concentrated in the 175-315°C boiling range, with a peak at 230°C [Pauls et al. 1990]. For Black Thunder coal liquid, 3.6 wt% of the naphtha (IBP - 193°C) and 10 wt% of the 193-266°F fraction are phenolic compounds and can be extracted easily by caustic washing [Burke et al. 1991]. This naphtha phenolic extract contains phenol, cresols, xylenols, ethyl phenol, methylethyl-phenol and propyl-phenol [Robbins et al. 1992].

Some coal liquids produced recently at Wilsonville are characterized in Table 1. Tables 2 through 4 compare the properties of respective fractions of these coal liquids with corresponding specifications for gasoline, jet fuel, and diesel fuel.

#### HYDROPROCESSING -- THE MAJOR TOOL FOR COAL-LIQUID REFINING

Based on the characteristics of coal liquids, hydroprocessing is obviously the most important refining technology for coal-liquid upgrading. Coal liquefaction is a hydrogenation process, and coal-liquid refining can be envisioned as an extension of the coal-to-liquid fuel conversion process. The hydrogenation conditions in the liquefaction step determine the yield and properties of the coal liquids produced, which in turn dictate the extent of upgrading required for coal-liquid fuel production.

Current liquefaction practice is to recycle resids to extinction to produce a total distillate product with an end point in the range of 370-427°C. With improved liquefaction operation, it is possible to lower the end point further to around 350°C, as suggested by some authors [Zhou and Rao, 1992]. This is particularly advantageous to the downstream refining facility which may have limited cracking (either catalytic or hydrocracking) capacity, and provides the added benefit of confining the toxicologically active polycyclic aromatic hydrocarbons within the boundary of the liquefaction plant. In fact, Exxon's new liquefaction process is generating 350°C- coal liquids, which make a naphtha plus distillate product slate [Stuntz 1991].

Hydroprocessing, e.g. hydrotreating and hydrocracking, of coal liquids is highly versatile in that the extent of hydrogenation can be adjusted to produce different product slates (maximum gasoline or maximum distillate) as well as product quality (primarily aromatics content).

#### UTILIZATION OF EXISTING PETROLEUM REFINERY INFRASTRUCTURE

It appears to be more realistic to consider the co-refining of coal liquids with petroleum in an existing petroleum refinery rather than in a grass-roots, dedicated coal-liquid refinery.

Coal liquids can be introduced into a refinery either as a single feed or as previously fractionated individual cuts. The unique properties of coal liquids warrant a different refining strategy than that for petroleum. Mixing the total coal liquid with petroleum would eliminate many possible refining schemes suitable for each of these two feedstocks. More flexibility in processing can be achieved if coal liquids are distilled in the liquefaction plant and individual fractions are introduced into the refinery at points where their properties are most compatible with petroleum counterparts.

Much work has been done on the hydrotreatment of total coal liquids; however, evidence shows that hydrotreating the individual naphtha, kerosene, and diesel fractions is advantageous from a product-quality standpoint. For example, jet fuels with higher smoke points may be obtained by hydrotreating the respective fractions rather than the total coal liquid [Sullivan 1987b, Zhou and Rao 1992]. Depending on the coal liquid properties, the product slate, and the refinery infrastructure, coal liquid fractions may be hydroprocessed together with or separately from their petroleum counterparts.

## REFINERY LINEAR PROGRAMMING

Linear programming (LP) techniques are used routinely within the refining industry to evaluate the economics of petroleum processing. Linear programming can also be applied to coal liquids to determine their value as refinery feedstocks. LP is potentially a very powerful tool since the products from most liquefaction processes are intermediates which must be further upgraded or blended with petroleum-derived intermediates to meet product specifications. Thus, LP allows the effects of variations in yields and quality between different liquefaction operations to be quantified, and can provide a benchmark for comparing and ranking different coal liquid products.

The effect of feeding coal-liquid fractions to a refinery is being studied with the linear programming technique and preliminary results are reported here. The LP model used in this study was developed by Bechtel, Inc. as part of the DOE-funded Direct Liquefaction Baseline Design project [Bechtel, work in progress]. It is a model of the typical midwestern U.S. refinery, producing the average U.S. midwest product slate. Incremental quantities of different coal-liquid cuts are introduced into the refinery model, which calculates the effect of each cut on refinery net profit. In general, liquids produced by direct liquefaction are found to be more valuable than crude petroleum. The results reported here are expressed as a coal liquid premium defined as the percentage difference between the value of the coal liquid and the price of crude oil.

## GASOLINE PRODUCTION FROM COAL NAPHTHA

Coal-liquid naphthas are similar to the naphtha fraction from a naphthenic crude oil. Data in Table 2 show that the oxidation stability, caused by heteroatoms (mainly oxygen), and lack of light ends are the two major problems in the manufacture of gasoline from coal liquids. Coal naphtha, however, has a high octane number and low aromatics content and is an ideal source for gasoline production. The clear motor octane of coal naphthas is in the range of 76-83 [Zhou and Rao, 1992]. The aromatics content of coal naphthas from recent TSL runs, contrary to conventional views, are fairly low (7-13 vol%), and the naphthene content is very high (60-70 vol%), as shown in Table 2. It is an excellent reformer feedstock to make gasoline components with a research octane number above 105 [Sullivan 1987b], which is attractive at the present time. However, conversion of naphthenes to aromatics by catalytic reforming may no longer be advisable due to provisions in the U. S. Clean Air Act Admendment. A cost-effective means of gasoline production from coal naphthas is to maintain the current level of naphthenes, which have fairly high octane numbers, and improve the oxidation stability of the coal naphtha via mild hydrotreating to remove the heteroatoms. Isomerization of light coal naphtha is also a promising option. Volatility requirements can be easily remedied by blending.

LP studies show that for a refinery not deficient in high- octane gasoline blendstocks, this scheme results in a premium for coal naphtha of 12% over the price of crude oil. Under the assumptions used in the calculation, straight blending of the hydrotreated coal naphtha is preferable to catalytic reforming which has a premium of 6.5%. This difference is due primarily to the loss of volume which occurs during reforming. In this study, the refinery product slate was assumed to be unchanged. Further studies are planned to explore various scenarios in which the refinery infrastructure and product slate are modified to take best advantage of coal liquid potentials. Higher premiums are anticipated.

### PHENOLICS EXTRACTION

Since oxygen is the major heteroatom found in coal liquids, hydrogen used for oxygen removal during hydrotreating accounts for the major part of hydrogen consumption. The oxygen compounds in the 232°C- fraction are mostly single-ring phenolics, which can be easily extracted by caustic washing.

A promising approach is, therefore, to extract these phenolics before hydrotreating as chemicals by-product. Preliminary work indicated that this has good potential for raising the coal-liquid premium for the naphtha fraction.

### JET FUEL PRODUCTION

As illustrated in Table 4, the coal-derived kerosene fractions have lower hydrogen contents than do naphthas from the same source. This follows the general trend that hydrogen content decreases with increasing boiling point. The hydrogen level of the coal-derived kerosene fraction is low compared with that of petroleum-derived jet fuels (H 13.5-14.0 wt%), and is a reflection of its high aromatics content, typically around 50%. As a result, the API gravity and smoke point, two major properties for jet fuels, are much lower than specifications.

The jet fuel fraction obtained from an EDS distillate by hydrotreating do not meet gravity and smoke point specifications [Erwin and Sefer 1989]. It was reported, however, that through appropriate hydrotreatment smoke points of at least 20 mm can be obtained for jet fuels from Illinois No. 6 coal liquids (aromatics content 10 vol% or lower) and for jet fuels from Wyodak coal liquids (aromatics content about 15 vol%) [Sullivan 1987a]. Hydrocracking appears to be a more efficient way of making specification jet fuels from coal liquids [Sullivan and O'Rear 1981]. In essence, this is a matter of the depth of hydrogenation. Jet fuels with no aromatics and no sulfur can be produced and meet all of the current ASTM specifications for jet fuel [Stuntz 1991].

Due to the compositional uniqueness, traditional density specification is more difficult to meet than smoke point for coal-derived jet fuel fractions, which comprise largely two-ring cycloparaffins. However, the high naphthene content of coal liquids makes them a remarkable feedstock for manufacturing high-density, high-energy jet fuels, a range-extender for high-mach aircrafts. More work is required in this area.

### DIESEL FUEL PRODUCTION

With an even lower hydrogen content than the kerosene fraction, the coal-derived middle distillates have low cetane numbers, usually in the twenties. Upgrading of the middle distillates is necessary to increase the hydrogen content and remove hetero-compounds. However, saturation of a large part of the aromatics in the diesel fuel fractions may not be justified economically, and the use of multi-purpose additives may be advisable [Sefer and Erwin 1989]. The coal-derived diesel fuel does show good susceptibility to ignition improvers [Sullivan et al. 1981].

With all the aromatic hydrocarbons in coal diesel fractions saturated, a zero-aromatics, zero-sulfur diesel fuel is made by Exxon, which has a cetane value in the 42-53 range and considerably reduced particulate emissions relative to a typical petroleum diesel fuel [Stuntz 1991].

Initial LP work indicates that low-severity hydrotreating results in a diesel blendstock with a premium of about 4% over crude oil. A better premium may be possible by adjusting the cut points of this fraction.

#### CRACKING

Coal-derived middle and heavy distillates can be cracked, either by catalytic cracking or hydrocracking, to boost yields of gasoline or light distillate fuels. In order to be a good cat-cracker feedstock comparable to petroleum feedstocks, coal distillates must be hydrogenated to a 11.5-12.0 wt% hydrogen content [Riedl and deRosset 1980].

A decision on whether the hydrotreated middle distillate should be used as a diesel fuel blending stock or subjected to catalytic cracking should be based largely on economic considerations. Product slate constraints, however, will probably dictate that a certain part of the middle distillate should be blended to diesel fuel and the rest cracked to generate gasoline blending components. Heavy distillate or vacuum gas oil, if produced by the liquefaction plant, should be cracked. Hydrocracking of coal-derived heavy distillates can produce quality gasoline, jet, and diesel fuels. The choice between catalytic cracking and hydrocracking depends on the refinery infrastructure. The mode of operation for the hydrocracker, all-gasoline mode or maximum-jet-fuel mode, depends on refinery economics. Further LP work is under way to study this and other related options.

#### CONCLUSION

Coal liquids can be refined by modern refining technologies, primarily hydroprocessing, into specification transportation fuels. Mild hydrotreatment of coal naphtha to produce a gasoline blendstock is preferred over catalytic reforming in the long run. The middle distillate can be hydro-upgraded into high-density jet fuel or diesel fuel with the use of an appropriate additive package. Heavy distillates may be cracked to boost gasoline yield. By adjusting the depth of hydrogenation, zero-aromatics liquid fuels can be obtained with high quality. A high degree of product slate flexibility is possible with coal-liquid refining. Suitable refining strategies will result in a considerable premium for coal liquids over the price of crude oils. More research is recommended on coal-liquid characterization, including detailed analysis and development of correlations for property prediction; and on coal-liquid processing, including experimental and LP studies.

#### ACKNOWLEDGEMENT

This work was sponsored by the U.S. Department of energy (DOE), Pittsburgh Energy Technology Center (PETC), in part under Contract No. DE-AC22-89PC89883 (CONSOL) and in part under Contract No. DE-AC22-89PC88400 (BRSC). Special thanks go to Mr. S.R. Lee (DOE/PETC) for his support and comments on this paper.

## REFERENCES

- Bechtel, Inc. work in progress. "Direct Coal Liquefaction Baseline Design and System Analysis," DOE Contract DE-AC22-90PC89857.
- Burke, F.P.; Winschel, R.A.; Robbins, G.A.; and Brandes, S.D. 1991. CONSOL Project Status Report under DOE Contract DE-AC22-89PC-89883, November 6, 1991.
- Erwin, J., and Sefer, N.R. 1989. "Synthetic Fuels from Coal-Derived Distillate as Jet Fuels for High Mach Aircraft," presented at ACS Meeting, Div. Petrol. Chem. September 10-15, 1989. Miami Beach, FL.
- Kramer, R.L. 1991. Conoco Research Report No. 6210-0003-T000-1-91, August 1991.
- Lee, J.M.; Cantrell, C.E.; Gollakota, S.V.; Davies, O.L.; Corser, M.M.; and Vimalchand, P. 1991. Prep. ACS National Meeting, Div. Fuel Chemistry, August 25-30, 1991. New York, N.Y. 36 (4), 1985.
- Pauls, R.E.; Bambacht, M.E.; Bradley, C.; Scheppele, S.E.; and Cronauer, D.C. 1990. Energy & Fuels, 4, 236.
- Riedl, F.J., and DeRosset, A.J. 1980. "Hydrotreating and Fluid Catalytic Cracking of SRC-II Process Derived Gas Oils," UOP Interim Report, DOE Contract No. EF-77-C-01-2566, July 1980.
- Robbins, G.A.; Brandes, S.D.; Winschel, R.A.; and Burke, F.P. 1992. CONSOL, Quarterly Technical Progress Report, Oct. 1 - Dec. 31, 1991. DOE Contract No. DE-AC22-89PC89883.
- Southern Electric International, Inc. 1991. "Advanced Coal Liquefaction Research Facility, Wilsonville, Alabama. Technical Progress Report, Run 258 with Subbituminous Coal," DOE Contract No. DE-AC22-82PC50041, May 1991.
- Stuntz, G.F. 1991. "Premium Products from Direct Coal Liquefaction," presented at Alternate Energy '91, April 16-19, 1991. Scottsdale, AR.
- Sullivan, R.F. 1987a. "High-Density Jet Fuels from Coal Syncrudes," presented at the Symposium on Structure of Future Jet Fuels, Div. Petroleum chemistry, ACS Meeting, April 5-10, 1987. Denver, CO.
- Sullivan, R.F. 1987b. "Refining and Upgrading of Synfuels from Coal and Oil Shales by Advanced Catalytic Processes," Final Report, prepared for USDOE, Contract No. DE-AC22-76ET10532, May 1987.
- Sullivan, R.F.; O'Rear, D.J.; and Frumkin, H.A. 1981. "Converting Syncrudes to Transportation Fuels," presented at 1981 Fuels and Lubricants Meeting, NPRA, November 5-6, 1981. Houston, TX.
- Vimalchand, P.; Lee, J.M.; Gollakota, S.V.; Davies, O.L.; Cantrell, C.E.; and Corser, M.M. 1991. "Recent Developments in Coal Liquefaction at Wilsonville Facility," presented at 16th Annual EPRI Conference, June 18 - 20, 1991. Palo Alto, CA.
- Winschel, R.A., and Zhou, P. 1991. "Inspection of Integrated Two-Stage Liquefaction Products by Petroleum Assay," presented at 16th Annual EPRI Conference on Fuel Science, June 16-21, 1991. Palo Alto, CA.
- Zhou, P.-Z., and Rao, S.N. 1992. "Assessment of Coal Liquids as Refinery Feedstocks," prepared for U.S. DOE/Pittsburgh Energy Technology Center, DOE Contract No. DE-AC22-89PC88400.

TABLE 1  
PROPERTIES OF WILSONVILLE TWO-STAGE LIQUIDS

| Coal                            | Spring Creek | Pittsburgh Seam | Black Thunder | Illinois No. 6 |
|---------------------------------|--------------|-----------------|---------------|----------------|
| Gravity, <sup>a</sup> API @15°C | 16.2-18.3    | 27.7            | 23.9          | 24.5           |
| Elemental                       |              |                 |               |                |
| Carbon, wt%                     | 86.2-86.9    | 86.9            | 87.4          | 87.2           |
| Hydrogen, wt%                   | 10.9-11.3    | 11.55           | 11.2          | 11.8           |
| Sulfur, wt%                     | 0.05-0.10    | 0.05            | 0.05          | 0.02           |
| Nitrogen, wt%                   | 0.40-0.52    | 0.1             | 0.3           | 0.22           |
| Oxygen, wt% (diff)              | 1.36-2.21    | 1.4             | 1.10          | 0.76           |
| H/C Atom Ratio                  | 1.51-1.58    | 1.59            | 1.54          | 1.62           |
| V, Ni, Fe, Cu, ppm              | -            | <4.5            | <25.0         | -              |
| Characterization Factor         | -            | 10.9            | 10.9          | -              |
| Ash, wt%                        | -            | 0.002           | 0.01          | -              |
| Conradson Carbon, wt%           | -            | 0               | 0             | -              |
| Pour Point, °C                  | -            | -59             | -26           | -              |
| Bromine Number, g/100g          | -            | 8               | 14            | -              |
| Aniline Point, °C               | -            | 23.8            | -             | -              |
| Kin. Viscosity, cSt, @38°C      | -            | 2.1             | 3.1           | -              |
| Phenolic-OH Conc., meq/g        | -            | 0.18            | -             | -              |
| Acidity, meq/g                  | -            | -               | 0.38          | -              |
| GC Simulated Dist., °C          |              |                 |               |                |
| IBP                             | 36-57        | -               | -             | -              |
| 10%                             | 118-180      | 85              | 80.5          | -              |
| 50%                             | 277-331      | 253             | 270           | -              |
| 95%                             | 363-417      | 362             | 379           | -              |

Data Source for Tables 1 through 4:

Burke et al. 1991.  
Kramer 1991.  
Visalchand et al. 1991.  
Winschel, Burke, and Zhou 1991.

Kowalski and Basu 1984.  
SEI 1991.  
Winschel and Zhou 1991.  
Zhou and Rao 1992.

TABLE 2  
PROPERTIES OF WILSONVILLE COAL-DERIVED NAPHTHAS

| Coal                            | Illinois No. 6 <sup>a</sup> | Pittsburgh Seam   | Black Thunder     | gasoline Specs      |
|---------------------------------|-----------------------------|-------------------|-------------------|---------------------|
| Cut, °C                         | IBP-182                     | IBP-193           | IBP-193           |                     |
| Gravity, <sup>a</sup> API @15°C | 43.1                        | 48.9              | 50.9              |                     |
| DB6 Distillation, °C            |                             |                   |                   |                     |
| 10%                             | 74 <sup>b</sup>             | 91                | 80 <sup>b</sup>   | 70 max              |
| 50%                             | 121                         | 126               | 116               | 77-121              |
| 90%                             | 173                         | 172               | 171               | 190 max             |
| EP                              | 197                         | 187               | 204               | 225 max             |
| RVP, kPa                        | -                           | 19.3              | 21.4              | 62 max <sup>c</sup> |
| Elemental, wt%                  |                             |                   |                   |                     |
| C                               | 85.2                        | 85.3              | 84.3              |                     |
| H                               | 12.9                        | 13.3              | 13.6              |                     |
| N                               | 0.008                       | <0.1              | 0.1               |                     |
| S                               | 0.36                        | 0.05              | 0.08              | 0.10 max            |
| O (diff)                        | 1.56                        | 1.25              | 1.92              |                     |
| Group Analysis, vol%            |                             |                   |                   |                     |
| Paraffins                       | 15.9                        | 19.3              | 38.0              |                     |
| Naphthenes                      | 60.7                        | 67.5              | 7.0               |                     |
| Aromatics                       | 23.4                        | 13.2              | 5.0               |                     |
| Olefins                         | 5.5                         | -                 | 5.0               |                     |
| Acidity, mg KOH/g               | -                           | -                 | 0.38              |                     |
| Phenolic-OH, meq/g              | -                           | 0.18              | 0.40              |                     |
| Motor Octane                    | 73.4                        | 86.5 <sup>d</sup> | 87.1 <sup>d</sup> |                     |
| Existent Gum, mg/g              | -                           | 7.6               | 40.2              | 5 max               |
| Copper Corrosion                | -                           | 1A                | 1A                | 1 max               |
| Oxidation Stability, min        | -                           | Pass              | Fail              | 240 min             |
| Yield, wt%                      |                             |                   |                   |                     |
| on Total Coal Liquid            | 18.4                        | 26.7              | 23.7              |                     |
| on maf Coal                     | -                           | 19.7              | -                 |                     |

<sup>a</sup> Wilsonville Run 244.  
<sup>b</sup> Class A.

<sup>c</sup> GC Simulated.  
<sup>d</sup> by GC method.

TABLE 3  
PROPERTIES OF WILSONVILLE KERSENE FRACTIONS

| Coal                  | Illinois<br>No. 6 | Pittsburgh<br>Seam | Black<br>Thunder | Jet A-1<br>Specs   |
|-----------------------|-------------------|--------------------|------------------|--------------------|
| Cut, °C               | 182-232           | 193-266            | 193-266          |                    |
| Gravity, °API @15°C   | 22.9              | 25.9               | 21.3             | 37-51              |
| DBG Distillation, °C  |                   |                    |                  |                    |
| 10%                   | 178 <sup>1</sup>  | 220                | 2121             | 205 max            |
| 50%                   | 200               | 227                | 242              |                    |
| 90%                   | 222               | 244                | 259              |                    |
| EP                    | 379               | 263                | 346              | 300 max            |
| RVP, kPa              | -                 | 9.6                | -                | 20.7 max           |
| Flash Point, °C       | -                 | 76.1               | 86.7             | 38 min             |
| Freezing Point, °C    | -                 | -53.5              | dark             | -47 max            |
| Elemental, wt%        |                   |                    |                  |                    |
| C                     | 84.4              | 87.0               | 85.8             |                    |
| H                     | 10.9              | 11.5               | 10.6             |                    |
| N                     | 0.22              | <0.1               | 0.3              |                    |
| S                     | 0.23              | 0.04               | 0.04             | 0.30 max           |
| Mercaptan S           | -                 | 0.003              | 0.009            | 0.003 max          |
| O (diff)              | 4.26              | 1.36               | 3.26             |                    |
| Group Analysis, vol%  |                   |                    |                  |                    |
| Paraffins             | -                 | -                  | -                |                    |
| Naphthenes            | -                 | -                  | -                |                    |
| Aromatics             | -                 | 44.0               | 50.0             | 25 max             |
| Olefins               | -                 | 3.0                | 3.0              | 5 max <sup>2</sup> |
| Naphthalene           | -                 | -                  | 4.94             |                    |
| Smoke Point, mm       | -                 | 10.8               | 9.8              | 25 min             |
| Acidity, mg KOH/g     | -                 | 0.05               | 0.92             | 0.1 max            |
| Phenolic-OH, meq/g    | -                 | 0.25               |                  |                    |
| Kin. Viscosity, cSt   |                   |                    |                  |                    |
| @ -20°C               | -                 | 1.75               | 18.94            | 8 max              |
| Existent Gum, mg/g    | -                 | 69.0               | 90.8             | 7 max              |
| Copper Corrosion      | -                 | 1A                 | 1A               | 1 max              |
| JFTOT                 | -                 | Fail               | -                | 25/3 Min.          |
| Net Heat Value, MJ/kg | -                 | 42.1               | 42.0             | 42.8 min           |
| Yield, wt%            |                   |                    |                  |                    |
| on Total Liquid       | 11.0              | 31.4               | 19.0             |                    |
| on maf Coal           | -                 | 23.1               | -                |                    |

<sup>1</sup> GC Simulated.

<sup>2</sup> applicable to Jet B.

TABLE 4  
PROPERTIES OF WILSONVILLE COAL-DERIVED MIDDLE DISTILLATES

| Coal                       | Illinois<br>No. 6 | Pittsburgh<br>Seam | Black<br>Thunder | No. 1<br>Diesel     |
|----------------------------|-------------------|--------------------|------------------|---------------------|
| Cut, °C                    | 182-343           | 266 <sup>+</sup>   | 266-343          |                     |
| Gravity, °API              | 18.6              | 16.3               | 17.7             |                     |
| GC Simulated Dist., °C     |                   |                    |                  |                     |
| 10%                        | 193               | -                  | 256              |                     |
| 50%                        | 250               | -                  | 289              |                     |
| 90%                        | 317               | 365                | 321              | 288 max             |
| EP                         | 379               | -                  | 346              |                     |
| Flash Point, °C            | -                 | -                  | 124              | 38 min              |
| Elemental, wt%             |                   |                    |                  |                     |
| C                          | 86.3              | 88.4               | 87.0             |                     |
| H                          | 10.7              | 10.5               | 10.7             |                     |
| N                          | 0.23              | 0.1                | 0.3              |                     |
| S                          | 0.22              | 0.04               | 0.03             | 0.50 max            |
| O (diff)                   | 2.48              | 0.96               | 1.75             |                     |
| H/C Atom Ratio             | 1.49              | 1.43               | 1.48             |                     |
| Aromatic Carbon, %         | 34.0              | -                  | -                |                     |
| Bromine No. g/100g         | -                 | 7.4                | 17               |                     |
| Viscosity, cSt, @40°C      | -                 | 8.97               | 6.2              | 1.3-2.4             |
| Ramsbottom Carbon, %       | 0.15              | -                  | -                | 0.15 max            |
| Hot C. Insolubles, %       | 0.48              | -                  | -                |                     |
| Ash, wt%                   | -                 | 0.02               | 0.00             | 0.01 max            |
| Copper corrosion           | -                 | 1A                 | 1A               | 3 max               |
| Cetane Index               | 21                | 26.5               | 27.7             | 40 min <sup>1</sup> |
| Yield, wt% on Total Liquid | 45.7              | 41.9               | 22.9             |                     |

<sup>1</sup> Cetane number.

## CATALYST SELECTION FOR HYDROTREATING DIESEL FUEL FROM RESIDUE HYDROCRACKING

Patricio S. Herrera, Michael C. Oballa, Arpad F. Somogyvari and Jacques Monnier\*  
NOVA HUSKY Research Corporation  
2928 16th - Street N.E., Calgary, Alberta, Canada, T2E 7K7  
\* Energy Research Laboratories, CANMET, Energy, Mines and Resources Canada  
555 Booth Street, Ottawa, Ontario, Canada, K1A 0G1

**Keywords:** Hydrotreating, aromatics reduction, sulfur reduction

### ABSTRACT

Six commercial catalysts ( $\text{NiMo}/\text{Al}_2\text{O}_3$  and  $\text{NiW}/\text{Al}_2\text{O}_3$ ) were evaluated for the simultaneous reduction of the aromatics and sulfur contents in the diesel fraction (177°C - 343°C) of a hydrocracked atmospheric residue.

The reactions were carried out in a fixed bed reactor operating in an upflow mode. Optimal operating variables were established to maximize aromatics conversion and sulfur removal. In order to rank catalysts according to their performance, short term screening runs were performed. The two best catalysts were selected for which long term runs were carried out. Though the hydrotreated products for all catalysts met required specifications, the optimal operating conditions used in this study were more severe than processing conditions used in existing hydrotreating units.

### INTRODUCTION

Diesel fuel properties are said to have an effect on the quantity and type of air polluting emissions from diesel engines. Specifically, the sulfur and aromatics contents of diesel fuels are singled out as the main sources of particulate emissions<sup>(1)</sup>. In Canada, the contribution of diesel particulates to the total discharges from transportation and industrial diesel engines was estimated at 29 and 23 thousand tons respectively per year<sup>(2)</sup>. In California, new and stringent emission standards are already set and other states are expected to follow California's example.

To comply with these new regulations, the oil refining industry has been evaluating a number of options to limit the sulfur and aromatics contents of diesel fuels. One way of achieving this goal involves a two-stage process: initial desulfurization with a deep desulfurization-type catalyst (Co-Mo/alumina) followed by aromatics saturation. The second stage may use a Ni-Mo/alumina or noble metal catalyst. Desulfurization would protect the noble metal catalyst against sulfur poisoning<sup>(3)</sup>.

On the other hand, there are new sulfur tolerant catalysts that would achieve both aromatics saturation and sulfur removal in one step<sup>(3-5)</sup>.

The work reported in this paper is part of a project to evaluate available commercial catalysts for simultaneously reducing sulfur and aromatics in diesel oil fractions to be produced at the Bi-Provincial Upgrader (BPU) in Lloydminster, Sask., Canada<sup>(6)</sup>. This

grassroots facility will upgrade a feedstock containing a 50/50 volumetric blend of Lloydminster/Cold Lake heavy oils to synthetic crude.

The project focused on attaining the proposed specifications for sulfur and aromatics contents in diesel fuel fractions. The selected approach was to study a one-step hydrotreating process using our particular feedstock and several new generation catalysts claiming to achieve the specified reductions.

## EXPERIMENTAL

**Equipment:** Hydrotreating experiments were carried out in a stainless steel tubular fixed bed reactor operated under the following experimental conditions: upflow mode, diluted catalyst bed (reaction zone = 225 mL), isothermal and plug flow, and once through. The experimental system, including the reaction unit, was described and illustrated elsewhere<sup>(7)</sup>.

**Catalysts:** All commercial catalysts except one (catalyst B) were of the Ni-Mo type on alumina carrier. Catalyst B was a layered arrangement of Ni-Mo and Ni-W catalysts supplied by the same source. Catalyst companies provided a catalyst they considered the most suitable to treat our feedstock. There were no apparent dissimilarities in catalyst properties based on vendor information.

**Feedstock:** The feedstock was the fraction boiling between 177°C - 343°C obtained from a hydrocracked 50/50 volumetric blend of Cold Lake/Lloydminster residue. The hydrocracked material was distilled on a TBP unit according to procedures described in ASTM D-2892. The properties of the average feed are given in Table 1.

**Analytical Methods:** Specific gravities were measured at 15.5°C using a Paar DMA instrument. Dynamic viscosities were determined at 25°C on a Brookfield DV II apparatus. Carbon and hydrogen were determined commercially on a Perkin Elmer 240B analyzer. Trace nitrogen was obtained by chemiluminescence using an Antek Model 771 analyzer, while trace sulfur was measured by microcoulometry using a Dohrmann instrument, model MCTS 130. The total per cent aromatics was determined by the fluorescent indicator adsorption (FIA) method (ASTM D-1319). Simulated distillations were performed according to ASTM D-2887. Low resolution mass spectrometry (MS) analyses for aromatic types were determined commercially by ASTM D-3239. Cetane number was determined by ASTM D613 and Aniline Point by ASTM D611.

## RESULTS AND DISCUSSIONS

The initial part of the study included catalyst activity runs to select the process conditions which produced a liquid product meeting the specifications established for the BPU middle distillate fraction (177°C - 343°C)<sup>(6)</sup>. These values correspond to, among others, sulfur content in product at 1000 wppm max. and cetane number at 40 min.

The base conditions chosen after the initial runs were:  $T = 380^{\circ}\text{C}$ ,  $P = 12.4 \text{ MPa}$  and  $\text{LHSV} = 0.75 \text{ h}^{-1}$ . A single catalyst (A) was used for all the initial runs.

The catalyst screening program involved experiments to rank six commercial catalysts according to their efficiencies in sulfur and aromatics conversions. Each catalyst was tested at base conditions and at various temperatures, pressures and liquid hourly space velocities (LHSV) to determine the influence of these parameters on catalyst performance. All experiments were performed using the same hydrogen-to-feed ratio ( $1000 \text{ Std.m}^3/\text{m}^3$ ).

The properties determined on the total liquid product obtained from each run included measurements of density, viscosity, sulfur and nitrogen content, simulated distillation, total aromatics by FIA and elemental analysis. The properties of the average feedstock and of the products obtained at base conditions are shown in Table 1.

#### AROMATICS CONVERSION

The aromatics content of the total liquid product was used (instead of the cetane number) to compare catalyst activities. The FIA method was used to measure concentrations of aromatics in feed and products. To confirm the FIA results and to expand the information on aromatics distribution, additional analyses using Robinson and Cook's mass spectrophotometric technique<sup>(8)</sup> were performed only on products obtained at base conditions. Table 2 shows the aromatics content of hydrotreated products determined by both procedures. The level of aromatics concentration recorded by the MS method was lower than that observed using FIA. The difference may be attributed to some of the problems observed with the FIA method: the analysis includes as aromatics other compounds such as diolefins and sulfur, nitrogen and oxygen containing materials<sup>(9)</sup>. Nevertheless, the trend observed with FIA for aromatics reduction with different catalysts was confirmed by MS results and, in addition, it was observed that conversion of diaromatics and polyaromatics to monoaromatics was almost complete.

The reduction in total aromatics with increase in reaction pressure is a well known aspect of the hydrotreating process<sup>(9,10)</sup>. In our work, the effect of pressure on aromatics conversion was studied over a wide pressure range at base values of temperature and LHSV (Figure 1). Our results indicate that in order to get aromatic conversions above 50% (or concentrations below 20 vol%), one has to operate at a pressure above 10 MPa. At higher pressures all catalysts exhibited higher aromatic conversions, confirming that the hydrogenation reaction is very much favored by pressure. Catalysts B and C clearly outperformed the others with respect to aromatics reduction. On the other hand, catalysts B and C also presented better hydrocracking activities by producing lighter fractions in the total liquid product (Table 1).

The influence of reaction temperature on aromatics conversion in middle distillate fractions has been studied before<sup>(11-13)</sup>. An optimum temperature of  $380^{\circ}\text{C}$  was determined<sup>(12)</sup> to achieve a maximum aromatics conversion. The base temperature found by us agrees with the optimum temperature previously measured. Our study covered the  $350 - 380^{\circ}\text{C}$  temperature range, at base values of pressure and LHSV.

Again catalysts B and C exhibited the best activity for aromatics saturation (Figure II). Aromatics conversion increased linearly with reaction temperature for all catalysts tested in the program. Even at the lowest end of the temperature range (350°C) catalyst B achieved aromatics conversion above 65% (or concentrations of 15 vol%). At 365°C, all catalysts attained conversions exceeding 50% which correspond to concentrations below 20 vol%.

The effect of LHSV on aromatics conversion, at base values of temperature and pressure, is shown in Figure III. At low LHSV, all catalysts achieved conversions above 80%. At the highest LHSV tested, 1.0 h<sup>-1</sup>, the conversion level surpassed 60% (or aromatics concentration below 18 vol%). Based on equal amount of conversion, the LHSV influence on aromatics reduction is not as marked as that produced by pressure or temperature.

According to the results presented, clearly aromatics saturation was more dependent on pressure than on any other parameter. Also, some of the combinations of the operating conditions reduced the aromatics concentration below the levels established in impending specifications for diesel fuels. The severe process conditions at which these requirements were met are, however, out of line with the operating parameters of existing diesel hydrotreating units.

#### **SULFUR AND NITROGEN CONVERSIONS**

Under all experimental conditions tested, sulfur conversions exceeded 90%. At base conditions removal of sulfur surpassed 94% (Table 1). Therefore, the target sulfur concentration was easily achieved by all catalysts at the operating conditions used. On the other hand, nitrogen conversions above 99% (corresponding to less than 5 wppm in product) were achieved in all of the runs performed. No significant differences were observed in the catalysts' performance from the point of view of sulfur and nitrogen removal.

#### **INFLUENCE OF CATALYST PROPERTIES**

The catalysts' properties were determined in an attempt to find the origin of the differences observed in catalysts' performance. We wished to compare the various conversions for each catalyst on an equal basis. The basis chosen was the unit surface area conversion. The catalyst components believed to affect in greater extent the conversions were nickel, molybdenum, phosphorus and tungsten. In Figure IV, the [Ni + Mo(W) + P] weight per unit surface area was plotted against the conversion for the same area. The results demonstrated that catalysts exhibiting higher coverage per unit area (B and C) were the ones performing better as far as aromatics, sulfur and nitrogen conversions are concerned. There was little correlation for independent components suggesting the existence of a synergism effect among all these elements.

#### **CATALYST DEACTIVATION EXPERIMENTS**

Long term runs of approximately 1000 hours were carried out using the two best catalysts from the screening experiments (B and C). The purpose of this task was to

study the rate of deactivation of the selected catalysts at base conditions. No marked difference in catalysts' performance was found except for hydrogen consumption (Table 3). It was the original intent of this part of the study to project catalyst life based on a deactivation curve. However, this was not possible because within the length of the runs, little deactivation occurred. The layered bed of NiMo and NiW on alumina (catalyst B) showed lower hydrogen consumption for similar aromatics conversions. The cetane number of liquid products showed similar results.

## CONCLUSIONS

All six commercial catalysts studied satisfied upcoming specifications on the sulfur content for diesel fuels. Also, at base conditions, all catalysts reduced the aromatics content of the feed to less than 20 vol%. The operating conditions at which these requirements were met are, however, out of line with the operating conditions of existing diesel hydrotreating units. This implies that a single stage process for hydrotreating middle distillates can only meet the impending specifications with a new reactor designed and built specifically for these operating conditions.

Two out of six catalysts (B and C) outperformed the others in aromatics conversion. It was found that the activity of these catalysts showed marked dependence on the total coverage of definite fresh catalyst components. After the catalyst deactivation experiments, the choice between catalysts B and C was based on economics because they exhibited similar technical performance.

## ACKNOWLEDGMENTS

The authors thank Mr. Leon Neumann who performed the hydrotreating experiments and was responsible for part of the analytical work. Our thanks also go the Analytical Services Group at NHRC. Part of this work was supported by a 50/50 cost-shared program between Husky Oil Ltd. and CANMET, EMR, Ottawa, under contract number 23440-0-9018/01-SQ.

## REFERENCES

1. Weaver, C.S.; Miller, C.; Johnson, W.A.; Higgins, T.S., SAE Technical Paper 860622 (1986).
2. *A Plan to Identify and Assess Emission Reduction Opportunities from Transportation*, Industrial Engines and Motor Fuels, Transportation Systems Division, Environment Canada, TP 9773E (May, 1989).
3. Cooper, B.H.; Stanislaus, A.; Hannerup, P.N., *Prepr. Am. Chem. Soc. Div. Fuel Chem.* 1992, **37**, 41.
4. Nash, R.M., *Oil and Gas Journal* 1989, **87** (22), 47-56.
5. Parkinson, G.; Johnson, E., *Chem. Eng.* 1989, **96** (9), 31-46.
6. Chase, S., Paper presented at the Sixth Annual Heavy Oil and Oil Sands Technical Symposium, Calgary, AB, March 1989.
7. Herrera, P.S.; Oballa, M.C.; Somogyvari, A.F., Paper presented at the 41st Annual Canadian Chemical Engineering Conference, Vancouver, B.C., Oct. 1991.
8. Robinson, C.J.; Cook, G.L., *Anal. Chem.* 1969, **41**, 1548.

9. Assim, M.Y.; Keyworth, D.A.; Zoller, J.R.; Plantenga, F.L.; Lee, S.L., Paper presented at the AKZO Catalysts Seminar, Calgary, AB, July 1990.
10. Nash, R.M., Paper presented at the NPRA Annual Meeting, San Francisco, CA, March 1989, paper AM-89-29.
11. Wilson, M.F.; Kriz, J.F., *Fuel* 1984, **63** (2), 190-196.
12. Wilson, M.F.; Fisher, I.P.; Kriz, J.F., *J. Catalysis* 1985, **95** (8), 155-166.
13. Wilson, M.F.; Mainwaring, P.R.; Brown, J.R.; Kriz, J.F., Preprints 10th Canadian Symposium on Catalysis, Kingston, Ontario, June 1986.

TABLE 1

AVERAGE FEEDSTOCK AND PRODUCT PROPERTIES AT BASE CONDITIONS

|                              | FEED STOCK | PROD. A | PROD. B | PROD. C | PROD. D | PROD. E | PROD. F |
|------------------------------|------------|---------|---------|---------|---------|---------|---------|
| Density (g/cm <sup>3</sup> ) | 0.8554     | 0.8308  | 0.8282  | 0.8251  | 0.8333  | 0.8266  | 0.8503  |
| Viscosity (cP)               | 3.2        | 2.0     | 2.6     | 2.3     | 2.7     | 2.7     | 3.6     |
| Carbon (wt%)                 | 86.96      | 86.01   | 85.38   | 85.67   | 86.13   | 85.99   | 86.14   |
| Hydrogen (wt%)               | 12.23      | 13.27   | 13.77   | 14.22   | 13.80   | 13.92   | 13.30   |
| Sulfur (wppm)                | 3858       | 112     | 181     | 195     | 138     | 82      | 64      |
| Nitrogen (wppm)              | 752        | 5       | <1      | <1      | 2       | 1       | <1      |
| Sim. Distribut. (wt%):       |            |         |         |         |         |         |         |
| IBP - 177°C                  | 0.9        | 4.7     | 6.8     | 5.8     | 4.7     | 5.6     | 3.5     |
| 177 - 249°C                  | 39.6       | 44.3    | 47.7    | 48.2    | 37.3    | 47.4    | 27.5    |
| 249 - 343°C                  | 58.6       | 50.1    | 43.7    | 44.7    | 57.0    | 45.6    | 64.1    |
| 343 - 524°C                  | 0.9        | 0.9     | 1.8     | 1.3     | 1.0     | 1.4     | 4.9     |

Notes: (i) A, B, C, D, E, F are commercial catalysts;

(ii) Base Conditions: T = 380°C; P = 12.4 MPa; LHSV = 0.75 h<sup>-1</sup>

TABLE 2  
TOTAL AROMATICS AT BASE CONDITIONS

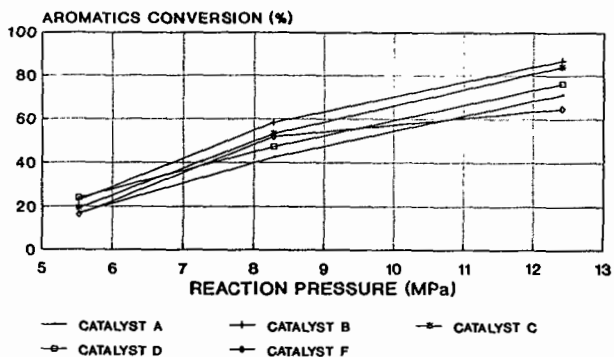
|                   | FEED-<br>STOCK | PROD.<br>A | PROD.<br>B | PROD.<br>C | PROD.<br>D | PROD.<br>E | PROD.<br>F |
|-------------------|----------------|------------|------------|------------|------------|------------|------------|
| F.I.A. (vol.%)    | 43.6           | 12.5       | 6.0        | 7.1        | 11.2       | 9.8        | 17.0       |
| Mass Spec. (wt%): |                |            |            |            |            |            |            |
| Monoaromatics     | 30.60          | 7.31       | 2.18       | 5.08       | 7.74       | 9.29       | 11.12      |
| Diaromatics       | 5.59           | 0.18       | 0.07       | 0.09       | 0.17       | 0.18       | 0.43       |
| Polyaromatics     | 0.05           | 0.01       | 0.00       | 0.08       | 0.13       | 0.03       | 0.61       |
| Aromatic Sulfur   | 0.74           | 0.03       | 0.04       | 0.00       | 0.02       | 0.00       | 0.12       |
| Total Aromatics   | 36.98          | 7.53       | 2.29       | 5.25       | 8.06       | 9.50       | 12.28      |

TABLE 3  
LONG TERM RUNS, AVERAGE QUALITY OF TOTAL LIQUID PRODUCTS

| CATALYST                               | B      | C      |
|--|--------|--------|
| Cetane Number (ASTM D613)              | 50.3   | 50.7   |
| Aniline Point, °C (ASTM D611) Modified | 70.70  | 71.25  |
| Sulfur (wppm)                          | 259    | 174    |
| Nitrogen (wppm)                        | 3      | <1     |
| FIA Aromatics (vol%)                   | 5.1    | 4.6    |
| Aromatics Conversion (%)               | 84.40  | 87.50  |
| Sulfur Conversion (%)                  | 91.07  | 94.00  |
| Nitrogen Conversion (%)                | 99.39  | 99.93  |
| Density (g/cm <sup>3</sup> )           | 0.8240 | 0.8225 |
| API Gravity                            | 40.2   | 40.5   |
| Viscosity (cP)                         | 2.4    | 2.4    |
| Carbon (wt%)                           | 85.98  | 86.25  |
| Hydrogen (wt%)                         | 13.56  | 13.74  |
| H <sub>2</sub> Consumption:            |        |        |
| L H <sub>2</sub> /L feedstock          | 56.2   | 74.6   |
| (SCF H <sub>2</sub> /BBL feedstock)    | (315)  | (419)  |

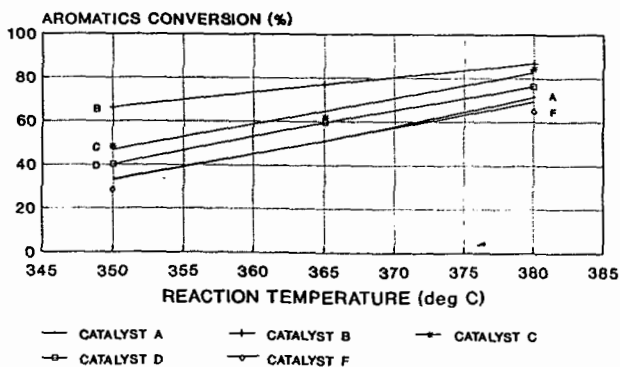
Note: Operating Conditions: T = 380°C; P = 12.4 MPa; LHSV = 0.75 h<sup>-1</sup>

FIGURE I: EFFECT OF REACTION PRESSURE ON AROMATICS CONVERSION



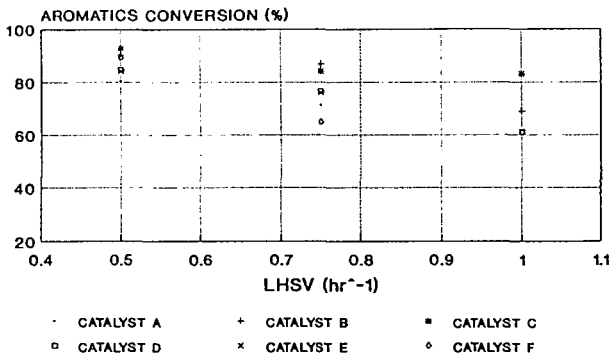
Temperature = 380 deg C  
 LHSV = 0.75 hr<sup>-1</sup>

FIGURE II: EFFECT OF REACTION TEMPERATURE ON AROMATICS CONVERSION



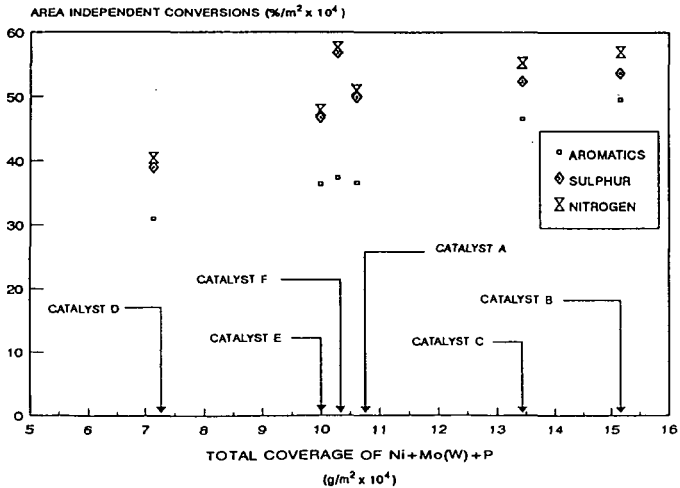
Pressure = 12.4 MPa  
 LHSV = 0.75 hr<sup>-1</sup>

FIGURE III: EFFECT OF LHSV ON AROMATICS CONVERSION



Temperature = 380 deg C  
 Pressure = 12.4 MPa

FIGURE IV: CONVERSION AS A FUNCTION OF CATALYST COMPONENTS COVERAGE



## PROMOTED HYDROTREATING CATALYSTS

A. S. Hirschon, L. L. Ackerman, and R. B. Wilson  
SRI International

Y. Horita and T. Komoto  
Nippon Steel Chemical Corporation

Keywords: Hydrotreating, HDN, catalysts

### INTRODUCTION

With dwindling supplies of high quality petroleum feedstocks, efforts are being taken to utilize alternative feedstocks such as heavy crudes and coal liquids as sources for chemicals and alternative fuels. However, these feedstocks are often heavily aromatic and contain large amounts of heteroatoms such as nitrogen, sulfur, and oxygen. Nitrogen and oxygen are so difficult to remove that extremely strenuous conditions are required. However, under these severe conditions the valuable aromatics are also excessively hydrogenated, wasting valuable hydrogen. Attempts to improve the current hydrotreating catalysts such as NiMo, CoMo, and NiW that have been developed for petroleum feedstocks have met with little success. What is needed are catalysts that are more selective toward hydrogenolysis activity rather than hydrogenation reactions. Therefore efforts are being conducted to find catalysts that can selectively remove heteroatoms, in particular, nitrogen. Workers have shown in systematic studies that for each row of the periodic table a correlation occurs between the position and the reactivity of the bulk metal towards hydrogenolysis reactions, with the lower rows being the most active.<sup>1-4</sup> Using this methodology, certain noble metals such as ruthenium have been identified as highly active hydrogenolysis catalysts.

Since the ratio of the hydrogenolysis to hydrogenation activity varies with the nature of the catalyst, various metals and metal combinations have been investigated in efforts to find catalysts with improved selectivity and high ratios of hydrogenolysis to hydrogenation activities.<sup>5-10</sup> Recently it has been shown that when ruthenium was used in conjunction with molybdenum, a very active and selective hydrodenitrogenation catalyst was formed. In this work we investigated several methods of preparation of this catalyst and their respective activities towards both model systems and coal tars.

### EXPERIMENTAL

#### Catalyst Preparation

Alumina extrudates were used for coal tar testing whereas powdered alumina was used for the model system testing. Molybdenum and nickel salts were impregnated into the alumina by standard incipient wetness techniques. Ruthenium was added as the carbonyl for the majority of the catalysts; the methodology for incorporation of ruthenium and activation of the catalyst is described in the text.

#### Catalyst Testing

The catalysts were evaluated for HDN and HDO using quinoline and diphenylether, respectively. Under nitrogen, 0.100 g of catalyst, 10 mL of a 0.197 M quinoline, and 0.086 M n-tetradecane (internal standard) and/or 0.150 M diphenyl ether were placed in a quartz liner in a 45-mL Parr bomb. The Parr bomb was pressurized with 500 psig of H<sub>2</sub> and heated for the desired times and

temperatures. The quinoline and the diphenyl ether were used to compare the catalysts for HDN and HDO activities, respectively. The HDN reactions were run at 350°C, and the HDO reactions were run at 250° to 300°C. The competitive HDN/HDO reactions were run at 350°C.

The HDN activities of the catalysts were compared by calculating the turnover frequencies (TF) for the disappearance of tetrahydroquinoline (THQ) and formation of propylbenzene (PB) and propylcyclohexane (PCH). Selectivities were determined from the relative distribution of PCH, PB, and propylcyclohexene (PCHE) when 5% of quinoline had been converted to these hydrocarbon products. HDO activities were compared by calculating the TF for the disappearance of diphenyl ether (DPE) and appearance of cyclohexane and benzene. HDO selectivities were determined from the relative proportions of benzene, cyclohexane, and phenol at a given level of conversion.

The activities of the catalysts were evaluated for the hydrotreatment of coal tars using a continuous flow reactor with 20 mL of catalyst at 360°C, 180Kg/cm<sup>2</sup> pressure hydrogen and LHSV of 0.5h<sup>-1</sup>. The reaction was monitored by elemental analysis of the product stream with samples taken after 100 h on-stream.

## RESULTS AND DISCUSSION

### Hydrogenolysis of Model Compounds

Since both nitrogen and oxygen containing molecules cause the most problems in upgrading coal derived liquids, both HDN and HDO reactivities on model systems were investigated. A summary of the effect of ruthenium promotion of supported NiMo and CoMo alumina catalysts on the HDN reaction of quinoline (Table 1) shows that the promoted CoMo gives exceptional performance; even greater than that of promoted NiMo under these conditions. Furthermore, the promotion shows a large increase in selectivity for the CoMo system from a PCH/PB ratio of 15:1 to 3:1, compared to an increase of 4.9:1 to 2.6:1 for the NiMo system. However, when the RuCoMo catalyst was examined for the HDO of diphenylether, the CoMo catalysts was actually found to be more reactive; but when examined in a competition study with both quinoline and diphenylether present, the reverse order was found and the promoted RuCoMo catalyst was both the most active and selective catalyst. Apparently the amine reduced the HDO activity of the CoMo catalyst to a greater extent than the RuCoMo catalyst. Thus we would expect that the ruthenium promoted catalysts would be most useful in hydrotreating coal liquids and other alternative fuels.

### Method of Activation and Preparation

The procedure we used for the formulation of the ruthenium promoted catalyst involved presulfiding the molybdenum based catalyst and then adding ruthenium carbonyl. The objective of this synthesis was to add the ruthenium to the sulfidryl groups of the sulfided metal (molybdenum for instance). This procedure was based on the methods of Yermakov, and was designed to produce a highly dispersed mixed metal cluster.<sup>11</sup> However, in common practice catalysts are not sulfided as an intermediate step, and therefore we varied the order of sulfiding and calcining as follows, to determine if there would be any effects on the activities and selectivities of these ruthenium promoted catalysts. Promoted molybdenum catalysts were prepared by three different methods. Method 1 consisted of impregnating the molybdenum catalyst with the ruthenium carbonyl in THF, evaporating the THF, and then first calcining and then sulfiding the product at 400°C. The method is similar to a conventional catalyst preparation, where each metal is sequentially added and calcined. The calcination step assures that the metals interact with the

support for high dispersion and to prevent loss of metal during use. Method 2 consisted of sulfiding the RuMo product without the second calcining step. In Method 3, we prepared the catalyst our normal way, first sulfiding the molybdenum catalyst and adding the ruthenium to the sulfided molybdenum catalyst, and then sulfiding again.

The activities and selectivities of the catalysts prepared by these methods are listed in Tables 3 and 4 for HDN reactions using quinoline as a model system. As seen in these tables, the selectivity of the catalyst produced by method 1 is high, giving a PCH/PB ratio of 3.0, but the overall activity is much lower than that for the other two methods, having a rate almost 200 times less active than for method 3. As seen for Methods 2 and 3, the activities are greatly improved, with method 3 being the most active for HDN activity. We believe that the difference between the activities is due to the sulfiding of the molybdenum prior to the promotion with Ru. Thus method 1 should give strong Al-O-Ru interactions, whereas method 3 should give Mo-S-Ru interactions, which we postulate will allow a synergy between the Mo and Ru.

### Testing of Catalysts on Coal Tars

In order to verify these results on model systems, samples of RuCoMo, RuNiMo, and RuMo were evaluated for hydrotreating of coal tars. Table 5 lists some of these results. As seen from this table, there were both similarities and differences from the results on the model systems. For instance, the promotion of the CoMo catalyst (2A) to form RuCoMo (2B) gave little difference in the HDN of the coal tar (HDN rates of 0.47 and 0.44, respectively). However, promotion of the CoMo catalyst gave a very dramatic increase in reactivity and selectivity for quinoline HDN. In contrast, the promotion of NiMo (1A) with ruthenium to form RuNiMo (1B) did indeed increase the reactivity towards coal tars, and increasing both the rate of nitrogen removal (from 0.43 to 0.55) as well as increasing the selectivity of HDN to hydrogenation reactions. Catalyst 3A and 3B were RuMo catalysts designed to compare the method of preparation as previously described in the model systems. Catalyst 3A was prepared by first sulfiding the molybdenum and then adding ruthenium (Method 3), and 3B was prepared by adding the ruthenium to the calcined molybdenum, calcining again, and then sulfiding (Method 1). Again, as with the model systems, the presulfiding increased the activity of the catalyst.

### CONCLUSIONS

Ruthenium promotion enhances HDN activity under low-severity hydrotreating of coal tars, confirming our previous studies with model systems. Promotion of CoMo is not as effective on coal tars as with model systems, and may depend upon the type of feedstock. However, promotion of NiMo gave enhanced HDN activity and selectivity for both systems. The key to the high activity and selectivity appears to be adding the ruthenium to a previously sulfided molybdenum catalyst. The reason for this high activity, we believe, is the formation of a Ru-S-Mo interaction, which may allow a better synergistic relationship. However, alternative explanations may be possible, and a more detailed study of these catalysts may lead to a better description of the active site.

### REFERENCES

1. H. Sinfelt, *Prog. Sol. St. Chem.* (1975), **10**, 55-69.
2. T. A. Pecoraro and R. R. Chianelli, *J. Catal.* (1981), **67**, 430

3. S. Harris and R. R. Chianelli, *J. Catal.* (1984), **86**, 400-412.
4. A. S. Hirschon and R. M. Laine, *Energy and Fuels*, (1988), **2**, 292-295.
5. A. S. Hirschon, R. B. Wilson, Jr. and R. M. Laine, *Amer. Chem. Soc. Div. Pet. Prepr.* (1987), **32**(2), 268-270.
6. A. S. Hirschon, R. B. Wilson Jr., and R. M. Laine, *Appl. Catal.* (1987), **34**, 311-316.
7. J. Shabtai, N. K. Nag, K. Balusami, B. Gajjar and F. E. Massoth, *Amer. Chem. Soc. Div. Pet. Prepr.*, **31** (1986) 231.
8. J. Shabtai, N. K. Nag and F. E. Massoth, *J. Catal.*, **104** (1987) 413.
9. T. G. Harvey and T. W. Matheson, *J. of Catal.*, **101**, (1986) 253-261.
10. S.-M. Koo, M. L. Hoppe, and R. M. Laine, *Amer. Chem. Soc. Div. Pet. Prepr.* (1992), **37**(1), 290-297.
11. I. Yermakov, *Catal. Rev.-Sci. Eng.*, (1976), **13**, 77-120.

Table 1

TURNOVER FREQUENCIES FOR QUINOLINE FOR QUINOLINE HDN<sup>a</sup>  
USING PROMOTED CATALYSTS

| No. | Catalyst | TF <sup>b</sup> |     |     |
|-----|----------|-----------------|-----|-----|
|     |          | THQ             | PCH | PB  |
| 1   | CoMo     | 54              | 8.9 | 0.5 |
| 2   | RuCoMo   | 141             | 27  | 8.0 |
| 3   | NiMo     | 86              | 15  | 1.7 |
| 4   | RuNiMo   | 128             | 14  | 5.5 |

<sup>a</sup>Reaction of 10 mL of 0.197 M quinoline in n-hexadecane and 0.100 g of sulfided catalyst at 350°C and 500 psi H<sub>2</sub>.

<sup>b</sup>TF = moles reactant or product/mol Metal/h.

Table 2

SELECTIVITY AT 5 mol % CONVERSION<sup>a</sup>

| No. | Catalyst | % PCH | % PB | % PCHE | PCH/PB |
|-----|----------|-------|------|--------|--------|
| 1   | CoMo     | 82.2  | 4.6  | 13.2   | 17.8   |
| 2   | RuCoMo   | 76.6  | 23.4 | 0      | 3.3    |
| 3   | NiMo     | 73.3  | 14.9 | 11.8   | 4.9    |
| 4   | RuNiMo   | 71.5  | 27.5 | 1.0    | 2.6    |

<sup>a</sup>Reaction of 10 mL of 0.197 M quinoline in n-hexadecane and 0.100 g of sulfided catalyst at 350°C and 500 psi H<sub>2</sub>.

Table 3  
EFFECT OF METHOD OF PREPARATION OF RuMo CATALYST  
FOR QUINOLINE HDN<sup>a</sup>

| No. | Method  | TF <sup>b</sup> |     |     |
|-----|---|-----------------|-----|-----|
|     |   | THQ             | PCH | PB  |
| 1   | Ru/O <sub>2</sub> /H <sub>2</sub> S <sup>c</sup>                  | 50              | 0.3 | 0.1 |
| 2   | O <sub>2</sub> /Ru/H <sub>2</sub> S <sup>d</sup>                  | 67              | 14  | 2.3 |
| 3   | O <sub>2</sub> /H <sub>2</sub> S/Ru/H <sub>2</sub> S <sup>e</sup> | 180             | 48  | 11  |

<sup>a</sup>Reaction of 10 mL of 0.197 M quinoline in n-hexadecane and 0.100 g of sulfided catalyst at 350°C and 500 psi H<sub>2</sub>.

<sup>b</sup>TF = moles reactant or product/mol Metal/h.

<sup>c</sup>Ru added to calcined Mo, calcining Ru, and then sulfiding.

<sup>d</sup>Ru added to calcined Mo, and then sulfiding.

<sup>e</sup>Ru added to sulfided Mo, and sulfided again.

Table 4  
SELECTIVITY AT 5 mol % CONVERSION<sup>a</sup>

| No. | Method  | % PCH | % PB | % PCHE | PCH/PB |
|-----|---|-------|------|--------|--------|
| 1   | Ru/O <sub>2</sub> /H <sub>2</sub> S <sup>b</sup>                  | 63    | 21   | 16     | 3.0    |
| 2   | O <sub>2</sub> /Ru/H <sub>2</sub> S <sup>c</sup>                  | 80    | 14   | 6      | 5.7    |
| 3   | O <sub>2</sub> /H <sub>2</sub> S/Ru/H <sub>2</sub> S <sup>d</sup> | 75    | 21   | 4      | 3.6    |

<sup>a</sup>Reaction of 10 mL of 0.197 M quinoline in n-hexadecane and 0.100 g of sulfided catalyst at 350 C and 500 psi H<sub>2</sub>.

<sup>b</sup>Ru added to calcined Mo, calcining Ru, and then sulfiding.

<sup>c</sup>Ru added to calcined Mo, and then sulfiding.

<sup>d</sup>Ru added to sulfided Mo, and sulfided again.

Table 5  
EFFECT OF CATALYST ON HYDROTREATMENT OF COAL TARS

| Run No. | Catalyst Type       | HDN                 |                      |                             | Hydrogenation       |                  |                   | Selectivity<br>K <sub>n</sub> /ΔH/C |
|---------|---------------------|---------------------|----------------------|-----------------------------|---------------------|------------------|-------------------|-------------------------------------|
|         |                     | N(wt%) <sup>a</sup> | DNR (%) <sup>b</sup> | K <sub>n</sub> <sup>c</sup> | C(wt%) <sup>a</sup> | H/C <sup>d</sup> | ΔH/C <sup>e</sup> |                                     |
| 1A      | NiMo                | 0.43                | 57.8                 | 0.43                        | 91.37               | 1.00             | 0.31              | 1.39                                |
| 1B      | RuNiMo              | 0.33                | 67.6                 | 0.55                        | 90.62               | 1.07             | 0.38              | 1.45                                |
| 2A      | CoMo                | 0.38                | 62.7                 | 0.47                        | 91.24               | 1.06             | 0.37              | 1.27                                |
| 2B      | RuCoMo              | 0.42                | 58.8                 | 0.44                        | 91.16               | 1.06             | 0.37              | 1.19                                |
| 3A      | RuMo-3 <sup>f</sup> | 0.40                | 60.8                 | 0.46                        | 90.61               | 1.08             | 0.39              | 1.17                                |
| 3B      | RuMo-1 <sup>g</sup> | 0.54                | 47.1                 | 0.32                        | 91.82               | 0.93             | 0.24              | 1.33                                |

<sup>a</sup>Wt % in product.

<sup>b</sup>Degree of nitrogen removal.

<sup>c</sup>Rate of nitrogen removal hr<sup>-1</sup>.

<sup>d</sup>Mole ratio.

<sup>e</sup>H/C(product)-H/C(feed).

<sup>f</sup>Mo(sulfided) + Ru.

<sup>g</sup>Mo + Ru, then sulfided.

## HYDROCRACKING OF HEAVY OILS: DEVELOPMENT OF STRUCTURE/REACTIVITY CORRELATIONS FOR KINETICS

Ralph N. Landau, Styliani C. Korré, Matthew Neurock and Michael T. Klein  
*Center for Catalytic Science and Technology, Department of Chemical Engineering  
University of Delaware, Newark, DE 19716*

and Richard J. Quann  
*Mobil Research and Development Corporation  
P.O. Box 480, Paulsboro, NJ 08066-0480*

### KEYWORDS

Hydrocracking, Phenanthrene, 1-methyl naphthalene, Linear Free Energy Relationships

### ABSTRACT

The catalytic hydrocracking reaction pathways, kinetics and mechanisms of 1-methyl naphthalene and phenanthrene were investigated in experiments at 350 °C and 68.1 atm H<sub>2</sub> partial pressure (190.6 atm total pressure), using a presulfided Ni/W on USY zeolite catalyst. 1-methyl naphthalene hydrocracking led to 2-methyl naphthalene, methyl tetralins, methyl decalins, pentyl benzene and tetralin. Phenanthrene hydrocracking led to dihydro, tetrahydro and octahydro phenanthrene, butyl naphthalene, tetralin to butyl tetralin and dibutyl benzene. The rate constants for the dealkylation of butyl tetralins produced in the phenanthrene hydrocracking network conform to a linear free energy relationship (LFER), with the heat of formation of the leaving alkyl carbenium ion as the reactivity index.

### INTRODUCTION

Catalytic hydrocracking is a versatile process for increasing the hydrogen to carbon ratio and decreasing the molecular weight of heavy oils. This versatility may prove extremely valuable in the search for optimal processing conditions and catalysts for production of "reformulated" gasolines. Associated reaction models will likely increase in detail as increasingly molecular output is desired. However, the complexity of hydrocracking feedstock structure and reactivity has kept traditional models somewhat global and, thus, often feedstock dependent. Therefore, the new, feedstock-sensitive, "molecular" models of hydrocracking reaction chemistry require the development of a critical mass of consistent molecular reaction pathways and kinetics as an essential data base. To this end, we report here on hydrocracking reaction pathways of 1-methyl naphthalene and phenanthrene, components among a broader set aimed at sampling the structural attributes of hydrocracking feedstocks. Special attention is devoted to the efficient organization of the resolved kinetic information into quantitative structure/reactivity correlations that will serve as a component of a broader kinetic data base.

The present work builds on the significant current understanding of the hydrocracking of paraffins (Froment, 1987) and extends to examine aromatic hydrocarbons. The aromatics' hydrocracking literature is less comprehensive. Several investigations on hydrocracking model bare ring polynuclear aromatic hydrocarbons involved  $\text{Al}_2\text{O}_3$  or  $\text{Si}/\text{Al}_2\text{O}_3$  catalysts (Qader, 1973; Shabtai et al., 1978; Lemberston and Guisnet, 1984). The effect of zeolite catalysts is examined in more recent publications (Haynes et al., 1983; Lapinas et al., 1987).

We report here on the reactions of 1-methyl naphthalene and phenanthrene. The experiments were focused on the target of discerning reaction families and characterizing them in terms of Quantitative Structure/Reactivity Correlations. We describe the work by first considering the experimental methods. The kinetics of 1-methyl naphthalene and phenanthrene hydrocracking are considered next. Finally, discernible linear free energy relationships are examined.

## EXPERIMENTAL

Cyclohexane (HPLC grade, 99.99%, Aldrich) served as the solvent for the study of the reactions of the remaining compounds. Phenanthrene (98%+, Aldrich), served as the prototype three-ring aromatic moiety. Its staggered structure, makes it thermodynamically more stable than anthracene, and thus more abundant in heavy oils. 1-methyl naphthalene (98%, Aldrich) could in principle be obtained from the phenanthrene network, but its high rank in the network made parameters estimated statistically insignificant. All reactants were used as received.

The catalyst was a Mobil conditioned Zeolyst 753 Ni/W on USY zeolite, received in standard 3.0 mm pellets. Prior to all experiments, it was sulfided for two hours at 400°C by a 10%  $\text{H}_2\text{S}$  in  $\text{H}_2$  gas stream (99%, Matheson Gas Products) at a flow rate of 30  $\text{cm}^3/\text{min}$ . The catalyst was equilibrated by reaction with phenanthrene at 350°C and 68.1 atm  $\text{H}_2$  for  $\approx 10$  hours to achieve a steady-state activity that lasted about 50 more hours on stream.

A one-liter spinning basket batch autoclave (modified from original as received from Autoclave Engineers) was the core of the reaction system. A detailed description of the system is available elsewhere (Landau, 1991). The catalyst basket was mounted on the autoclave's agitator which was equipped with baffles to ensure turbulence. Varying the stirring speed revealed the absence of diffusion limitations for a stirring rate of 10  $\text{s}^{-1}$  or greater. Also, phenanthrene hydrocracking with powdered catalyst (50-200 mesh) in a slurry exhibited the same kinetic behavior as with the 3.175mm pellets, which suggested that internal transport limitations were not important.

Experiments were routinely performed at 350°C and 68.1 atm  $\text{H}_2$  (190.6 atm total pressure, the balance from cyclohexane vapor pressure), with 10g of catalyst in the spinning basket arrangement. The stirring rate was 15  $\text{s}^{-1}$ , increased by 50% for 10 min. immediately following the injection. Total pressure was regulated with continuous hydrogen makeup. Sampling was scheduled to remove no more than 5% of the total liquid volume.

Products were identified using a Hewlett Packard 5970 Mass Selective Detector and a Hewlett Packard 5880A Gas Chromatograph, employing a fused silica capillary column and flame ionization detector. Dibenzyl ether (Aldrich, > 99.9%) was used as an external standard. Finally, the

## RESULTS

### Hydrocracking of 1-methyl naphthalene

Reaction of 25% wt 1-methyl naphthalene took place in cyclohexane as a solvent at 68.1 bar H<sub>2</sub> at 350 °C, and led to 6 identified isomeric lumps, representing 99%+ material balance closure. Kinetics are summarized in Fig. 1. There are two primary products of 1-methyl naphthalene hydrocracking, both with high selectivity : methyl tetralins (lump including 1, 2, 5, and 6-methyl tetralins) and 2-methyl naphthalene (isomerization product). The balance consists of methyl decalins, pentyl benzenes and tetralins.

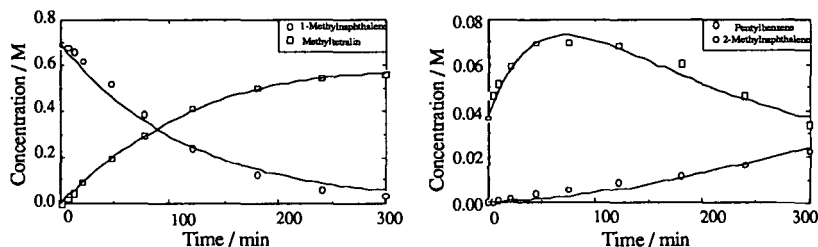


Fig. 1 : Temporal yields of some 1-methyl naphthalene hydrocracking products. Solid lines represent parameter estimation results

Delplot analysis classifies pentyl benzenes as secondary products (direct cracking of methyl tetralins), as well as methyl decalins. Tetralin appeared to be weakly primary product, which implies that their formation is the result of disproportionation reactions of methyl tetralins with the solvent, since no bare-ring naphthalene has been observed.

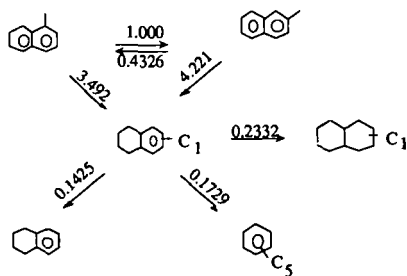


Fig. 2: Proposed network for 1-methyl naphthalene hydrocracking (normalized with  $1.49 \cdot 10^{-3} \text{ l/gcat/min.}$ )

Parameter estimation for the above network provided more insight into the pathways. Isomerization of 1-methyl naphthalene occurred at a slower rate than its hydrogenation, while 2-

methyl naphthalene hydrogenated at a slightly higher rate than 1-methyl naphthalene. Further reactions of methyl tetralins (hydrogenation to decalins, cracking to pentyl benzenes) occurred with rate parameters one order of magnitude lower.

### Hydrocracking of Phenanthrene

Reaction of 3.4 wt% phenanthrene in cyclohexane solvent and at 68.1 atm H<sub>2</sub> at 350 °C led to 11 identified isomeric product lumps, representing 95%+ material balance closure. Each lump represents grouping of molecular weight isomers. For example the tetrahydro phenanthrenes lump includes molecules with cyclohexyl and methyl cyclopentyl saturated rings. *Sym*- and *asym*- octahydro phenanthrenes are in the same lump, and "butyl tetralin" refers to any tetralinic unit sheet with a side chain of four carbon atoms, regardless of its position on the unit sheet.

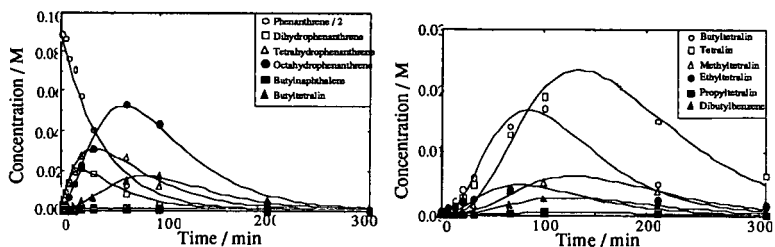


Fig. 3: Temporal yields of some phenanthrene hydrocracking products. Solid lines represent model correlations.

Reaction kinetics are summarized in Fig. 3, which shows, by the initial positive slopes, that dihydrophenanthrene (DHP) and tetrahydro phenanthrenes (THP) were the primary products, DHP forming with higher initial selectivity. Octahydro phenanthrenes (OHP) had very low initial selectivity and were interpreted as secondary products, evolving from THP. Butyl tetralins, tetralins and dibutyl benzenes were higher rank products, evolving mainly from OHP. Butyl naphthalenes, propyl- and methyl tetralins were all clearly of tertiary or higher rank.

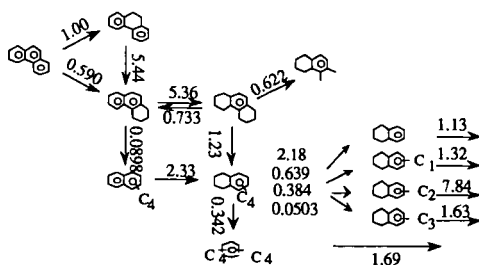


Fig. 4: Proposed network for phenanthrene hydrocracking (normalized with  $1.49 \cdot 10^{-3} \text{ l/gca/min.}$ )

DHP did not appear to dehydrogenate back to phenanthrene, as reported over non-acidic catalyst supports (Girgis and Gates, 1991), but rather hydrogenated further to THP. This difference was probably due to the higher H<sub>2</sub> partial pressure employed in this work. THP in turn underwent further hydrogenation to OHP; this was more selective than ring opening to n-butyl naphthalene. The terminal naphthenic ring in OHP was cracked to butyl tetralin, and cleavage of the butyl side chain occurred at various positions.

The optimized kinetic parameter fitting on all the network components of Fig. 4 is presented in Fig. 3, as modeled species' concentration vs. time. Clearly the fit is good. The chemical significance of the rate constants regressed is thus the remaining issue. This is considered more fully below.

### LFER DEVELOPMENT

The organization and chemical significance of these kinetics data can be enhanced by the existence of linear free energy relationships (LFER). A LFER will exist for a reaction family with similar transition state sterics (essentially constant A-factor) and reactivities that differ because of differences in activation energies. This will assume the form of a linear correlation between the reactivity of a molecule, as it is expressed through its rate parameter, and its structure, as expressed by a reactivity index pertinent to each reaction. The existence of a LFER not only helps to establish the reaction mechanism, but can also concisely summarize an enormous amount of information in a handful of slopes and intercepts. The data bases constructed in this way will be general and flexible enough to draw useful correlations for process modeling.

The applicability of LFERs in heterogeneous catalysis has been hindered in part because of the uncertainty of controlling elementary steps (Dunn, 1968). Observable kinetics are generally the expression of many elementary steps acting in concert. However, Mochida and Yoneda (1967) uncovered a linear relationship between the logarithm of the observed rate constant for dealkylation of a particular alkyl benzene and the enthalpy change for hydride abstraction from the related paraffin,  $\Delta H_C^+(R)$  (Olah et al., 1964). The mechanistic information in this correlation is the suggestion of a rate limiting step for the dealkylation reactions that correlates with the formation of the alkyl carbenium ion. It is also possible that several steps correlate in concert with the same reaction family index. In any case, the modeling value of this correlation is that it allows for the *a priori* prediction of other dealkylation reactions. We follow this perspective in the search for useful correlations to summarize hydrocracking kinetics data.

The butyl tetralin dealkylation reactions observed during hydrocracking of phenanthrene seemed a reasonable point to search for a relationship like that found by Mochida and Yoneda (1967). Careful scrutiny of the kinetic parameters regressed reveals a trend for the dealkylation of butyl tetralins. The dealkylation rate constants increase as the stability of the leaving alkyl carbenium ion increases. This is consistent with the energetics of the formation of the alkyl carbenium ions. This suggests that the formation of the alkyl carbenium ion could contribute to the controlling energetics of the process.

This information was tested more quantitatively using a linear free energy relationship for the butyl tetralin dealkylation reactions with the stability of the dealkylating carbenium ion as the reactivity index. Two options for the value of the reactivity index were available, reflecting the nature of the alkyl carbenium ion: the energetics of either the primary (n-alkyl) or the most stable alkyl carbenium ion could be used. The experimental data were not sufficiently precise to adjudicate.

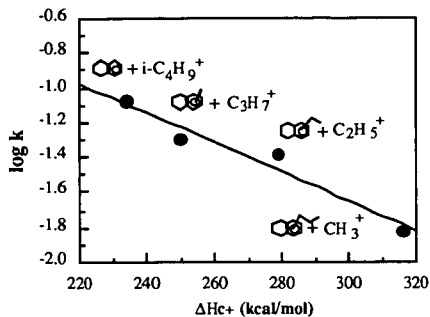


Fig. 5: LFER for the butyl tetralin dealkylation reactions. ( $k$  in  $\text{min.}^{-1}$ )

## CONCLUSIONS

1-methyl naphthalene hydrocracking resulted in isomerization to 2-methyl naphthalene, as well as hydrogenation to methyl tetralins. Hydrogenation of the single ring in methyl tetralin was one order of magnitude slower than hydrogenation of methyl naphthalenes, and comparable to the naphthenic ring opening reactions. Phenanthrene hydrocracking proceeded mainly through sequential hydrogenation to dihydro, tetrahydro and octahydro phenanthrene, followed by opening of the terminal naphthenic rings and dealkylation of the butyl side chains.

Reasonable structure/reactivity correlations were obtained for the rate parameters of the dealkylation of butyl tetralins produced from phenanthrene hydrocracking. The heat of formation of the leaving alkyl carbenium ion ( $\text{CH}_3^+ - \text{C}_5\text{H}_{11}^+$ ) as used from Mochida and Yoneda (1967) was established as a suitable reactivity index.

## ACKNOWLEDGEMENT

The authors acknowledge the financial support of Mobil Research and Development Corporation (Paulsboro Research Laboratory), and the State of Delaware, as authorized by the State Budget Act of Fiscal Year 1989.

## REFERENCES

- Bhore, N. A., Klein, M.T., and Bischoff, K.B. (1990). The Delplot Technique: A New Method for Reaction Pathway Analysis. *Ind. Eng. Chem.*, **29**(2), 313-316.
- Dunn, I.J. (1968). Linear Free Energy Relationships in Modeling Heterogeneous Catalytic Reactions. *J. Catal.*, **12**, 335-340.
- Froment, G.F. (1987). Kinetics of the Hydroisomerization and Hydrocracking of Paraffins on a Platinum Containing Bifunctional Y-Zeolite. *Catal. Today*, **1**, 455-473.

- Girgis, M.J., and Gates, B.C. (1991). Reactivities, Reaction Networks, and Kinetics in High-Pressure Catalytic Hydroprocessing. *Ind. Eng. Chem. Res.*, **30**(9), 2021-2058.
- Haynes, H.W.J., Parcher, J.F., and Helmer, N.E. (1983). Hydrocracking Polycyclic Hydrocarbons over a Dual-Functional Zeolite (Faujasite)-Based Catalyst. *Ind. Eng. Chem. Process Des. Dev.*, **22**, 401-409.
- Landau, R.N. (1991) Chemical Modeling of the Hydroprocessing of Heavy Oil Feedstocks. PhD Thesis, University of Delaware.
- Lapinas, A.T., Klein, M.T., Gates, B.C., Macris, A., and Lyons, J.E. (1987). Catalytic Hydrogenation and Hydrocracking of Fluoranthene: Reaction Pathways and Kinetics. *Ind. Eng. Chem. Res.*, **26**, 1026-1033.
- Lemberon, J.-L., and Guisnet, M. (1984). Phenanthrene Hydroconversion as a Potential Test Reaction for the Hydrogenating and Cracking Properties of Coal Hydroliquefaction Catalysts. *Appl. Catal.*, **13**, 181-192.
- Mochida, I., and Yoneda, Y. (1967). Linear Free Energy Relationships in Heterogeneous Catalysis I. Dealkylation of Alkylbenzenes on Cracking Catalysts. *J. Catal.*, **2**, 386-392.
- Olah, G.A., Baker, E.B., Evans, J.C., Tolgyesi, W.S., McIntyre, J.S., and Bastien, I.J. (1964). Stable Carbonium Ions. V. Alkylcarbonium Hexafluoroantimonates. *J. Am. Chem. Soc.*, **86**(1360-1372).
- Pines, H. (1981). The Chemistry of Catalytic Hydrocarbon Conversions. New York, N. Y.: Academic Press.
- Qader, S. A. (1973). Hydrocracking of Polynuclear Aromatic Hydrocarbons over Silica-Alumina Based Dual Functional Catalysts. *J. Inst. Pet.*, **59**, 178-187.
- Shabtai, J., Veluswami, L., and Oblad, A.G. (1978). Steric Effects in Phenanthrene and Pyrene Hydrogenation Catalyzed by Sulfided NiW/Al<sub>2</sub>O<sub>3</sub>. *Am. Chem. Soc., Div. Fuel Chem. Prepr.*, **23**(1), 107-112.

## ASPHALTENE AND RESID PYROLYSIS 2: THE EFFECT OF REACTION ENVIRONMENT ON PATHWAYS AND SELECTIVITIES.

Muzaffer Yasar, Daniel M. Trauth and M.T. Klein

Center for Catalytic Science and Technology  
Department of Chemical Engineering  
University of Delaware  
Newark, Delaware 19716.

### Keywords

Asphaltene, Kinetic, Pyrolysis.

### Abstract

Resids and isolated asphaltenes from four feedstocks were pyrolyzed at temperatures of 400, 425 and 450 °C for holding times ranging from 20 to 180 minutes in micro-batch reactors. Reaction products were recovered as gas, maltene, asphaltene and coke lumps. The maltene, asphaltene and coke product fractions were collected by a solvent extraction sequence where heptane-soluble material was defined as maltene, toluene-soluble material as asphaltene, and toluene-insoluble material as coke. Gas chromatography revealed the presence of C<sub>1</sub>-C<sub>5</sub> paraffins, C<sub>2</sub>-C<sub>5</sub> olefins, isoparaffins, H<sub>2</sub>S and CO<sub>2</sub>.

Results were summarized by a lumped reaction network which allowed for quantitative kinetics. Comparison of relative kinetics and apparent activation energies yielded insight into thermal reaction pathways, feedstock effects, and asphaltene environment effects. At 400°C and 425°C, isolated asphaltene reacted selectively to maltenes. At 450°C asphaltene reacted predominately to coke. Isolated maltene pyrolysis indicated that asphaltene and coke formed in series, i.e., M→A→C.

### Introduction

The increased usage of heavy petroleum feedstocks has focused attention on problems associated with the refining of heavy feedstocks, such as solids formation and catalyst deactivation. On a feedstock structural level, these problems are associated with high aromaticity, high molecular weight, and high heteroatom content<sup>1</sup>.

Asphaltene is the aromatic-soluble and paraffinic-insoluble fraction of crude oil. Understanding the effects of environment on asphaltene reaction pathways can provide insight into the processing problems of heavy crudes. Previous asphaltene and resid thermal pyrolysis studies<sup>2</sup> have yielded information on environmental and feedstock effects. The current work is an extension of that study. Arabian Heavy Resid (AHR) and Arabian Light Resid (ALR) were subject to pyrolysis in an isothermal sand bath at 400, 425, and 450°C for holding times between 20 and 180 minutes. The isolated maltene from ALR was also pyrolyzed at 425°C. Gaseous products were collected and analyzed by GC. A soxhlet sequence was used to separate maltene, asphaltene and coke. The time dependence of the product distributions was used to calculate lumped kinetic rate constants. Arrhenius parameters were calculated for each network step.

### **Experimental Methods**

#### **1) Samples**

Asphaltenes were precipitated from the resids at a weight ratio of 40/1, n-heptane to resid. The mixture was stirred for 1 hr at 60 °C, and then allowed to cool under continuous stirring for 4 hr. The solution was then allowed to settle overnight prior to filtering. Maltenes were collected by evaporating the n-heptane from the filtrate. The asphaltene was subject to soxhlet extraction to verify the absence of maltenes.

The samples were characterized by elemental analysis, simulated distillation, proton NMR, SARA (saturate, aromatic, resin, asphaltene) and molecular weight by VPO. Molecular weight experiments were carried out at 130°C in nitrobenzene. Molecular weights were extrapolated from measurements at three concentrations. The results are given in Table (I). VPO measurements showed that Maya isolated asphaltene and Arabian Heavy resid had the highest molecular weight in their respective classes. Elemental analysis indicated that heteroatoms were concentrated in the asphaltene fraction. Simulated distillation analysis revealed some variability in cut point for the resids.

## 2) Pyrolysis Reactions

Reactions were carried out in micro-batch reactors. Briefly, a glass tube containing the sample was loaded into the reactor. It was purged several times with high pressure nitrogen to minimize potential oxidation reactions then reacted in an isothermal sandbath. Reaction products were separated into gas, maltene, asphaltene and coke fractions. Gas products were collected and then analyzed by gas chromatography equipped with a thermal conductivity detector and a 6 ft propak Q column. Maltene, asphaltene and coke fractions were collected by a soxhlet extraction sequence. The yield of each fraction was calculated gravimetrically.

## Results and Discussions

### 1) Isolated asphaltenes

Figures (1a-c) show the kinetics of pyrolysis of isolated asphaltenes. The curves drawn through experimental data represent a first-order model fit. Asphaltene reactivities were as follows: AH~AL~H>M at 400 and 425°C. At 450°C asphaltene conversion was extremely rapid.

### 2) Asphaltene in resid

Figures (2a-c) depicts the time dependence of the ratio of the weight of asphaltene to initial weight of asphaltene in the resid. Clearly the reaction paths of asphaltene are influenced by the resid environment. The amount of AL asphaltene approximately doubled at 400°C. At 425 and 450°C the amount of AL asphaltene rapidly rose to 2-3 times its initial value. Further reaction returned the AL asphaltene amount to a value below this initial level. Asphaltene levels in the other three resids did not increase above the ordinate at any reaction temperatures. Reactivities were as follow: H>AH~M>AL

### 3) Maltene from isolated asphaltene

Figures (3a-c) summarize the temporal variation of the maltene weight fraction. At 400°C the yield of maltene was nearly the same for all feedstocks. H maltene yield

increased at all temperatures. H had highest maltene yield at 450 °C. M produced the most maltene at 425°C. AH and AL produced the greatest amounts at 400 and 425°C.

The maxima exhibited by all isolated asphaltenes at reaction temperatures of 425 and 450°C are indicative of secondary cracking and possible condensation reactions. The complex behavior is indicative of a chemically complex mixture.

#### 4) Maltene from resids

The temporal variations of the maltene weight fractions for AH, AL, H and M resids are shown in Figures (4a-c). As temperature increased the maltene disappearance rate increased for all resids. After 20 minutes, the disappearance rate of maltenes was similar for all feedstocks.

#### 5) Isolated maltenes and reaction pathways

Experimental results from isolated AL maltenes pyrolysis, as shown in figure (5), suggest that isolated maltenes produced asphaltene and then coke in series. These experiments revealed that the previously proposed pathways<sup>2</sup> could be simplified since coke was not formed directly from maltene. The network is shown in Figure (6).

#### Reaction Kinetics

Optimized rate constants for the network of Figure (6) were obtained as described elsewhere.<sup>3</sup> Briefly, a simplex minimization program<sup>4</sup> coupled to the DGEAR<sup>5</sup> routine minimized the error in the solution of a first-order differential equations developed from figure (6).

The predicted rate constants are shown in Table II. For both isolated asphaltenes and resid,  $k_4$ , the rate constant for the reaction of maltene to gas was negligible. The rate constant for the reactions of asphaltene to maltene and maltene to asphaltene,  $k_1$  and  $k_5$ , were highest for resids. The selectivities,  $k_1/k_5$ , were between 4.5 and 8.6 for four resids at all temperatures.

The activation energies calculated from network parameters for each reaction step are summarized in the table III both for resids and asphaltenes.

## **Conclusions**

- 1) AL, AH and H isolated asphaltenes reacted at the similar rates at 400 and 425°C; The M isolated asphaltene reacted more slowly. All of the isolated asphaltenes reacted at about the same rate at 450°C.
- 2) At 400 and 425°C, the isolated asphaltenes reacted selectively to maltene. At 450°C H isolated asphaltene formed more maltene than M, AL and AH.
- 3) H asphaltene reacted faster than M, AL and AH in the resid at all temperatures. AL asphaltene in the resid reacted most slowly.
- 4) Resids and isolated AL maltene pyrolysis showed that important amounts of asphaltene and coke could be formed by maltenes.

## **References**

- 1) Speight, J.G. 1990. Fuel Science and Technology Handbook. Marcel Dekkar, New york.
- 2) Trauth, D.M., M. Yasar, M. Nuerock, A. Nigam, M.T. Klein and S.G. Kukes. Asphaltne and Resid Pyrolysis: Effect of Reaction Environment. Accepted for publication in Fuel Science and Technology International 1991.
- 3) Nuerock, M., A. Nigam, D. Trauth, and M.T.Klein. 1990. Asphaltene Pyroysis Pathways and Kinetics: Feedstock Dependence. Preprints AIChE Meeting, San Diego, CA, August 1990 (submitted to AIChE symposium series).
- 4) Press, W.H., Flanner, S. A. Teukolsky, and W.T. Vetterling. 1986. Numerical Recipes. Cambridge University Press.
- 5) IMSL Inc. 1989. IMSL User's Manual, Volume 1, v1.1.

**TABLE I**

Chemical analysis of Hondo, Maya, Arabian Light, and Arabian resids and their isolated asphaltens by Elemental, VPO, Proton NMR, Simulated Distillation, ORA, a Soxhlet Extraction techniques (R=resid, A=asphaltene, - =not measured).

| Analysis                  | Hondo<br>(R) | Maya<br>(R) | A. Light<br>(R) | A. Heavy<br>(R) | Hondo<br>(A) | Maya<br>(A) | A. Light<br>(A) | A. Heavy<br>(A) |
|---------------------------|--------------|-------------|-----------------|-----------------|--------------|-------------|-----------------|-----------------|
| % Carbon                  | 81.15        | 85.66       | 84.41           | 83.80           | 80.35        | 83.08       | 82.13           | 82.00           |
| % Hydrogen                | 9.95         | 10.41       | 10.02           | 9.31            | 7.96         | 7.27        | 7.59            | 6.69            |
| % Nitrogen                | 1.01         | 0.465       | 0.15            | 0.44            | 1.87         | 1.09        | 0.75            | 0.93            |
| % Sulfur                  | 6.90         | 3.17        | 4.04            | 5.31            | 7.89         | 7.11        | 6.17            | 7.43            |
| % Oxygen                  | 1.02         | 0.50        | 0.008           | 0.020           | 0.110        | 0.170       | 0.036           | 0.074           |
| % Vanadium                | 0.017        | 0.005       | 0.002           | 0.007           | 0.040        | 0.032       | 0.010           | 0.022           |
| % Nickel                  | 0.010        | 0.005       | -               | -               | -            | -           | -               | -               |
| % Iron                    | 1.47         | 1.46        | 1.40            | 1.33            | 1.19         | 1.05        | 1.11            | 0.98            |
| H/C                       | 0.011        | 0.005       | 0.002           | 0.005           | 0.020        | 0.011       | 0.008           | 0.010           |
| N/C                       | 0.032        | 0.014       | 0.018           | 0.024           | 0.037        | 0.032       | 0.028           | 0.034           |
| S/C                       | 0.009        | 0.004       | 0.009           | 0.013           | 0.016        | 0.008       | 0.013           | 0.015           |
| O/C                       |              |             |                 |                 |              |             |                 |                 |
| MW by VPO                 | 862          | 944         | 1022            | 1535            | 2871         | 5292        | 1950            | 2119            |
| 1H NMR                    | -            | -           | -               | -               | 20.6         | 28.1        | 28.8            | 29.8            |
| % H (ME)                  | -            | -           | -               | -               | 57.6         | 60.9        | 44.9            | 46.7            |
| % H (N + MY)              | -            | -           | -               | -               | 10.6         | 5.8         | 12.2            | 14.8            |
| % H (alpha)               | -            | -           | -               | -               | 11.2         | 5.2         | 14.2            | 9.7             |
| % H (aromatic)            | -            | -           | -               | -               | -            | -           | -               | -               |
| Simulated<br>Distillation |              |             |                 |                 |              |             |                 |                 |
| %800-1000°F               | 12.5         | 19.0        | 10.1            | 9.8             | -            | -           | -               | -               |
| %1000°F+                  | 87.5         | 81.0        | 89.9            | 90.2            | -            | -           | -               | -               |
| ORA                       |              |             |                 |                 |              |             |                 |                 |
| %Oils                     | 31.7         | 12.3        | -               | -               | -            | -           | -               | -               |
| %Resins                   | 55.2         | 71.6        | -               | -               | -            | -           | -               | -               |
| %Asphaltens               | 12.5         | 15.1        | -               | -               | -            | -           | -               | -               |
| Soxhlet<br>Extracted      |              |             |                 |                 |              |             |                 |                 |
| %Maltens                  | 77           | 88          | 94              | 85              | -            | -           | -               | -               |
| %Asphaltens               | 23           | 12          | 6               | 15              | -            | -           | -               | -               |
| SARA                      |              |             |                 |                 |              |             |                 |                 |
| %Saturates                | 13           | 26          | 30              | 30              | -            | -           | -               | -               |
| %Aromatics                | 43           | 51          | 45              | 44              | -            | -           | -               | -               |
| %Resins                   | 21           | 11          | 19              | 16              | -            | -           | -               | -               |
| %Asphaltens               | 23           | 12          | 6               | 2               | -            | -           | -               | -               |

**Table II**

Network Kinetics of the Pyrolysis of Hondo and Maya Resids and their Isolated Asphaltene  
(First order units are 1/(hr\*wt%))

| Rate Parameters. | Hondo Resid | Maya Resid | Arabian Light Resid | Arabian Heavy Resid | Hondo Asphaltene | Maya Asphaltene | Arabian Light Asphaltene | Arabian Heavy Asphaltene |
|------------------|-------------|------------|---------------------|---------------------|------------------|-----------------|--------------------------|--------------------------|
| <b>400°C</b>     |             |            |                     |                     |                  |                 |                          |                          |
| k1               | 123.62      | 54.018     | 2.5800              | 13.351              | 0.9369           | 0.6465          | 0.7330                   | 48.943                   |
| k2               | 0.3433      | 0.2689     | 0.1680              | 0.3369              | 3.2014           | 1.5201          | 3.0133                   | 2.9273                   |
| k3               | 0.2559      | 0.1699     | 0.1390              | 0.1313              | 0.4196           | 0.1503          | 0.3022                   | 0.3012                   |
| k4               | 0.0025      | 0.0003     | 0.0001              | 0.0003              | 0.0048           | 0.0038          | 0.0000                   | 0.0003                   |
| k5               | 20.044      | 8.1600     | 0.3860              | 2.8021              | 0.5875           | 0.6825          | 0.2540                   | 81.565                   |
| <b>425°C</b>     |             |            |                     |                     |                  |                 |                          |                          |
| k1               | 293.14      | 115.08     | 12.757              | 33.350              | 2.5700           | 1.5813          | 0.9720                   | 114.81                   |
| k2               | 1.4586      | 0.8568     | 1.1251              | 0.8183              | 3.3700           | 2.6710          | 4.3890                   | 6.4369                   |
| k3               | 0.0006      | 0.3545     | 0.3565              | 0.3300              | 0.5290           | 0.0010          | 0.5077                   | 0.7720                   |
| k4               | 0.0765      | 0.0003     | 0.0003              | 0.0005              | 0.0200           | 0.4889          | 0.0000                   | 0.0007                   |
| k5               | 33.910      | 14.400     | 2.2291              | 7.3300              | 1.1400           | 0.6977          | 0.5592                   | 163.81                   |
| <b>450°C</b>     |             |            |                     |                     |                  |                 |                          |                          |
| k1               | 572.53      | 348.60     | 34.121              | 79.350              | 3.0725           | 59.438          | 4.3110                   | 368.58                   |
| k2               | 1.7511      | 1.4741     | 1.9663              | 1.9153              | 4.2704           | 203.45          | 7.3411                   | 13.687                   |
| k3               | 1.1886      | 0.7349     | 1.3054              | 0.9250              | 1.1481           | 0.0039          | 1.5570                   | 2.2512                   |
| k4               | 0.0007      | 0.0008     | 0.0007              | 0.0009              | 0.0018           | 0.9305          | 0.0910                   | 0.0021                   |
| k5               | 97.398      | 59.571     | 4.8265              | 16.380              | 0.3793           | 0.4078          | 9.1011                   | 280.02                   |

**Table III**

Arrhenius parameters for resids and asphaltenes, (Ea (kcal/mol), \* = not calculated).

| Parameters                 | k1    | k2    | k3    | k4    | k5                              | k1    | k2    | k3    | k4    | k5    |
|----------------------------|-------|-------|-------|-------|---------------------------------|-------|-------|-------|-------|-------|
| <b>Hondo Resid</b>         |       |       |       |       | <b>Hondo Asphaltene</b>         |       |       |       |       |       |
| Ea                         | 29.69 | 31.81 | *     | *     | 30.45                           | 23.16 | 5.53  | 19.33 | *     | *     |
| log A                      | 11.74 | 9.94  | *     | *     | 11.48                           | 7.54  | 2.28  | 5.86  | *     | *     |
| <b>Maya Resid</b>          |       |       |       |       | <b>Maya Asphaltene</b>          |       |       |       |       |       |
| Ea                         | 35.98 | 33.04 | 28.32 | 18.80 | 38.24                           | 86.79 | 93.82 | *     | 106   | *     |
| log A                      | 13.38 | 10.19 | 8.42  | 2.53  | 13.26                           | 27.79 | 30.36 | *     | 32.53 | *     |
| <b>Arabian Light Resid</b> |       |       |       |       | <b>Arabian Light Asphaltene</b> |       |       |       |       |       |
| Ea                         | 50.07 | 47.88 | 43.22 | 42.05 | 49.07                           | 33.98 | 17.19 | 31.58 | *     | 68.74 |
| Log A                      | 16.71 | 14.87 | 13.15 | 9.58  | 15.58                           | 10.81 | 6.05  | 9.68  | *     | 2.16  |
| <b>Arabian Heavy Resid</b> |       |       |       |       | <b>Arabian Heavy Asphaltene</b> |       |       |       |       |       |
| Ea                         | 34.47 | 33.61 | 37.72 | 21.22 | 34.18                           | 38.97 | 34.57 | 38.87 | 38.23 | 23.89 |
| Log A                      | 12.32 | 10.44 | 11.36 | 3.36  | 11.55                           | 14.31 | 11.60 | 12.08 | 8.86  | 9.68  |

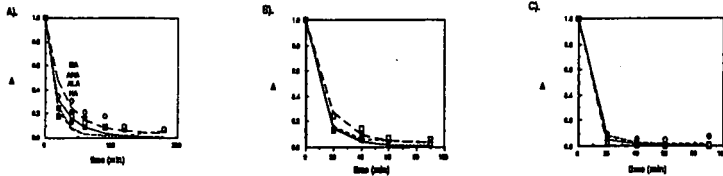


Figure 1. Temporal variation of isolated asphaltene: A) 400°C, B) 425°C, C) 450°C

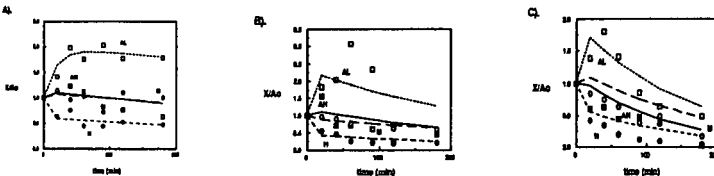


Figure 2. Temporal variation of asphaltene yield in a ratio of asphaltene weight to initial asphaltene weight for resids: A) 400°C, B) 425°C, C) 450°C

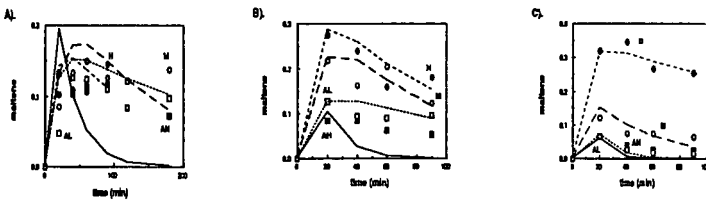


Figure 3. Temporal variation of maltene weight fraction for asphaltenes. A) 400°C, B) 425°C, C) 450°C.

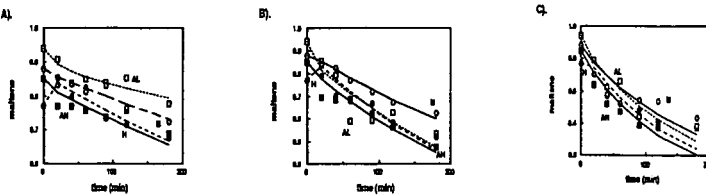


Figure 4. Temporal variation of maltene weight fraction for resids. A) 400°C, B) 425°C, C) 450°C.

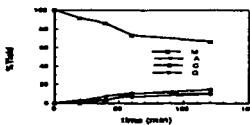


Figure 5. Isolated maltene pyrolysis at 425°C.

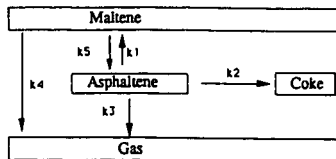


Figure 6. Lumped resid/ asphaltene model

## PERFORMANCE OF HYBRID CATALYST SYSTEM IN TWO-STAGE COAL LIQUEFACTION

J. M. Lee, P. Vimalchand, O. L. Davies, and C. E. Cantrell  
Southern Electric International, Inc.  
P. O. Box 1069, Wilsonville, Alabama 35186

Keywords: two-stage liquefaction, catalyst, distillate

### INTRODUCTION

The Clean Coal Research Center at Wilsonville has developed alternate technologies for producing low cost fuels from coal. Process developments of close-coupled integrated (CC-ITSL) configurations using the thermal/catalytic or catalytic/catalytic mode of operation were discussed in earlier articles<sup>1,2</sup>.

This paper is primarily focused on the low-rank Black Thunder subbituminous coal performance at steady-state operation with catalyst replacement in the thermal/catalytic mode. Process development results from four runs are discussed: Runs 258, 260, 262 and 263. Three different operation modes with supported, dispersed slurry and hybrid catalyst systems were tested. Runs 258 and 260 studied the supported catalyst system using Shell (or Criterion) 324 catalyst in the second stage without addition of a dispersed catalyst. Runs 262 and 263 (second part) tested the hybrid system using a dispersed molybdenum (Molyvan L or 822 precursor) and Criterion 324 supported catalyst in the second stage. Run 263 (first part) tested the dispersed slurry catalyst system using Molyvan L and 822 as precursors. Half-volume reactors were used for Runs 258, 262 and 263; a combination of full- and 3/4-volume reactors was used for Run 260. Iron-oxide (+ dimethyl disulfide) addition was 1-2 wt % MF coal.

The primary objective of this study was to maximize the distillate production with good quality in order to improve the process economics. High distillate yield and coal throughput increase the distillate production. The distillate production can be enhanced by improving coal reactivity, catalyst conversion activity, and distillate selectivity. The performance of a dispersed molybdenum catalyst was evaluated processing a low-rank coal. Solids buildup in reactor transfer lines and interstage separator was investigated for possible reduction or elimination by using a dispersed molybdenum catalyst. The dispersed molybdenum catalyst may give acceptable conversions at moderate reaction temperatures and reduce the coking reactions, that cause solids to deposit in the transfer lines, by hydrogenating thermally produced free radicals and possibly through the prevention of retrogressive reactions<sup>3</sup>. Dispersed molybdenum catalysts using Molyvan L and Mo octoate as precursors were tested in bench-scale two-stage liquefaction with Illinois No. 6 coal using Amocat 1C bimodal supported catalyst by Amoco Oil Company<sup>4</sup>, and UOP<sup>5</sup> and Dow Chemical Company<sup>6</sup> studied dispersed catalysts in bench-scale single stage. Several investigators have studied with dispersed molybdenum and iron catalysts to improve liquefaction conversion and their results can be found in the literature<sup>7-15</sup>. Typical analyses of Black Thunder coal processed for this study are summarized in Table 1. Properties of Shell (or Criterion) Ni-Mo catalyst and dispersed molybdenum precursors tested are shown in Table 2.

## PROCESS DESCRIPTION

The current catalytic close-coupled integrated two-stage liquefaction (CC-ITSL) process consists of two H-OIL<sup>®</sup> ebullated-bed reactors and a Residuum Oil Supercritical Extraction-Solids Rejection (ROSE-SR<sup>SM</sup>) unit<sup>14</sup>. Both the reactor designs utilize "H-OIL<sup>®</sup>" technology supplied by Hydrocarbon Research, Inc. The ebullated-bed design helps to maintain a uniform temperature distribution in the reactor. The reactor is used as a thermal reactor in the thermal mode of operation without a supported catalyst. The ROSE-SR<sup>SM</sup> is a proprietary extraction process at conditions close to the critical point of the deashing solvent. It was developed and licensed by the Kerr-McGee Corporation.

## RUN EXPERIMENTS

Key process variables studied in Runs 258, 260, 262 and 263 are listed below to maximize the distillate production by increasing distillate yield and coal throughput processing Black Thunder subbituminous coal.

- (1) Catalyst activity
  - Shell (or Criterion) 324 unimodal supported
  - dispersed molybdenum (Molyvan L/822 precursors)
  - iron-oxide + DMDS (dimethyl disulfide)
- (2) Steady-state operation with catalyst replacement
  - 1.5 to 3 lb/ton MF coal in catalytic stage
- (3) Molybdenum addition concentration (100-1000ppm MF coal)
- (4) Iron-oxide addition concentration (1-2 wt % MF coal)
- (5) Recycle resid concentration
  - 35-45 wt % in the process solvent
- (6) High/low thermal severity mode
- (7) Heavy vacuum gas oil recycle
- (8) Coal space velocity
  - 45-110 lb MF coal/hr/ft<sup>3</sup>-catalyst in catalytic
  - 30-90 (x1/C) lb MF coal/hr/ft<sup>3</sup>-reactor in thermal
  - (C: constant equating thermal to catalytic reaction volume in the thermal/catalytic mode)
- (9) Reaction temperature
  - 760-860/760-810°F in the first/second stage
- (10) Inlet hydrogen partial pressure
  - 2450-2850 psia in the first stage
  - 2400-2550 psia in the second stage
- (11) Slurry composition (25-30 wt % coal, 20 wt % CI)
- (12) Interstage separation
- (13) Reactor operation parameters
  - temperature profiles, exotherms
  - ebullation rate, gas flow, slurry flow
  - slurry viscosity, etc.

Several steady-state operation periods in Runs 258, 262 and 263 with half-volume reactors in operation were selected for comparison of distillate production in three different operation modes with the supported, dispersed slurry and hybrid catalyst systems. Experimental results with Black Thunder subbituminous coal are summarized in the following along with the theoretical distillate production projected for the "all-distillate" product slate with resid extinction using a CSTR first order kinetic model<sup>15</sup>. Illinois No. 6 bituminous coal result from Run 257J using Amocat 1C in the catalytic/catalytic mode is also included for comparison.

| run               | catalyst  | temper. cat. rep. |                   | recycle resid (wt %) | dist.prod. (lb/hr) |                   |
|-------------------|---|-------------------|-------------------|----------------------|--------------------|-------------------|
|                   |   | 1st/2nd (°F)      | 1st/2nd (lb/t MF) |                      | exp.               | the. <sup>a</sup> |
| (1)               | w/ supported catalyst in the second stage                 |                   |                   |                      |                    |                   |
| 258H              | Shell 324   | 840/790           | -/1.5             | 40                   | 127                | 126               |
| 258I              | Shell 324   | 850/790           | -/1.5             | 40                   | 132                | 126               |
| (2)               | w/ dispersed molybdenum slurry catalyst                   |                   |                   |                      |                    |                   |
| 262F <sup>b</sup> | Molyvan L   | 825/810           | 200 <sup>c</sup>  | 40                   | 152                | 137               |
| 263E              | Molyvan L   | 840/810           | 100 <sup>c</sup>  | 40                   | 147                | 150               |
| 263H              | Molyvan 822   | 840/810           | 100 <sup>c</sup>  | 45                   | 150                | 158               |
| (3)               | w/ hybrid catalyst with dispersed and supported catalysts |                   |                   |                      |                    |                   |
| 262E              | <sup>d</sup>  | 825/810           | -/3 <sup>e</sup>  | 40                   | 185                | 181               |
| 263I              | <sup>d</sup>  | 840/810           | -/3 <sup>e</sup>  | 45                   | 195                | 207               |
| 263J              | <sup>d</sup>  | 840/810           | -/3 <sup>e</sup>  | 40                   | 188                | 197               |
| (4)               | w/ Illinois coal in catalytic/catalytic mode              |                   |                   |                      |                    |                   |
| 257J              | Amocat 1C   | 810/760           | 3/1.5             | 50                   | 137                | 133               |

<sup>a</sup> Using CSTR 1st order kinetic model for resid extinction<sup>15</sup>.

<sup>b</sup> Some Criterion catalyst was left in the second reactor.

<sup>c</sup> Unit: ppm based on MF coal.

<sup>d</sup> With a combination of Molyvan L and Criterion 324.

<sup>e</sup> Molyvan L addition at 100 ppm based on MF coal.

## RESULTS AND DISCUSSION

### DISTILLATE PRODUCTION COMPARISON

#### Supported, Dispersed Slurry and Hybrid Catalyst Systems

The hybrid system (Runs 262E and 263IJ) with a combination of dispersed molybdenum and Criterion supported catalysts showed the highest distillate production, 185-195 lb/hr, among three catalyst systems tested. Corresponding coal space velocities for these runs were 59-62 MF lb/hr-ft<sup>3</sup>-catalyst in 2nd stage or 24-26 (xl/C) MF lb/hr-ft<sup>3</sup>-reactors in CCR unit. The distillate production of the hybrid system was 30% higher than that of the dispersed molybdenum slurry catalyst system (147-152 lb/hr in Runs 262F and 263EH at 20 (xl/C) coal space velocity); 50-60% higher than that of the Criterion supported catalyst system (127-132 lb/hr in Run 258H1 at 17 (xl/C) coal space velocity).

The hybrid system with Black Thunder subbituminous coal in the thermal/catalytic mode of operation produced 40-55% higher distillate than the Amocat 1C supported catalyst system with Illinois No. 6 bituminous coal in the catalytic/catalytic mode of operation (Run 257J at 18 (xl/C) coal space velocity). This result suggests that Black Thunder subbituminous coal can produce more distillate than Illinois No. 6 bituminous coal, if process operating conditions are optimized for better coal and resid conversions, even though subbituminous coal has lower distillate yield and selectivity. It seems that due to the addition of the dispersed molybdenum to the supported catalyst system, the hybrid system enhances the distillate production by improving coal and resid conversions, employing higher thermal severity compared to Run 257J with Illinois coal and Amocat 1C catalyst. However, as reported in the previous Run 261 with Illinois bituminous coal using a new bimodal supported catalyst (EXP-AO-60)<sup>15</sup> in the catalytic/catalytic mode with full-volume reactors in operation, the

low/high severity operation significantly improved the distillate production by approximately 40-50%, employing higher thermal severity, increased recycle resid concentration and higher catalyst replacement. Further studies are required for better comparison with bituminous coals using half-volume reactors in operation.

#### Distillate Product Yield and Selectivity

The addition of a dispersed molybdenum allowed operation at lower thermal severity in the first stage, while the second stage operated at higher thermal severity compared to the supported catalyst system, resulting in higher C4+ distillate product yield and selectivity to resid + UC conversion as summarized below. The potential C4+ distillate yield is estimated by adjusting the resid yield for the "all-distillate" product slate with resid extinction by using an achievable common organic rejection (OR) and distillate selectivity measured in each run.

| run   | catalyst system | distillate yield, wt % MAF coal experimental | theoretical (OR) | distillate selectivity, % |
|-------|-----------------|--|------------------|---------------------------|
| 258HI | supported       | 55-58  | 60 (14)          | 64-68                     |
| 263EH | slurry          | 61   | 62-63 (14)       | 72-73                     |
| 263IJ | hybrid          | 58-61  | 61-62 (13-14)    | 71-72                     |

#### EFFECT OF MOLYBDENUM CONCENTRATION

Varying the molybdenum concentration from 100 to 1000 ppm (based on MF coal) seemed not to affect the resid + UC conversion, but increasing the molybdenum concentration slightly improved coal conversion. Good performance was observed at a low 100 ppm concentration in both slurry and hybrid catalyst systems. Distillate properties were generally the same within the range of molybdenum concentration studied.

The addition of Molyvan L or 822 as a dispersed molybdenum seemed to improve the overall two-stage resid and coal conversions allowing lower temperature and higher space velocity operation. In the hybrid system, with a combination of dispersed and supported catalysts, the resid + UC conversion was 5-10 wt % MAF coal higher and the coal conversion was 3-5 wt % higher than using the catalysts separately, when compared at the same thermal reaction severity operation. The use of just dispersed slurry catalyst (Molyvan L or 822) or Criterion supported catalyst gave similar overall two-stage coal and resid + UC conversions, and conversions improved by the combination of Criterion and Molyvan L or 822 catalysts.

#### COAL CONVERSION AND ORGANIC REJECTION

Figure 1 illustrates the effect of coal conversion on organic rejection. A good linear correlation was observed with low-rank coals and are summarized as follows.

$$Y = 173.3 - 1.69 X; r^2 = 0.84$$

where Y is the organic rejection (wt % MAF coal), X is the coal conversion (wt % MAF coal), and  $r^2$  is the determination coefficient. The X-intercept in Figure 1 indicates that a deeply cleaned coal could achieve a low organic rejection (4 wt % MAF coal), if extrapolated to 100 wt % coal conversion. A similar observation with bituminous coals was reported in the previous work<sup>2,15</sup>.

## CATALYST AND THERMAL ACTIVITIES IN RESID + UC CONVERSION

Supported catalyst and thermal activities were calculated assuming that the resid + UC conversion reaction follows first-order kinetics for a continuous stirred tank reactor<sup>2</sup>. Cracking activity (resid conversion) is not the only function of the catalyst. Hydrogenation activity of the catalyst was not considered in these catalyst activity analyses. Catalyst activity analysis is based on the overall activity of combined catalytic and thermal conversions in the catalytic stage.

The Arrhenius plot for temperature dependence (Figure 2) compares first stage thermal conversion activities in Runs 258, 260, 262 and 263 processing Black Thunder subbituminous coal operating in three different modes with supported, dispersed slurry and hybrid catalyst systems. The hybrid system with a combination of Molyvan L or 822 and Criterion 324 catalysts showed the highest thermal conversion activity, compared to the dispersed slurry and supported catalyst systems. The presence of Criterion supported catalyst in the second stage improved the resid + UC conversion in the first stage, due to improved hydrogenation by the supported catalyst in the second stage, producing better recycle process solvent and resulting in better thermal conversion in the first stage. It appears that the dispersed molybdenum catalyzes thermal hydrogenation of coal- and resid-derived free radicals<sup>3</sup> through stabilization by hydrogen transfer from the process solvent, resulting in higher thermal conversion in the hybrid system. The dispersed catalyst system had a higher thermal conversion activity than the supported catalyst system. Apparent activation energies (30000-31000 Btu/lb-mole) for the hybrid and dispersed slurry systems were lower than that (53000-64000 Btu/lb-mole) for the supported catalyst system, although their conversion activity levels were higher than the supported system.

Figure 3 compares second stage conversion activities for Runs 262 and 263. The catalytic resid + UC conversion activity of the hybrid system with a combination of Molyvan L or 822 and Criterion 324 was much higher than the thermal conversion activity of the dispersed slurry catalyst system using Molyvan L or 822 alone. The calculated average rate constant values were 45-115% higher than those obtained without Criterion catalyst. The hybrid system catalytic activity was obtained with 3 lb/ton MF coal catalyst replacement. It seems that the dispersed molybdenum may not be greatly involved in hydrogenation and hydrocracking of the process solvent compared to the supported catalyst, since operations with the dispersed slurry catalyst gave significantly lower hydrogen and higher heteroatoms contents of distillate and process streams. It is possible that nickel or support material of the supported catalyst, which are missing components of the dispersed molybdenum, may play a significant role in hydrogenation and hydrocracking. Apparent activation energy for the hybrid catalyst system was 48000 Btu/lb-mole, higher than that with the supported catalyst (30000-40000 Btu/lb-mole). This high value might have been affected by molybdenum concentration variation in the range of 100-1000 ppm MF coal.

## SOLIDS BUILDUP IN PROCESS LINES AND INTERSTAGE SEPARATOR

Problems associated with the formation of deposits in both the process lines and interstage separator between two reactors were discussed in the previous work processing subbituminous coals<sup>16</sup>, and two different solids deposition mechanisms suggested by Davis et al. were coking and mineral

deposition<sup>17</sup>. In recent Runs 262 and 263, the addition of Molyvan L or 822 as a dispersed slurry catalyst prevented reactor line plugging. However, solids did deposit in the interstage separator. A different interstage separator design could resolve the deposit problem.

#### DISTILLATE PRODUCT QUALITY

Table 3 summarizes distillate product qualities from Runs 258HI, 262E, 263EHJ, 257I and 261BD. During Run 259 with Pittsburgh coal and Shell 324, which was the first run tested with a better distillation separation system, the boiling end point of the distillate product was reduced to 715-760°F<sup>2</sup>. In Run 261BD with Illinois coal and EXP-AO-60 bimodal catalyst, the end point was 772-780°F. Runs 257I and 258HI end point data were estimated by assuming steady recycle of heavy distillate as in Runs 259 and 261.

The major observation from Runs 262 and 263 in Table 3 was that operations in the hybrid system with a combination of Molyvan L or 822 and Criterion catalysts produced better quality distillate than just using dispersed slurry catalyst (periods 262E and 263J vs. 263EH). Hydrogen content increased to 11.0-11.4 wt %, while heteroatoms decreased to 0.6 wt % nitrogen and 1.7-2.1 wt % oxygen, respectively. The end point of the distillate product was similar for both catalyst systems (717-755°F). Note that the supported catalyst only system (258HI) had similar distillate product quality as the hybrid system. The presence of Criterion supported catalyst in the second stage seems to improve the product quality in both the hybrid and supported catalyst systems by increasing hydrogenation and heteroatoms removal.

#### CONCLUSIONS

- Processing Black Thunder subbituminous coal, the hybrid system with a combination of dispersed molybdenum slurry and supported catalysts improved the distillate production by 30-60% compared to using the dispersed slurry and supported catalysts separately.
- The addition of Molyvan L or 822 at a low 100 ppm MF coal as a dispersed molybdenum catalyst precursor significantly improved coal and resid conversions, allowing operation at lower thermal severity in the first stage and higher severity in the second stage compared to the supported catalyst system, resulting in higher C<sub>4</sub>+ distillate product yield and selectivity to resid + UC conversion.
- Operations in the hybrid system with a combination of Molyvan L or 822 and Criterion catalysts produced better quality distillate than just using dispersed slurry catalyst only. The boiling end point of the distillate product was similar for both catalyst systems (717-755°F).
- The supported catalyst only system had similar distillate product quality as the hybrid catalyst system. It seemed that the presence of Criterion supported catalyst in the second stage improved the product quality in both the hybrid and supported catalyst systems by increasing hydrogenation and heteroatoms removal.
- The dispersed molybdenum seemed to catalyze thermal hydrogenation of coal- or resid-derived free radicals through stabilization by hydrogen transfer from the process solvent, resulting in higher thermal conversion in the hybrid catalyst system, while seemed to have a less role in hydrogenation and hydrocracking of the process solvent compared to the supported catalyst.

- The addition of Molyvan L or 822 as a dispersed molybdenum catalyst precursor improved process operability by preventing reactor line plugging.
- Black Thunder subbituminous coal produced more distillate than Illinois No. 6 bituminous coal, when process operating conditions were optimized for better coal and resid conversions, even though the subbituminous coal had lower distillate yield and selectivity.

#### ACKNOWLEDGMENTS

This work was supported by the U. S. Department of Energy under Contract DE-AC22-82PC50041, and the Electric Power Research Institute under Contract RP1234-1-2, and was managed by the Southern Company Services, Inc. Dr. Ed Klunder is DOE project manager and Mr. Bill Weber is EPRI project manager. The authors appreciate the contributions made by the technical department staff (M. Sherbert, F. Morton, M. Corser and S. Gollakota). The authors also acknowledge J. Howard, T. Pinkston, G. Styles, N. Stewart, D. Cronauer, A. Basu, R. Lumpkin, G. Robbins, H. Schindler and E. Moroni for their supports.

#### REFERENCES

1. R. V. Nalitham, J. M. Lee, C. W. Lamb, and T. W. Johnson. Fuel Processing Technology, Vol. 17, 1987, pp. 13-27.
2. J. M. Lee and C. E. Cantrell. Fuel Processing Technology, Vol. 29, 1991, pp. 171-197.
3. B. Bockrath, E. Illig, and M. Keller. ACS Div. Fuel Chem., Prep., 37(1), 133 (1992).
4. A. Swanson. ACS Div. Fuel Chem., Prep., 37(1), 149 (1992).
5. J. Gatsis, R. Roemisch, M. Miller, C. Piasecki, and H. Fullerton. ACS Div. Fuel Chem., Prep., 37(1), 160 (1992).
6. N. Moll and G. Quarderer. Chemical Engineering Progress, 75(11), 1979.
7. A. Cugini, D. Krastman, and R. Hickey. Proceedings of the Eighth Annual International Pittsburgh Coal Conf., Pitts., PA, Oct., 1991.
8. A. Cugini, B. Utz, D. Krastman, R. Hickey, and V. Balsone. ACS Div. Fuel Chem., Prep., 36(1), 91 (1991).
9. A. Hirschon and R. Wilson. ACS Div. Fuel Chem., Prep., 36(1), 103 (1991).
10. F. Derbyshire and T. Hager. ACS Div. Fuel Chem., Prep., 37(1), 312 (1992).
11. D. Sommerfeld, J. Jaturapitpornsakul, L. Anderson, and E. Eyring. ACS Div. Fuel Chem., Prep., 37(2), 749 (1992).
12. C. Burgess, L. Artok, and H. Schobert. ACS Div. Fuel Chem., Prep., 37(1), 200 (1992).
13. C. Curtis and H. Kim. ACS Div. Fuel Chem., Prep., 35(4), 1064 (1990).
14. Catalytic, Inc., Topical Report. DOE Cont. No. DE-AC22-82PC50041, EPRI Cont. No. RP1234-1-2, Doc. No. DOE/PC/50041-82.
15. J. Lee, C. Cantrell, S. Gollakota, O. Davies, M. Corser, and P. Vimalchand. Proceedings of the Sixteenth Annual EPRI Conference on Fuel Science, June 1991.
16. J. M. Lee, S.V. Gollakota, and O.L. Davies. Proceedings of the Fifteenth Annual EPRI Conference on Fuel Science, June 1990.
17. A. Davis, H. Schobert, G. Mitchell, and L. Artok. DOE Technical Progress Reports, No. DOE-PC-89877-3 and -7 (1990 and 1991).

TABLE 1. FEED COAL ANALYSIS  
(BLACK THUNDER MINE - WYODAK ANDERSON SEAM)

FC: 49% mf, HV: 11800 Btu/lb mf, Reactives: 92 mmf vol%  
Ultimate: 69.5% C, 5.1% H, 1.0% N, 0.6% S, 7.3% Ash, 16.5% O

TABLE 2. CATALYST PROPERTIES

Shell (or Criterion) 324 unimodal supported catalyst  
1/16" size, 2.7% Ni, 13.2% Mo  
SA: 165 m<sup>2</sup>/g, PV: 0.48 cc/g, CBD: 54 lb/ft<sup>3</sup>  
Dispersed molybdenum slurry catalyst  
Molyvan L: 8.1% Mo, 12.3% S, 6.4% P, no N  
Molyvan 822: 4.9% 6.0% no yes

TABLE 3. TOTAL DISTILLATE PRODUCT QUALITY COMPARISON

| Run Coal             | 258H                    | 258I | 262E | 263E | 263H | 263J | 257I              | 261B | 261D |
|----------------------|-------------------------|------|------|------|------|------|-------------------|------|------|
|                      | -----Black Thunder----- |      |      |      |      |      | -----Illinois---- |      |      |
| Wt % C               | 86.1                    | 86.0 | 86.3 | 85.8 | 85.1 | 86.3 | 87.4              | 87.3 | 87.5 |
| H                    | 11.2                    | 11.3 | 11.4 | 10.1 | 10.4 | 11.0 | 12.1              | 11.4 | 11.3 |
| N                    | 0.5                     | 0.5  | 0.6  | 0.9  | 0.9  | 0.6  | 0.1               | 0.2  | 0.3  |
| S                    | 0.06                    | 0.06 | 0.05 | 0.02 | 0.05 | 0.04 | 0.01              | 0.04 | 0.03 |
| O (dir.)             | 2.2                     | 2.2  | 1.7  | 3.9  | 3.6  | 2.1  | 0.4               | 1.1  | 0.9  |
| °API                 | 18                      | 18   | 24   | 15   | 18   | 22   | 21                | 23   | 22   |
| Wt % Naptha          | 21                      | 21   | 20   | 10   | 12   | 16   | 18                | 19   | 14   |
| Mid.D1               | 15                      | 15   | 10   | 14   | 17   | 14   | 11                | 11   | 16   |
| Mid.D2               | 59                      | 62   | 44   | 38   | 40   | 40   | 64                | 40   | 40   |
| Gas Oil              | 5                       | 2    | 26   | 38   | 31   | 30   | 7                 | 30   | 30   |
| End point °F (D1160) | 667                     | 665  | 748  | 755  | 719  | 717  | 665               | 772  | 780  |
|                      | (estimated)             |      |      |      |      |      | (est.)            |      |      |

FIGURE 1 ORGANIC REJECTION VS COAL CONVERSION  
Low-Rank Coal Correlation in CC-ITSL Process

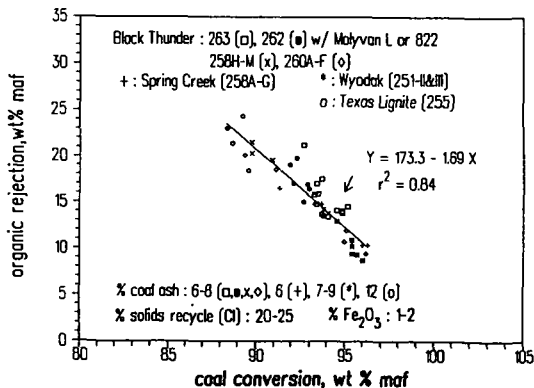


FIGURE 2

**1ST STAGE THERMAL ACTIVITY COMPARISON**  
**(Black Thunder Subbituminous Coal)**  
 Arrhenius Plot (CSTR 1st Order Resid+UC Conversion)

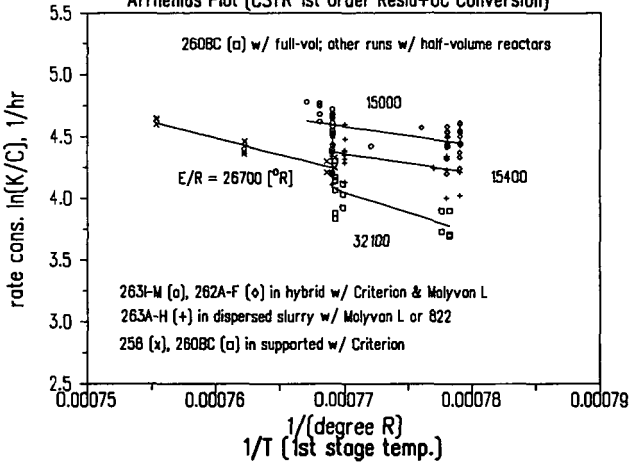
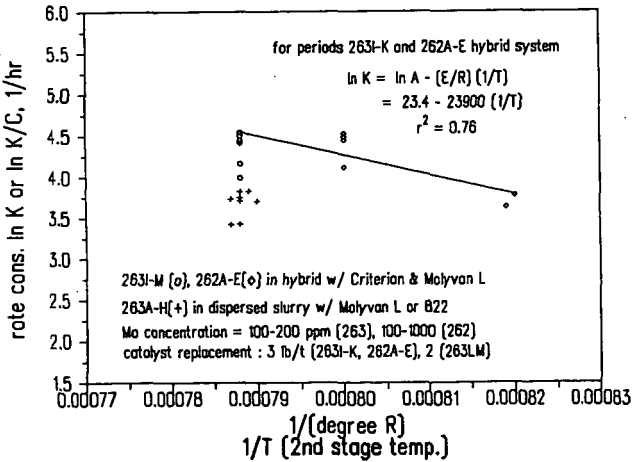


FIGURE 3

**2ND STAGE CONVERSION ANALYSIS (RUNS 263,262)**  
 Catalytic (Hybrid) vs. Thermal (Dispersed Slurry)



## CHLORIDATION AND ACTIVITY OF Pt/Al<sub>2</sub>O<sub>3</sub> CATALYSTS

Robert A. Keogh, Dennis E. Sparks, Gerald A. Thomas, and  
Burtron H. Davis

Center for Applied Energy Research  
University of Kentucky  
3572 Iron Works Pike  
Lexington, KY 40511

**Keywords:** chloridation, Pt/Al<sub>2</sub>O<sub>3</sub>, Isomerization

### INTRODUCTION

Current advanced coal liquefaction processes produce a naphtha that contains a high fraction of naphthenes. This will likely remain true for any improved process at lower temperatures. Conversion of this naphtha to gasoline by today's reforming processes will lead to a gasoline with a very high percentage of aromatics. Environmental considerations require that the aromatic and olefinic content of gasolines be drastically reduced. Petroleum refiners are making an intense effort to produce a gasoline containing more alkanes; for the short term alkylate will be utilized to accomplish this.

The high naphthene content of naphtha from coal liquefaction means that it would not be a suitable transportation fuel for the future. Tomorrow's clean gasoline will be low in heteroatoms and will contain mainly isoparaffins instead of aromatic and naphthenic hydrocarbons. Thus, if coal liquefaction is to advance from an emerging technology to a viable commercial process, a means must be found to reform the naphtha to a clean gasoline that will find acceptance in the market place.

Currently naphtha reforming is conducted at high temperatures and produces a high concentration of aromatics. The objective of this study is to reverse this trend in reforming by operating at low temperatures where thermodynamics favors a high concentration of isoparaffins.

An approach taken was to effect isomerization using an active catalyst (e.g., 1-3). Although a wide range of catalysts were investigated, much effort was centered on a heavily chlorided Pt-alumina catalyst. For example, Pt on a special silica-alumina could only operate at 350°C, and heavily chlorided Pt-alumina catalysts have been used for isomerization of alkanes at higher temperatures (350°C or greater). However, for naphtha reforming to produce alkanes it is desirable to operate at lower temperatures to be able to obtain a high octane product. It is likely that the chlorided Pt-alumina catalyst will have sufficient activity to produce a high fraction of the isoparaffins; however, the question concerning the ability of the catalyst to operate effectively in the presence of a high concentration of naphthenes (such as found in a coal-derived naphtha) requires further study. An objective of this paper was to develop a method to obtain a heavily chlorided Pt-alumina catalyst and to determine the activity and selectivity of these catalysts in reforming coal-derived naphtha and model compounds.

### EXPERIMENTAL

Two aluminas, one a commercially available pellet (S.A. = 196 m<sup>2</sup>/g) and one which was made in-house (S.A. = 149 m<sup>2</sup>/g), were used in this project. The alumina powder was

made by precipitating  $\text{AlCl}_3 \cdot 6\text{H}_2\text{O}$  (.5M in Al) with  $\text{NH}_4\text{OH}$  to a pH of 7.6. The gel was copiously washed with distilled  $\text{H}_2\text{O}$  and dried. The dried alumina was calcined at  $500^\circ\text{C}$  in air for 16 hours. Platinum was impregnated on the aluminas with chloroplatinic acid. An acetone solution containing the desired concentration of Pt was added to the alumina carrier and stirred overnight. The acetone was removed by rotoevaporation. The catalyst was dried overnight and stirred in a dessicator. Surface areas were determined by the BET method.

A plug flow reactor system was used for reduction, chloridation and activity testing of the catalysts.

Chloride analysis were done using standard ion chromatography techniques.

Methylcyclohexane and n-pentane were obtained commercially and dried using molecular sieves (3A) prior to use. All gases ( $\text{N}_2$  and  $\text{H}_2$ ) were ultra high purity (99.999%) and passed over molecular sieves prior to introduction into the reactor system. The naphtha sample was obtained from the Wilsonville advance liquefaction pilot plant. The naphtha was hydrotreated in the CAER PIPU pilot plant prior to use with the chlorided  $\text{Pt}/\text{Al}_2\text{O}_3$  catalyst.

## RESULTS AND DISCUSSION

A. Chloride Pretreatment. In the initial set of chloriding experiments, the Pt impregnated alumina powder (S.A. =  $149 \text{ m}^2/\text{g}$ ) catalysts were used. The catalyst was reduced prior to the pretreatment using a temperature of  $450^\circ\text{C}$  and 260 psig  $\text{H}_2$  (100 sccm/min.) overnight. Chloriding was done at  $300^\circ\text{C}$  using nitrogen at 250 psig pressure (100 sccm/min.) and  $\text{CCl}_4$  as the chloriding agent. The  $\text{CCl}_4$  partial pressure in the gas phase was controlled by the temperature of the vessel containing liquid  $\text{CCl}_4$  that was used to saturate the nitrogen stream. Gas samples were taken to monitor the  $\text{CO}_2$  content of the product gas by gas chromatography. In addition, gas samples were analyzed in the region of maximum  $\text{CO}_2$  production and in the initial stage of chloridation by GC/MS. No  $\text{COCl}_2$  or  $\text{CO}$  were found in the product gas stream in any of the samples using nitrogen as the carrier. The only compounds detected were  $\text{N}_2$ ,  $\text{CO}_2$ , and at the end of the final time period of chloridation,  $\text{CCl}_4$ . Thus,  $\text{CCl}_4$  reacts with alumina to produce  $\text{CO}_2$  as the only carbon containing product; however, it is not known whether the chloride containing species is  $\text{AlOCl}$ ,  $\text{AlCl}_3$ , or some more complex alumina compound is formed. However, it appears that chloriding occurs in steps with the first product being an alumina oxy chloride followed by subsequent formation of  $\text{AlCl}_3$ . Thus, for discussion purposes the reaction is written in two steps:



The four Pt/Al<sub>2</sub>O<sub>3</sub> catalysts were chlorided using this method. A typical CO<sub>2</sub> generation curve obtained using the .4 wt.% Pt/Al<sub>2</sub>O<sub>3</sub> catalyst is shown in Figure 1. Because of the dead volume between the CCl<sub>4</sub> saturator and the catalyst bed, the time taken as zero does not coincide with the time that CCl<sub>4</sub> first contacts the catalyst bed. As can be seen in this figure, the CO<sub>2</sub> generated goes through a maximum at .31 mole % in 90 minutes. The low amount of CO<sub>2</sub> generated, which was typical for this set of catalysts suggested that the amount of chloride added would be lower than the 8-13 wt.% required for an active isomerization catalyst (4). Analysis of the catalyst indicated that the chloride content was  $3.66 \pm .30$  wt.%. The chloride content of these Pt/Al<sub>2</sub>O<sub>3</sub> catalysts did not exceed 4 wt.% and appeared to correlate with the maximum CO<sub>2</sub> content generated during the chloriding pretreatment.

The next set of experiments performed in an attempt to increase the chloride content of the catalyst used the commercially available Al<sub>2</sub>O<sub>3</sub> pellets. The method for the chloriding pretreatment was also changed. Nitrogen was used for the CCl<sub>4</sub> entrainment at atmospheric pressure and 100 sccm/min. The reactor temperature remained the same (300°C). The CO<sub>2</sub> concentrations generated during the chloridation of the alumina pellets are shown in Figure 2. As can be seen, the amount of CO<sub>2</sub> produced was significantly greater than the amount shown in Figure 1. The maximum CO<sub>2</sub> generated (23.2 mole %) was also obtained at a shorter reaction time (10 min.). The chloride content of the catalyst was determined to be 13.70 wt.%. These data suggested that the observed increase in chloride added to the alumina pellets may be due to the form of the catalyst (pellets vs. powder).

In the next chloriding experiment, the alumina pellets were ground to -100 mesh (S.A. = 200 m<sup>2</sup>/g) to determine if the form of the catalyst affects the amount of chloride addition. The powdered alumina was chlorided using the same procedure as that used for the alumina pellets. The CO<sub>2</sub> generated during the chloridation of this sample is shown in Figure 2. As can be seen, the maximum CO<sub>2</sub> content is lower and required a longer reaction time to obtain. This correlates with the lower chloride content (5.79 wt.%) of the powdered catalyst. One possible explanation for the data shown in Figure 2 is that for the alumina pellets, the CCl<sub>4</sub> penetrates the pellet and reacts rapidly (reactions [1] and [2]) with the alumina to produce a chlorided alumina compound and produce CO<sub>2</sub>. The penetration of CCl<sub>4</sub> into the pellet and the escape of the CO<sub>2</sub> out of the pellet was not believed to be diffusion limited. It is believed that the diffusion of AlCl<sub>3</sub> from the interior of the catalyst or particle is slow because of diffusion, or a process that resembles diffusional limitations. Thus, it is viewed that AlCl<sub>3</sub> forms uniformly throughout the catalyst particle or pellet but that it is lost from the catalyst bed by desorption from the surface boundary of the catalyst particle or pellet. The geometric surface boundary of the pellet is much smaller than that of the same amount of catalyst when it is present in powder form. Hence, it is believed that the rate of chloridation is similar in both the powder and the pellet. However, desorption to the gas in the void volume and transport from the catalyst bed is much slower for the pellet than for the powder.

With the development of a method of chloride addition which produced an alumina with a sufficiently high chloride content, the next set of experiments used the alumina pellets impregnated with 2 wt.% Pt. This catalyst was reduced as described above and chlorided using the same procedure as in the alumina pellet experiments. In addition this catalyst was also chlorided without prior reduction. The chloride content of the resulting catalysts are shown in Figure 3. The data shown in Figure 3 indicate that the addition of Pt to the alumina pellets decreases the chloride content of the catalysts when compared to that of

the alumina pellets. The reduced catalyst produced a slightly higher chloride content than the catalyst which was not reduced prior to chloridation. Without further data, it is not possible to unambiguously determine the cause for the lower chloride content; however, the data does suggest that the impregnation of the alumina with the Pt has removed a number of sites that react with the  $\text{CCl}_4$ .

The data presented above indicate that a 2%  $\text{Pt}/\text{Al}_2\text{O}_3$  (pellet) can be chlorided to produce a catalyst containing a high chloride content (7.22 wt.%) and that the extent of chloride addition can be monitored by the amount of  $\text{CO}_2$  produced during this pretreatment. The reproducibility of this method is illustrated in Figure 4 which shows the  $\text{CO}_2$  generation curves for a number of chloride pretreatments. Note that in Test #11, the chloriding pretreatment was terminated just after the  $\text{CO}_2$  production reached a maximum. The resulting catalyst had a 5.93 wt.% chloride content. This run suggests that using this method of monitoring the extent of chloridation can accurately produce a series of catalysts with varying chloride contents.

**B. Isomerization Activity.** The isomerization activity of the 2%  $\text{Pt}/\text{Al}_2\text{O}_3$  catalysts which have different chloride contents is shown in Figure 5. For all of the reaction temperatures studied, the  $\text{Pt}/\text{Al}_2\text{O}_3$  (pellet) catalyst containing 7.22 wt.% Cl affected significantly higher conversions of n-pentane. The product distribution obtained for both of these catalysts were similar. The major product of the runs was isopentane (> 99%). In addition, minor amounts (ca. 0.1 - 0.2 wt.%) of isohexanes were also produced. Very little hydrogenolysis was observed for both of the catalysts. The data obtained from these isomerization runs with n-pentane suggest that the higher conversions are obtained with catalysts with high chloride concentrations.

The chlorided 2 wt.%  $\text{Pt}/\text{Al}_2\text{O}_3$  (pellet) was also tested with methylcyclohexane (MCH) using a number of reactor temperatures. The results indicated that although conversion of MCH were relatively high, the major products were 2-carbon cyclopentanes (~ 95+ wt.%) which indicated that little ring-opening of the MCH was accomplished. In an attempt to change the selectivity of the catalysts for the conversion of MCH, the total hydrogen pressure of the reactor was increased while holding the temperature constant. The effect of pressure on the conversion of MCH is shown in Figure 6. Increasing the reactor pressure from 100 to 730 psig slightly increases the conversion from 60 to 80 wt.%. However, the increase in pressure significantly changes the product distribution (Figure 7). The 2-carbon cyclopentanes, which are the major products of the conversion of MCH at lower pressures, significantly decrease in concentration with increasing pressure. It appears from these data that in order to obtain ring opening at lower temperatures, higher reactor pressures are required.

A hydrotreated naphtha derived from processing an Illinois #6 coal at Wilsonville was obtained as a reforming feedstock using the chlorided 2%  $\text{Pt}/\text{Al}_2\text{O}_3$  (pellet) catalyst. The catalyst exhibited an initial high activity in producing branched alkanes; however, this activity decreased rapidly with time on stream. It appears that the low concentration of heteroatoms remaining in the hydrotreated naphtha poisons the catalyst rapidly.

## SUMMARY

The extent of chloridation of a  $\text{Pt}/\text{Al}_2\text{O}_3$  catalyst can be monitored by determining the  $\text{CO}_2$  concentration in the product gas stream. The pellet form of the catalyst can be pretreated to produce a catalyst with a higher chloride content when compared to the powdered form

of the catalyst. The Pt/Al<sub>2</sub>O<sub>3</sub> catalyst containing the higher chloride content has a significantly higher isomerization activity using n-pentane as the feedstock. In order to open the cycloalkane ring to produce branched alkanes, higher reactor pressures are required at low reaction temperatures.

#### ACKNOWLEDGMENT

This work was supported by the DOE contract #De-AC22-90PC90049 and the Commonwealth of Kentucky. The authors also acknowledge the personnel at the Wilsonville liquefaction facility for providing the naphtha samples and for their helpful advice.

#### REFERENCES

1. E. F. Schvarzenback, *Proc. Am. Petrol. Inst.*, **37**, Section III, 354 (1957).
2. D. H. Belden and V. Haensel, *Proc. Am. Petrol. Ind.*, **37**, Section III, 354 (1957).
3. T. Y. Yan, T. J. Huang, W. O. Haag, U.S. Patent 4,049,539, September, 1977.
4. A. G. Goble, P. A. Lawrance, *Proc. 3rd Int. Cong. Catalysis*, Amsterdam, Vol. 1, 320, 1964.

Chloridation tests, using 0.4 wt% Pt on alumina powder,  
5.00 gram catalyst load, reduced overnight at 450 C, 250 psig H<sub>2</sub>,  
65.00 gram carbon tetrachloride load in chloriding bomb,  
chlorided at 300 C, 250 psig, 100 sccm nitrogen

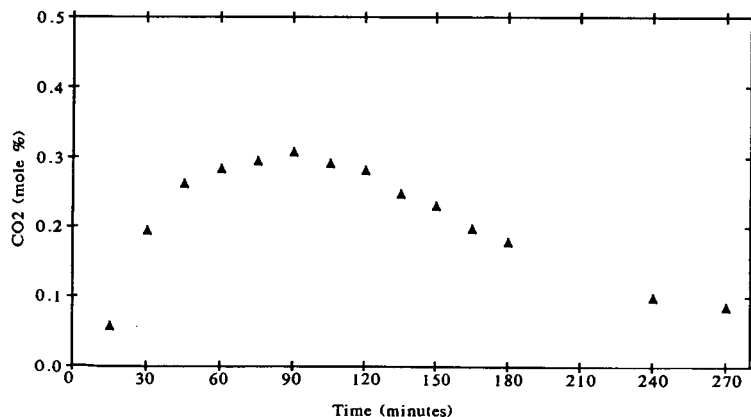


Figure 1. Carbon dioxide content of product gas during chloridation.

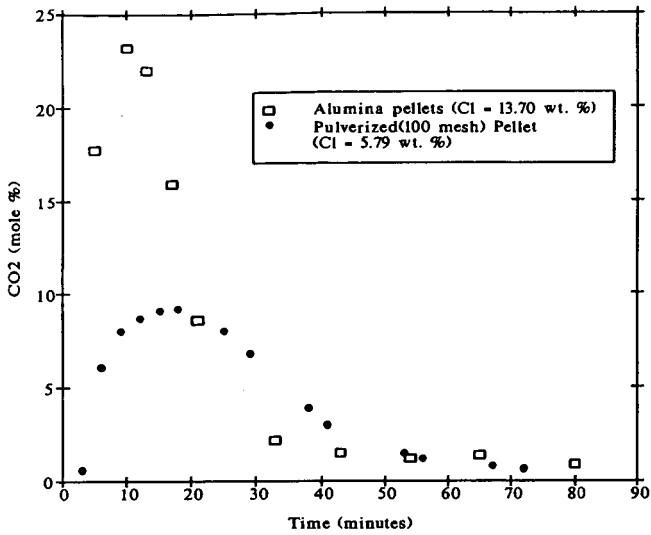


Figure 2. CO<sub>2</sub> production during chloridation of alumina catalysts (5.00 gram load, 65.00 g CCl<sub>4</sub> load in chloriding bomb, chlorided at 300 C, 1 at, N<sub>2</sub> @ 50 sccm).

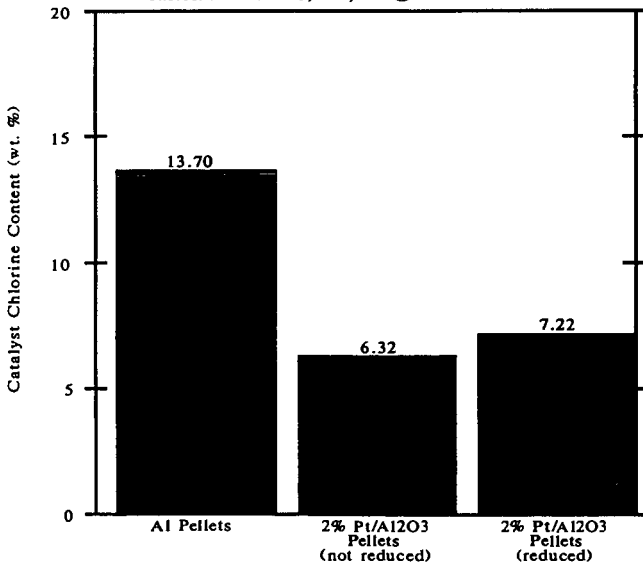


Figure 3. The effect of Pt impregnation and reduction on chloride addition. (same conditions as Figure 2.)

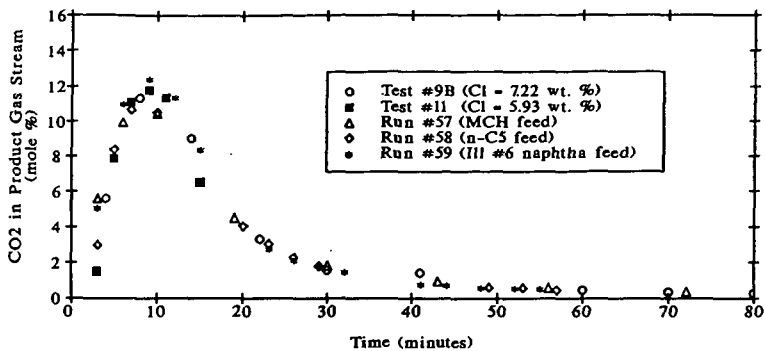


Figure 4. Reproducibility in the chloriding of a 2 % Pt/Al<sub>2</sub>O<sub>3</sub> catalyst (pellet) (same conditions as in Figure 2).

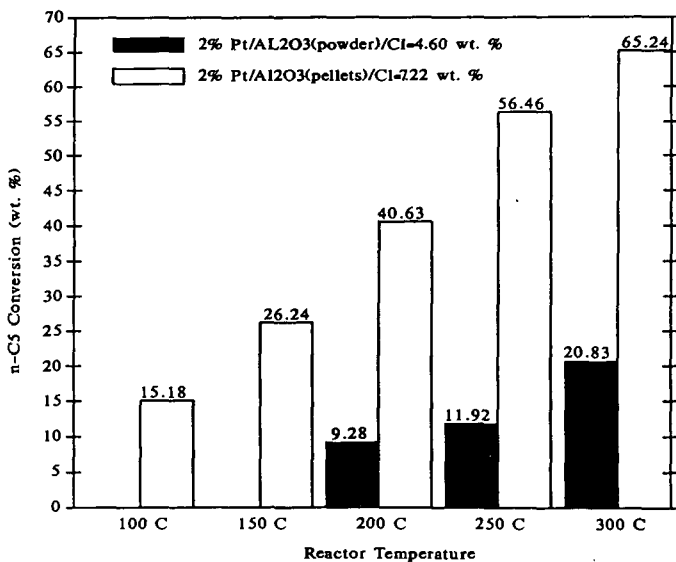


Figure 5. Comparison of n-C<sub>5</sub> conversions using catalysts with different Cl contents (WHSV=1.0, pressure=100psig).

Chlorided 2.0 wt% Pt on alumina pellets  
 methyl cyclohexane + 0.25 wt% CCL<sub>4</sub>  
 hydrogen:methylcyclohexane feed mole ratio = 3:1  
 250 C, 100-730 psig, WHSV- 2.0 g/hr per g catalyst

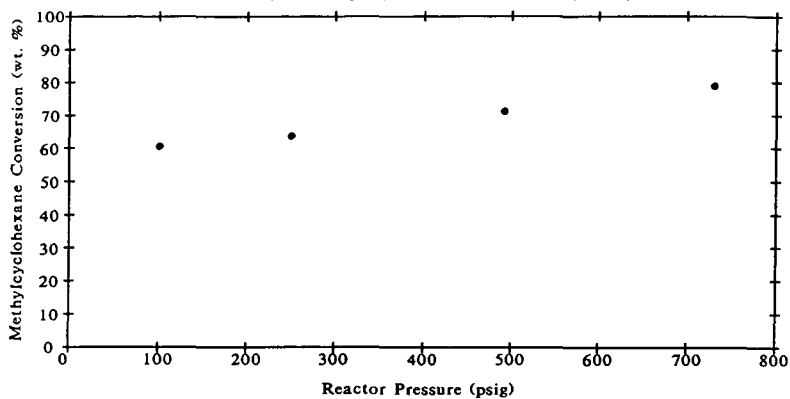


Figure 6. Effect of hydrogen pressure on MCH conversion.

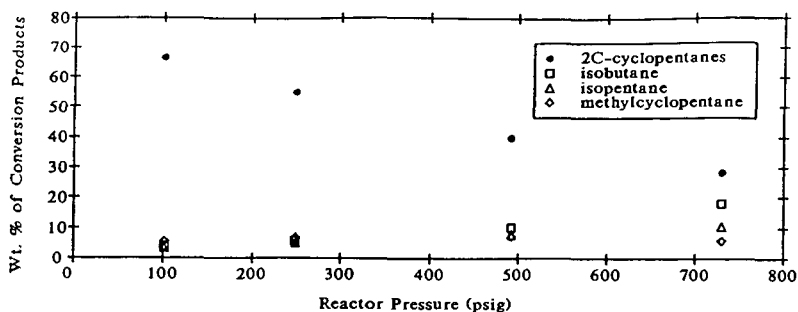


Figure 7 Effect of H<sub>2</sub> pressure on product selectivity (same conditions as Figure 6).

## THE APPLICATION OF FT-IR METHODS TO THE CHARACTERIZATION OF COAL LIQUEFACTION PROCESS STREAMS

Hsisheng Teng, Michael A. Serio, Rosemary Bassilakis,  
Kim S. Knight, Stephen C. Bates and Peter R. Solomon

Advanced Fuel Research, Inc.  
87 Church Street  
East Hartford, CT06108

**Keywords:** Coal Liquefaction, FT-IR, Fiber Optics

### INTRODUCTION

Fourier transform infrared spectroscopy (FT-IR) is one of the most versatile analytical techniques available for the study of fossil fuel structure and reaction chemistry [1-5]. Among its advantages are: 1) its ability to study feedstocks and reaction products as solids, liquids and gases, since almost all have characteristic absorptions in the infrared; 2) its high sensitivity, allowing the study of strongly absorbing materials such as coal and char, and the use of techniques such as attenuated total reflectance (ATR) or photoacoustic spectroscopy; 3) its speed, allowing the possibility of following chemical reactions on-line. Because of these advantages, FT-IR spectroscopy has achieved increasing use in fuel science.

The objective of this work was to evaluate the use of two FT-IR methods for characterization of distillation resids from coal liquefaction process streams. The first method is quantitative FT-IR analysis of samples pressed into KBr pellets to determine functional group concentrations. The second method is Thermogravimetric Analysis with FT-IR analysis of evolved products (TG-FTIR). In addition, the application of on-line FT-IR Fiber Optic (F-O) ATR analysis to coal liquefaction processes is addressed.

### EXPERIMENTAL

#### Characterization of Coal Liquefaction Products

The samples used in this study were supplied by Consolidation Coal Company (CONSOL), PA, along with chemical and structural information obtained with various techniques. These samples included: 1) Three feed coals (Wyodak, Illinois, and Pittsburgh); 2) Nine whole resid samples produced by distillation of process oils generated from the three different feed coals and obtained from three different sampling points (interstage, recycle, second stage) during liquefaction runs at the Wilsonville (AL) facility; 3) Nine THF soluble portions of the above whole resids; 4) Four additional solids free resids obtained during a catalyst aging study at the HRI (NJ) facility; 5) A single whole process oil for Pittsburgh coal obtained from the Wilsonville facility. These samples were analyzed by both FT-IR and TG-FTIR.

**FT-IR Analysis** - The samples are analyzed as KBr pellets in a Nicolet 7199 FT-IR. For quantitative analysis of such spectra, a curve analysis program is employed to synthesize the IR spectra [1-3]. The program uses a basic set of adsorption peaks identified with various functional groups. The synthesis routine can produce a spectrum which matches the actual spectrum well. The correction of a whole resid spectrum for scattering and minerals is demonstrated in Figure 1.

**TG-FTIR Analysis** - The apparatus consists of a sample suspended from a balance in a gas stream within a furnace. As the sample is heated in helium, the evolving volatile products are carried out of the furnace directly into a gas cell for analysis by FT-IR [5]. The results of a typical resid pyrolysis experiment are shown in Figure 2. The system continuously monitors the time-dependent evolution of the gases and tars, and weight of the non-volatile material. At the end of the pyrolysis experiment, oxygen is introduced to burn the residue to obtain the ash content of the sample.

#### **In-Situ FT-IR/F-O/ATR Measurements**

A coal liquefaction test cell which incorporates a FT-IR/F-O system is shown in Figure 3. The reactor is made of 3/8" stainless tubing and Swagelok tube fittings. This reactor can withstand a pressure as high as 3800 psig at 400 °C. A sapphire fiber, which is 15" (38 cm) in length and 0.25 mm in diameter, is used as an ATR sensor in the reactor. A zirconium fluoride fiber cable is used as a transmitting fiber to link between the sensor fiber and the FT-IR spectrometer and detector.

Liquefaction of demineralized Zap lignite was performed in the test cell, with 1 g of coal sample mixed with 6 ml of tetralin. The experiment was performed by heating the reactor from room temperature to 400 °C at 20 °C/min, and sustaining the final temperature for 40 minutes. The F-O/ATR spectra of the tetralin/coal liquid mixtures in the reactor were taken at regular intervals. Tetralin spectra at the relevant temperatures were taken and compared with those from coal liquefaction experiments.

## **RESULTS AND DISCUSSION**

### **Characterization of Coal Liquefaction Products**

Characterization of the samples using the FT-IR and TG-FTIR methods provides a good understanding of the average chemical structure of products from the various stages of a coal liquefaction process. In order to demonstrate the reliability of these two FT-IR techniques, correlation and comparison of the results in this study with those supplied by CONSOL using different methods are described below.

#### **FT-IR Analysis**

**Aromatic and Aliphatic Hydrogen (Proton) Distribution** - The comparison of the aromatic to total hydrogen ratio ( $H_a/H_{tot}$ ) using FT-IR analysis with the aromatic proton fraction from the <sup>1</sup>H-NMR method for the THF soluble samples is shown in Figure 4a. Figure 4b shows the comparison of the aliphatic hydrogens for the same set of samples. The results show that the FT-IR  $H_a/H_{tot}$  agrees reasonably well with the fraction of aromatic protons derived from the <sup>1</sup>H-NMR method. The same is true of the aliphatic hydrogen. These figures contain two lines. The solid line is the mean value of the ratios between the two sets of measurements. The dashed line is a parity line. Figures 4a and 4b provide a relation between the results obtained by these two methods:

$$\begin{aligned} H_a/H_{tot} (\%, \text{ THF sol.}), \text{ FT-IR} &= 0.77 [\text{Aromatic Proton Fraction } (\% \text{ THF sol.}), \text{ }^1\text{H-NMR}] \\ H_a/H_{tot} (\%, \text{ THF sol.}), \text{ FT-IR} &= 1.1 [\text{Aliphatic Proton Fraction } (\% \text{ THF sol.}), \text{ }^1\text{H-NMR}] \end{aligned}$$

**Hydroxyl Groups** - Both this study and CONSOL used an FT-IR method to determine the

concentration of hydroxyl groups in the samples. CONSOL used the -OH stretch band found between 3200 and 3400  $\text{cm}^{-1}$  to determine the phenolic -OH concentration from measurements on THF-soluble portions of the samples. In this study, the concentration of hydroxyl groups was determined using the 3200  $\text{cm}^{-1}$  O-H stretch to avoid the interference from the KBr-H<sub>2</sub>O band which peaks at 3400  $\text{cm}^{-1}$  [1]. The hydroxyl results obtained in this study and by CONSOL are in good agreement, considering the differences in sample preparation and the quantitative analysis routines. The relation between them is:

$$-\text{OH (wt\%, THF sol.)}, \text{FT-IR} = 0.90 [\text{Phenolic-OH (wt\%, THF sol.)}, \text{FT-IR} | \text{CONSOL}]$$

**Oxygen Analysis** - In general, most of the oxygen atoms in coal and coal products are contained in hydroxyl, ether, and carbonyl functional groups. In this study, oxygen contents of the samples were determined through quantitative analysis of hydroxyl and ether by the FT-IR method, assuming that the amount of oxygen in carbonyl functions is negligible. The oxygen contents of the samples provided by CONSOL were determined by difference in elemental analyses. The oxygen data in this study and from CONSOL for the whole resids and whole process oil show reasonable agreement, although the data are somewhat scattered. The relation between these two different methods is:

$$\text{O-Content (wt\%, MAF)}, \text{FT-IR} = 1.1 [\text{O-Content (wt\%, MAF)}, \text{Elemental Difference}]$$

**Hydrogen Analysis** - The total hydrogen content for each of the samples was determined by summing up the aliphatic, aromatic, and hydroxyl hydrogen determined by FT-IR. The hydrogen analysis provided by CONSOL was determined with a Leco CHN-600 elemental analysis instrument. The results of these two methods are in good agreement. The relation between them is:

$$\text{H-Content (wt\%, MAF)}, \text{FT-IR} = 1.1 [\text{H-Content (wt\%, MAF)}, \text{Elemental Analysis}]$$

**Carbon Analysis** - The carbon content of each sample was determined by mass balance difference with oxygen and hydrogen contents obtained with the FT-IR method, assuming that the fraction of others, such as nitrogen and sulfur, is negligible. The values supplied by CONSOL were obtained from carbon analysis with the Leco CHN-600 instrument. A comparison shows that these two sets of data from different methods are in good agreement, and the relation between them is:

$$\text{C-Content (wt\%, MAF)}, \text{FT-IR} = 1.0 [\text{C-Content (wt\%, MAF)}, \text{Elemental Analysis}]$$

**Ash** - FT-IR analysis can determine the contents of major minerals, i.e. mixed clays, Kaolinite, Quartz, and Calcite. The total ash content determined by FT-IR is the sum of these four minerals. Since the FT-IR measurement of minerals includes the associated water and is done at ambient temperature, it is expected to be higher than the high temperature ash determinations supplied by CONSOL. However, it is also true that the FT-IR method does not determine pyrite, so it may underestimate the ash content for coals which contain large amounts of this mineral. The comparison of the ash contents determined with FT-IR and by CONSOL is shown in Figure 4c. The results show that the trends in the FT-IR values of the total ash content agreed well with the values supplied by CONSOL, although the latter numbers were lower as expected. The relation between the two measurements is:

$$\text{Ash (wt\%, dry)}, \text{FT-IR} = 1.3 [\text{Ash (wt\%, dry)}, \text{Combustion}]$$

### **TG-FTIR Analysis**

**Proximate Analysis of Feed Coals** - Pyrolysis up to 900 °C followed by combustion of the residue, when carried out in the TG-FTIR apparatus, gives a good proximate analysis for feed coals. The proximate analysis with TG-FTIR reveals the contents of ash, volatile matter, fixed carbon, and moisture in coal.

Pyrolysis of coal at temperatures as high as 900 °C will produce a char with a high carbon content (>95%, MAF). Therefore, the char yield (MAF) in pyrolysis represents the fixed carbon content in the coal. The comparison of the fixed carbon content obtained by TG-FTIR and that supplied by CONSOL is shown in Figure 4d. It shows that the two sets of values are in good agreement and the relation between them is:

Fixed Carbon (wt%, dry), TG-FTIR = 1.0 [Fixed Carbon (wt%, dry), Proximate Analysis]

The ash content is determined by burning the char in the presence of oxygen. A comparison of ash analyses is shown in Figure 4e, and the results show a good agreement. The relation between the two sets of data is:

Ash (wt%, dry), TG-FTIR = 1.1 [Ash (wt%, dry), Proximate Analysis]

The volatile matter of coal includes all the species evolved during pyrolysis. These species are gases and tars, which are measured by TG-FTIR during the process of pyrolysis. The comparison of the volatile matter contents determined by TG-FTIR with those provided by CONSOL from proximate analysis is shown in Figure 4f. The results show that they are in good agreement with each other and the relation is:

Volatile (wt%, dry), TG-FTIR = 1.0 [Volatile (wt%, dry), Proximate Analysis]

The moisture content of coal is determined by TG-FTIR prior to pyrolysis. The results obtained by TG-FTIR are not in good agreement with those supplied by CONSOL, although the trend is correct. The relation between them is:

Moisture (wt%, as rec.), TG-FTIR = 0.45 [Moisture (wt%, as det.), Proximate Analysis]

This difference is not surprising since the moisture content depends on how the sample is stored and handled.

**Ash Analysis for Resids** - The ash content of the distillation resids was determined using TG-FTIR by burning the char residue from the resids in the presence of oxygen. The comparison of the resid ash content obtained with TG-FTIR and that supplied by CONSOL is shown in Figure 5a. The results show that the ash contents determined by TG-FTIR are in very good agreement with those provided by CONSOL. The relation between the two sets of data is:

Ash (wt% dry), TG-FTIR = 1.0 [Ash (wt%, dry), Combustion]

**Char Analysis for Resids** - Coal chars produced at temperatures above 900 °C consist mainly of large condensed aromatic rings. It is expected that the char yield from resid pyrolysis would have a proportional relation with the content of condensed aromatics. The comparison of the char yield for pyrolysis performed in the TG-FTIR and the condensed aromatic proton fraction from NMR is shown in Figure 5b for the THF soluble fractions. The results show that the char

yield in resid pyrolysis increases with increasing condensed aromatic proton fraction. The relation between the two sets of values is:

$$\text{Char (wt\%, THF sol.)}, \text{ TG-FTIR} = 0.65 [\text{Cond. Aromatic Proton (\%, THF sol.)}^1 \text{H-NMR}]$$

### Data Interpretation in the Context of the Liquefaction Process

The samples from the Wilsonville facility were taken from three locations to represent different degrees of coal processing. The Interstage Product samples were distillation resids obtained from a high pressure flash separation system located between the first stage and second stage reactors. The 2nd Stage Product samples were resids collected from the bottom product hold tank of a separation system following the second stage reactor. The Recycle samples were resids obtained from the solvent surge tank. The Recycle samples are the partially deashed products of the 2nd Stage Product. The structural differences of the samples, revealed in the analytical data, are due to differences in the feed coals and to different degrees of coal processing in liquefaction, as discussed below.

A comparison of -OH contents from THF soluble fractions of the resid samples from different degrees of processing is shown in Figure 6. The results show that the Interstage Product has a higher -OH content than the 2nd Stage Product due to upgrading by the second reactor. The TG-FTIR results show a corresponding reduction of CO evolution in pyrolysis for the 2nd Stage Product, as discussed below. Figure 6 shows a slight -OH reduction due to the deash process. In general, the -OH content of the resids decreases in the order Interstage > 2nd Stage > Recycle. The trends for char yield from TG-FTIR analysis follow the same general order, which is consistent with the role of oxygen functions in retrogressive reactions under pyrolysis [6] and liquefaction conditions [7].

Since the oxygen content of the feedstock would be reduced in the liquefaction process, the amount of CO evolution in pyrolysis is expected to decrease in the order coal > Interstage > 2nd Stage > Recycle, and the results shown in Figure 7 for the whole resids indicate that this is the case. If the results in Figures 6 and 7 are compared, it can be seen that the -OH content and the CO evolution from pyrolysis are related.

Similar to the result of CO evolution in pyrolysis, more CH<sub>4</sub> is evolved in coal pyrolysis than in resid pyrolysis. Because most of the CH<sub>4</sub> forming components in coal are consumed in the liquefaction process in which gaseous product CH<sub>4</sub> is separated from the process stream to become fuel gas, it is reasonable to see less CH<sub>4</sub> evolution in resid pyrolysis. A comparison of CH<sub>4</sub> yields from pyrolysis of the feed coals and various whole resid samples is shown in Figure 8. Since CH<sub>4</sub> forming components would be further reduced by the Second stage reactor, it is also not surprising to see less CH<sub>4</sub> evolution in the pyrolysis of the 2nd Stage Product than the Interstage Product. The amounts of CH<sub>4</sub> evolution from the 2nd Stage Product and from the Recycle are similar, which reveals that the deash process has little effect on the CH<sub>4</sub> forming structures in resids. In general, the amount of CH<sub>4</sub> evolution in the pyrolysis of liquefaction products follows the order coal > Interstage > 2nd Stage ~ Recycle.

The hydrogen content analyses indicate a slight increase in hydrogen concentration in the whole resids from the second stage reactor by comparing the 2nd Stage Product with the Interstage Product (except for Pittsburgh resid). These results are shown in Figure 9. This figure also shows the expected increase in hydrogen concentration for the resid products when compared to the feed coal. Also, as the material is upgraded, the absolute amount of aromatic hydrogen decreases, as shown in Figure 10.

The HRI samples represent production of material from a Continuous Two-Stage Liquefaction facility for different periods of time in a single run. Interpretation of the data reveals a consistent variation of the properties of the samples with the length of run period. The interpretation of these variations is discussed below and is based on information supplied by CONSOL on variations in run conditions as function of time.

The variation of the hydrogen content of the sample with the length of the run period is shown in Figure 11. The results show that the total hydrogen and aliphatic hydrogen content decrease with increasing run time, whereas the aromatic hydrogen shows an opposite trend. The decrease of the hydrogen content of the liquefaction product with run time may be attributable to catalyst aging as well as to a reduction in the solvent/coal ratio and an increase in solvent cut point. It is reasonable to observe a reduction in the aliphatic hydrogen content since the hydrogenation rate slows down with time due to catalyst aging. The increase in  $H_a$  with run time may also result from the increasing reaction temperature which would tend to increase the amount of aromatic hydrogen.

The variation of the hydroxyl and ether contents of the samples with the length of the run period is shown in Figure 12. The results show an increase of the hydroxyl content with run time. The change in -OH concentration is due to catalyst aging as well as to the reduction in the solvent/coal ratio and to the increase in solvent cut point. The FT-IR results also show an increase in the ether content with time. The increase of the ether content in the liquefaction products can be attributed mostly to the catalyst aging which would result in a lower rate of bond cleavage on ether linkages. A second possibility is an increase in the amount of ethers formed from retrogressive reactions involving hydroxy and dihydroxy functionalities structures.

#### **In-Situ FT-IR/F-O/ATR Measurements**

In order to accommodate the temperature (~400°C) and pressure (~3000 psig) requirements of a coal liquefaction process, a sapphire fiber optic element was used in the ATR mode for in-situ measurements. This cuts out the information below about 2500  $\text{cm}^{-1}$ , but still allows significant amounts of chemical structural information to be obtained.

Since tetralin is the solvent used in coal liquefaction experiments, it is of interest to know how tetralin behaved under temperature conditions similar to those of coal liquefaction. Non-isothermal experiments which simulate the conditions of coal liquefaction are carried out in the test cell, and the infrared spectra from the F-O/ATR spectroscopy at different temperatures were obtained. Figure 13 shows the tetralin absorbance spectra in the C-H stretching region at different temperatures. Since tetralin does not contain oxygen functional groups, the focus of the analysis was on the C-H stretching region.

It can be seen from the spectra that the infrared absorbance decreases with temperature. This result is expected, since the depth of penetration of the infrared evanescent wave into the sample decreases with temperature. The temperature effect on F-O/ATR spectroscopy requires further study in order to obtain quantitative results.

Since it was known [8] that tetralin would undergo hydrogen transfer reactions to form a mixture of aliphatic and alkyl aromatic compounds by heat treatment, the aliphatic to aromatic ratio in the system would therefore vary with temperature. Based on Figure 13, one should be able to determine the aliphatic to aromatic hydrogen ratios at different temperatures from the absorbance ratios of 2930  $\text{cm}^{-1}$  to 3020  $\text{cm}^{-1}$ , if the extinction coefficients for each species were

known. This issue, for pure tetralin as well as coal liquefaction measurements, will be discussed in a future publication.

It has been reported [9] that the alkyl  $\text{CH}_2$  gives rise to a symmetric stretching mode at  $2870\text{ cm}^{-1}$ , and the  $-\text{CH}_2-$  at  $2850\text{ cm}^{-1}$ . Since tetralin does not contain methyl structures, the  $2860$  and  $2840\text{ cm}^{-1}$  peaks shown in Figure 13 are actually from the splitting of the methylene symmetric stretching at  $2850\text{ cm}^{-1}$ . By thermal treatment, tetralin will undergo decomposition to form its derivatives, which contain methyl groups. The methyl symmetric stretching at  $2870\text{ cm}^{-1}$  would interfere with the  $2860\text{ cm}^{-1}$  peak from the methylene, and, therefore, the former peak would not be distinct if its concentration is low. Because of this interference, we cannot see a  $2870\text{ cm}^{-1}$  peak emerging at higher temperatures in Figure 13. However, if a series of absorbance spectra from coal liquefaction experiments are examined, as shown in Figure 14 for demineralized Zap, the emergence of the methyl  $2870\text{ cm}^{-1}$  absorbance underneath the methylene  $2860\text{ cm}^{-1}$  absorbance can be clearly seen. A curve resolving technique has recently been developed in our group to resolve overlapped absorption bands. This technique will be applied to the F-O/ATR spectra to improve quantitative analysis.

The O-H stretching region for the liquefaction run is shown in Figure 15. The absorbance spectrum of O-H stretching is usually a broad band, ranging between  $3100$  and  $3600\text{ cm}^{-1}$  and centered near  $3400\text{ cm}^{-1}$  [10]. Figure 15 shows that the absorbance by hydroxyls increases with the degree of liquefaction, indicating increasing amount of OH-containing coal fragments dissolved in the liquid phase.

## CONCLUSIONS

Both FT-IR and TG-FTIR have been clearly shown to provide a wide variety of useful information for process stream characterization. Both techniques can be applied to whole process oils, resids, or distillates, including ash components, and require relatively small samples (<50 mg). Significant differences are observed between process stages, coal types, and with catalyst aging. A summary of the composition parameters that can be obtained by FT-IR and TG-FTIR is shown in Table 1. In many respects, FT-IR is probably the single most useful technique for this purpose, since it can provide measurements on both organic and mineral components. It has also demonstrated that on-line FT-IR measurements could be made in-situ using a sapphire fiber optic element in the Attenuated Total Reflectance mode.

## ACKNOWLEDGEMENTS

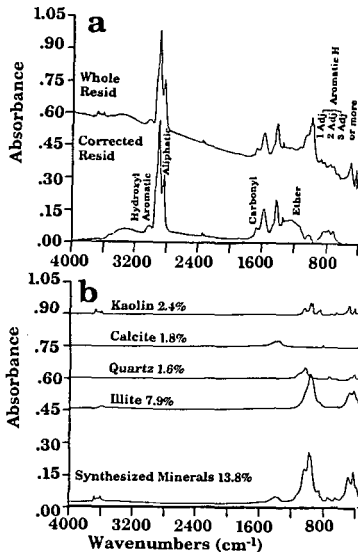
This work was supported by a subcontract from the Consolidation Coal Company under DOE Contract No. DE-AC22-89PC89883, and by the DOE SBIR program under Grant No. DE-FG05-91ER81151. The authors also wish to acknowledge Dr. Susan Brandes and Mr. Richard Winschel of CONSOL Research and Development for many helpful discussions, and Mr. William Stevenson, Dr. Mark Druy, and Mr. Paul Glatkowski of Foster-Miller, Inc. of Waltham, Mass. for assisting with the FT-IR/F-O/ATR measurements. Marie DiTaranto of Advanced Fuel Research did the FT-IR analyses. Robert Carangelo and Erik Kroo consulted on the interpretation of the FT-IR, TG-FTIR and FT-IR/F-O/ATR results.

## REFERENCES

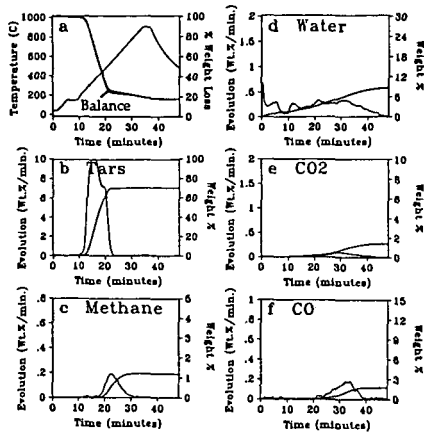
1. Solomon, P.R., and Carangelo, R.M., Fuel, **61**, 663 (1982).
2. Solomon, P.R., and Carangelo, R.M., Fuel, **67**, 949 (1988).
3. Solomon, P.R., Hamblen, D.G., and Carangelo, R.M., Am. Chem. Soc. Symp. Ser., **205**, 77 (1982).
4. Painter, P.C., Snyder, R.W., Starsinic, M., Coleman, M.M., Kuehn, D.W., and Davis, A., Am. Chem. Soc. Symp. Ser., **205**, 47 (1982).
5. Carangelo, R.M., Solomon, P.R., and Gerson, D.J., Fuel, **66**, 960(1987).
6. Solomon, P.R., Serio, M.A., Desphande, G.V., and Kroo, E., Energy & Fuels, **4**, (1), 42 (1990).
7. Serio, M.A., Solomon, P.R., Kroo, E., Bassilakis, R., Malhotra, R., McMillen, D., Prepr. Pap. - Am. Chem. Soc., Div. Fuel Chem., **35**, (1), 61 (1990).
8. Vlieger, J.J., Kieboom, A.P.G., and Bekkum, H., Fuel, **63**, 334, (1984).
9. Willard, H.H., Merritt, L.L., Jr., Dean, J.A., and Settle, F.A., Jr., Instrumental Methods of Analysis, 6th Edition, D. van Nostrand Co., New York (1981), Chapter 7.
10. Painter, P.C., Sobkowiak, M., and Youtcheff, J., Fuel, **66**, 973 (1987).

TABLE 1. SUMMARY OF FT-IR AND TG-FTIR MEASUREMENTS

| FT-IR MEASUREMENT                            | ALTERNATIVE TECHNIQUE |
|--|-----------------------|
| Hydroxyl Hydrogen                            | Chemical Titration    |
| Aliphatic Hydrogen                           | <sup>1</sup> H-NMR    |
| Aliphatic Carbon*                            | <sup>13</sup> C-NMR   |
| Aromatic Hydrogen                            | <sup>1</sup> H-NMR    |
| Hydrogen Content                             | Elemental Analysis    |
| Carbon Content*                              | Elemental Analysis    |
| Hydroxyl Oxygen                              | Chemical Titration    |
| Ether Oxygen                                 | ---                   |
| Carbonyl Oxygen**                            | ---                   |
| Total Ash                                    | TGA                   |
| Mineral Components                           | ICP                   |
| TG-FTIR MEASUREMENT                          | ALTERNATIVE TECHNIQUE |
| <b>Direct</b>                                |                       |
| Volatile Content                             | Proximate Analysis    |
| Fixed Carbon                                 | Proximate Analysis    |
| Total Ash                                    | Proximate Analysis    |
| Moisture                                     | Proximate Analysis    |
| C,H,N,S                                      | Elemental Analysis    |
| <b>Indirect</b>                              |                       |
| Char Yield → Condensed Aromatics             | <sup>1</sup> H-NMR    |
| CO Yield → Phenolic Content                  | FT-IR                 |
| CH <sub>4</sub> Yield → Methyl Group Content | <sup>13</sup> C-NMR   |
| Tar Evolution Profile → Boiling Range        | Distillation          |



**Figure 1.** Quantitative FT-IR Analysis of the Coal Liquefaction Product. Correction of Resid Spectrum for Scattering and Minerals. a) Correction of Resid Spectrum; b) Determination of Mineral Spectrum by Addition of Reference Spectra. Data for Whole Resid Sample (interstage) from Illinois No. 6 Coal.



**Figure 2.** TG-FTIR Results for Interstage Oil Resid from Illinois No. 6 Coal.

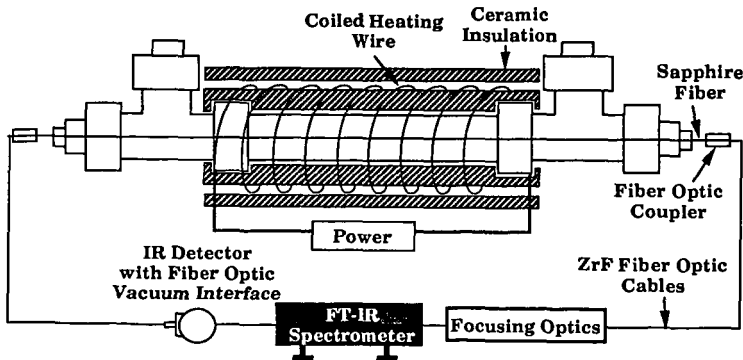


**Figure 3.** Schematic of FT-IR Fiber-Optic ATR System for Coal Liquefaction.

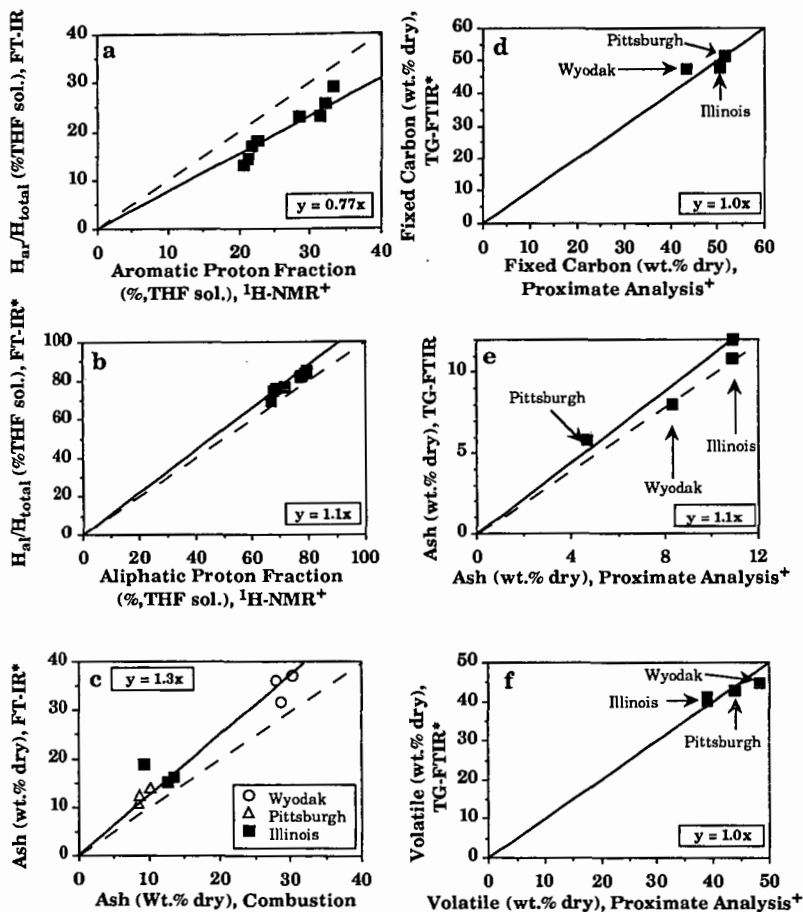


**Figure 4.** Correlation and Comparison of the Results from FT-IR Techniques and Other Methods. a) Resid Aromatic Hydrogen Distribution; b) Resid Aliphatic Hydrogen Distribution Resid; c) Resid Ash Content; d) Coal Fixed Carbon; e) Coal Ash Content; f) Coal Volatile. \* Present Study; + Data Supplied by CONSOL.

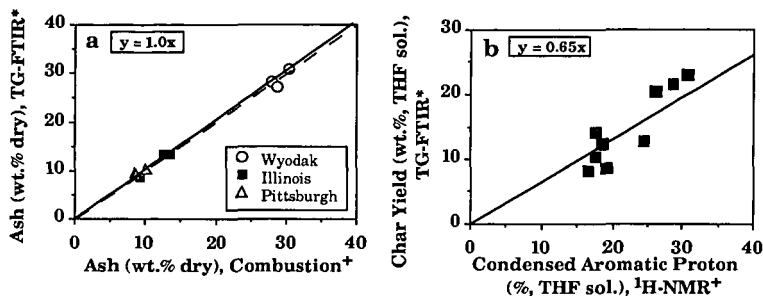


Figure 5. Correlation and Comparison of the Results from FT-IR Techniques and Other Methods. a) Resid Ash Content; b) Char Yield with Condensed Aromatic Proton Fraction. \* Present Study; + Data Supplied by CONSOL.

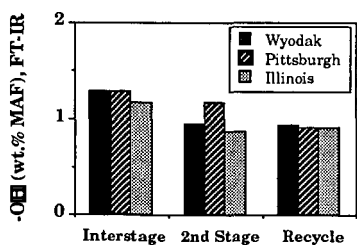


Figure 6. -OH Content at Different Stages for Wilsonville Resids.

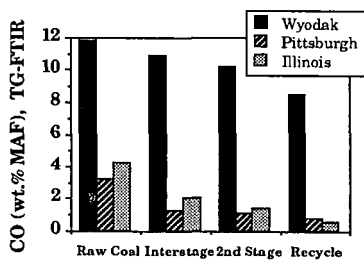


Figure 7. CO Evolution from Pyrolysis of Wilsonville Resids.

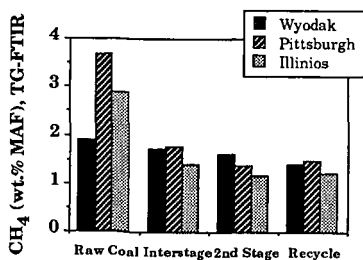


Figure 8. CH<sub>4</sub> Evolution from Pyrolysis of Wilsonville Resids.

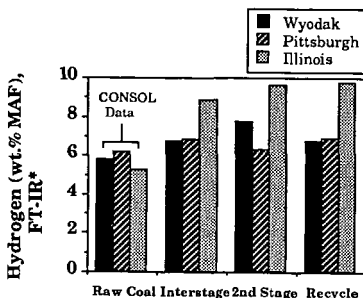


Figure 9. Hydrogen Content at Different Stages for Wilsonville Resids.

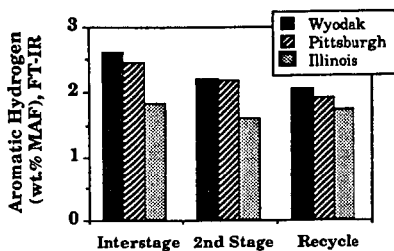


Figure 10. Aromatic Hydrogen Content at Different Stages for Wilsonville Resids.

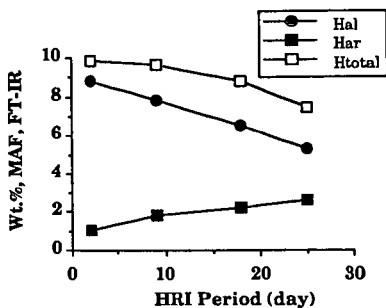


Figure 11. Hydrogen Analysis for HRI Liquids.

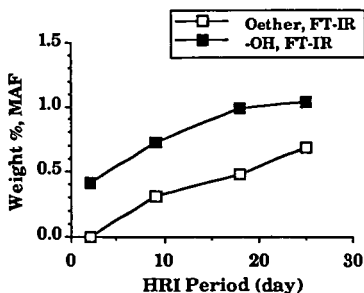


Figure 12. Oxygen Functional Group Analysis for HRI Liquids.

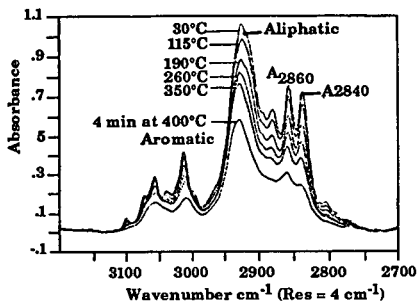


Figure 13. The Absorbance Spectra of Tetralin from F-O/ATR Spectroscopy in a Non-Isothermal Experiment.

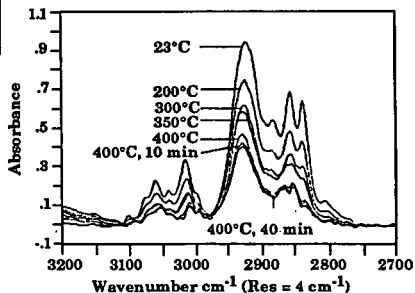


Figure 14. The C-H Stretching Region of the Absorbance Spectra from F-O/ATR Measurements under Coal Liquefaction Conditions for Demineralized Zap.

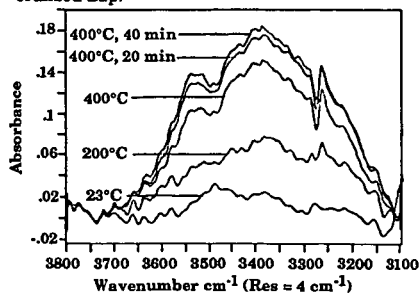


Figure 15. The O-H Stretching Region of the Absorbance Spectra from F-O/ATR Measurements under Coal Liquefaction Conditions for Demineralized Zap.

## SYMPOSIUM ON PROCESSING AND PRODUCT SELECTIVITY OF SYNTHETIC FUELS

Presented before the Division of Fuel Chemistry  
American Chemical Society  
Washington, D.C., August 23-28, 1992

### ASSAY OF DIESEL FUEL COMPONENTS PROPERTIES AND PERFORMANCE

by Jimell Erwin  
Southwest Research Institute  
P.O. Drawer 28510  
San Antonio, TX 78228  
(512) 522-2389

#### Introduction

The increasingly stringent restrictions on exhaust emissions from diesel fuel powered vehicles pose a challenge for both existing petroleum fuels and proposed fuels from alternative sources. The EPA regulation limit governing particulates reduced to 0.25 g/bhp-hr in 1991 for trucks and to 0.1 g/bhp-hr for city buses in 1993. In 1994, the limit will drop to 0.1 g/bhp-hr for all vehicles. It is expected that Canada will adopt the same limits at a later date and Mexico will have similar standards for urban vehicles. EPA has not prescribed the method for meeting the emissions requirements for diesel engines. Engine manufacturers have performed significant development on cleaner engines without meeting the proposed standard in all cases. EPA issued regulations that limit sulfur content of diesel fuel to 0.05 weight percent and imposed a minimum 40 cetane index to "cap" aromatics content at present levels.<sup>1</sup> The California Air Resources Board has also announced regulations effective in 1993 that control diesel fuel sulfur content to less than 0.05 weight percent plus aromatics to less than 10 volume percent.

The objectives in the current work included producing a consistent set of performance, emission, and composition measurements on a set of diesel fuel components distinguished by source and processing history emphasizing aromatics. The components were reduced in sulfur and aromatic content by pilot plant hydrogenation before distillation into selected ranges of boiling points. The resulting fractions of feedstocks and products were analyzed for chemical composition and physical properties that would be most revealing for ignition quality and particulate generation.

This report presents the results to date of this work in progress. With the broad objective of relating diesel exhaust emissions and performance to chemical composition and physical properties, the more specific concerns of the effect of alkane branching and aromatic substituents will be addressed later. The choice of starting materials will give insight about source and upgrading method as they affect ignition quality and emissions from different samples meeting the same limits on sulfur and aromatics but with different processing histories.

#### Background

Contemporary diesel fuel is a blend of several refinery streams chosen to meet specifications. The need to increase yield of transportation fuel from crude oil has resulted in converting increased proportions of residual oil to lighter products. This is accomplished by thermal, catalytic, and hydrocracking of high molecular weight materials rich in aromatic compounds. The current efforts to reformulate California diesel fuel for reduced emissions from existing engines is an example of the other driving force affecting refining practice. Although derived from petroleum crude oil, reformulated diesel fuel is an alternative to current specification-grade diesel

fuel, and this alternative presents opportunities and questions to be resolved by fuel and engine research.

It has been observed that sulfur and aromatics concentrations increase with boiling point. For example, lower concentrations of aromatics and sulfur typically occur in D-1 fuel whose boiling range of 300-550°F is lower than D-2 fuel with 350-650°F. What has not been shown is which of the highest boiling components are most responsible for particulate emissions or which components of refinery streams would benefit the most from processing to reduce emissions precursors. The approach used for determining the effects of fuel composition on engine behavior has been to blend or measure full boiling range fuels for engine tests. For instance, the work at the University of Wisconsin<sup>2</sup> and the University of Pennsylvania<sup>3</sup> found little effect on performance and emissions attributable to fuel composition. Other studies had different results. Weidmann found that fuel properties have a small, measurable effect on emissions using a VW 1.67 liter, 4-cylinder engine.<sup>4</sup> Hydrocarbon emissions were found to be a function of fuel cetane number with volatility exerting a stronger influence for low cetane number fuels. Particulate formation was a strong function of fuel density and distillation range.

Fortnagel et al., found HC, NO<sub>x</sub>, CO, and a particulate emissions to be subject to aromatic content in a Mercedes Benz, prechamber-type engine.<sup>5</sup> A study by Gairing found large effects on exhaust emissions and fuel consumption attributable to fuel properties.<sup>6</sup> The diversity of these results is typical of the literature and emphasizes the strong influence that the engine type has on emissions from a given fuel. These studies were also performed with full-boiling fuels that made no attempt to segregate fuel properties by boiling range. Cookson attempted to determine the effect of hydrocarbon type composition on the diesel index (Method IP21) and the cetane index (ASTM D976) in 54 fuels, again using full-boiling materials.<sup>7</sup>

The approach to be used in the current work will attempt to improve on the resolution of previous studies done with full-boiling test fuels by examining the four starting materials in narrow fractions of the diesel fuel boiling range. We will then correlate the resulting measurements with emissions and performance indicators.

## Experimental

**Materials** → Of the refinery streams blended into diesel fuel, the higher boiling and more aromatic ones are implicated in particulate and hydrocarbon emissions. Accordingly, feedstocks for this study were chosen to include products from resid conversion and gas oil cracking. The test components chosen were:

- full-boiling straightrun diesel (SRD)
- light cycle oil from catalytic cracking (LCO)
- light coker gas oil (LCGO)
- coal-derived Fischer-Tropsch distillate (FT)

The parentheses enclose the abbreviated designations used in this paper. The opportunity to include the highly paraffinic FT liquid extended the objectives to see the effect of a material which might provide future solutions to diesel emission problems. These four materials were characterized by a set of laboratory analyses as shown in Table 1.

**Processing** → The four feedstocks were processed to reduce sulfur and aromatics then distilled into analytical samples. The processing and distillation sequence is shown in Figure 1. The LCO and LCGO were hydrogenated at two severities to reduce sulfur to 0.05 M% and aromatic concentration (by ASTM D1319) to 10 V%. The SRD was naturally low in sulfur and was hydrotreated at one severity to reduce aromatics to 10 V%. The FT required no hydrogenation. The process variables for the hydrogenations are summarized in Table 2.

| TABLE 1. FEEDSTOCK PROPERTIES    |             |                     |                |                   |                 |  |
|----------------------------------|-------------|---------------------|----------------|-------------------|-----------------|--|
| Test                             | ASTM Method | Straight Run Diesel | Lt. Cycle Oil  | Lt. Coker Gas Oil | Fischer-Tropsch |  |
| Density                          | D 1298      | 0.8458              | 0.9490         | 0.8676            | 0.7770          |  |
| Specific Gravity<br>°API<br>g/ml |             | 35.8<br>0.8453      | 17.6<br>0.9485 | 31.6<br>0.8671    | 50.6<br>0.7767  |  |
| Distillation, °F                 | D 86        |                     |                |                   |                 |  |
| IBP/5%                           |             | 353/428             | 367/457        | 385/420           | 368/396         |  |
| 10/30%                           |             | 466/523             | 476/509        | 435/462           | 407/449         |  |
| 50/70%                           |             | 551/581             | 536/573        | 492/528           | 502/550         |  |
| 90/95%                           |             | 635/657             | 634/656        | 574/590           | 592/606         |  |
| EP                               |             | 672                 | 689            | 608               | 620             |  |
| Carbon, Wt%                      | D 3178      | 86.82               | 88.84          | 85.18             | 84.92           |  |
| Hydrogen, Wt%                    |             | 13.31               | 9.84           | 12.58             | 15.12           |  |
| Sulfur, Wt%                      | D 2622      | 0.052               | 0.69           | 1.41              | 0.003           |  |
| Hydrocarbon Type, Vol %          | D 1319      |                     |                |                   |                 |  |
| Aromatics                        |             | 23.6                | 75.45          | 52.4              | 0.9             |  |
| Olefins                          |             | 1.0                 | 3.64           | 5.9               | 0.9             |  |
| Saturates                        |             | 74.7                | 20.91          | 41.7              | 98.2            |  |
| Viscosity @ 40°C                 | D 445       | 3.52                | 3.16           | 2.56              | 2.42            |  |
| @ 100°C                          |             | 1.34                | 1.20           | 1.10              | 1.05            |  |
| Refractive Index @ 20°C          | D 1218      | 1.4718              | 1.5537         | 1.4797            | 1.4342          |  |
| Cetane Index                     | D 976       | 52.6                | 26.1           | 39.3              | 75.4            |  |
|                                  | D 4737      | 54.6                | 23.89          | 38.9              | 81.4            |  |
|                                  |             |                     |                |                   |                 |  |
| UV Aromatics Analysis            | TOTAL       | 11.4                | 43.7           | 15.7              | 0.2             |  |
| Wt% Aromatic Carbon              | MONO        | 4.3                 | 6.3            | 8.4               | 0.0             |  |
|                                  | DI          | 5.8                 | 28.3           | 5.9               | 0.0             |  |
|                                  | TRI         | 1.3                 | 9.1            | 1.4               |                 |  |
| Cloud point, °C/°F               | D2500       | 1/34                | -10/14         | Too dark          | -20/-4          |  |
| Pour point, °C/°F                | D 97        | -1/30               | -12/10         | -30/-22           | -20/-4          |  |
| Aniline point, °C/°F             | D 611       | 73.0/163            | 9.8/50         | 47.6/118          | 92.8/199        |  |
| Smoke point, mm                  | D 1322      | 17.2                | 6.2            | 13.3              | +35             |  |

Each of the four feedstocks and their five products were distilled under vacuum into congruent (corresponding cut point) boiling range fractions. The following boiling point ranges were selected for the cuts:

| Fraction 1 | Fraction 2 | Fraction 3 | Fraction 4 | Fraction 5 | Fraction 6 | Fraction 7 |
|------------|------------|------------|------------|------------|------------|------------|
| IBP -      | 440° -     | 480° -     | 520° -     | 560° -     | 600° -     | 640° - EP  |
| 440°F      | 480°F      | 520°F      | 560°F      | 600°F      | 640°F      |            |

Approximately 40 liters of each material were charged to a stainless steel kettle and column, which was operated along the lines of a ASTM D1160 distillation. The resulting 63 samples were further subsampled for separation by ASTM D2549 into saturates and aromatics fractions.

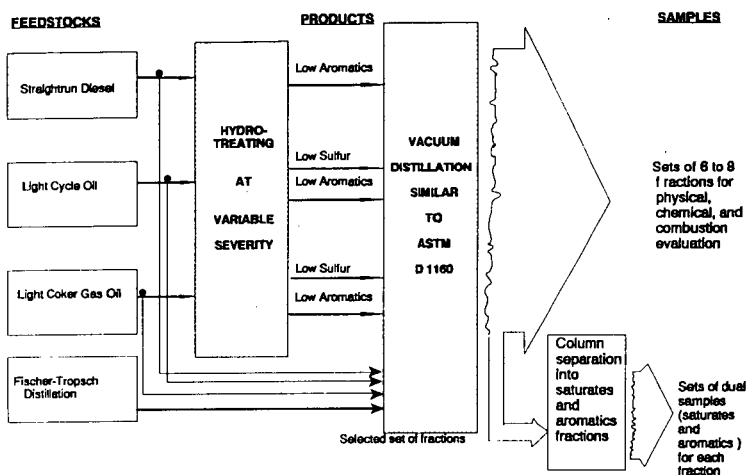


Figure 1. Sequence of Processing for the Diesel Fuel Assay

| TABLE 2. PROCESSING PARAMETERS |                  |                     |                               |                      |                           |
|--------------------------------|------------------|---------------------|-------------------------------|----------------------|---------------------------|
|                                | $T_{av}$ ,<br>°F | $P_{tot}$ ,<br>psig | Feed,<br>gal-hr <sup>-1</sup> | $H_{2,ox}$ ,<br>SCFH | LHSV,<br>hr <sup>-1</sup> |
| <b>STRAIGHT RUN DIESEL</b>     |                  |                     |                               |                      |                           |
| High severity - low aromatics  | 630              | 1500                | 1.6                           | 60                   | 1.03                      |
| <b>LIGHT CYCLE OIL</b>         |                  |                     |                               |                      |                           |
| Low severity - low sulfur      | 710              | 650                 | 1.9                           | 110                  | 1.05                      |
| High severity - low aromatics  | 686              | 2300                | 0.74                          | 130                  | 0.41                      |
| <b>LIGHT COKER GAS OIL</b>     |                  |                     |                               |                      |                           |
| Low severity - low sulfur      | 650              | 600                 | 2.2                           | 140                  | 1.22                      |
| High severity - low aromatics  | 676              | 2200                | 0.98                          | 117                  | 0.56                      |

Combination of adjacent cuts were made in the middle of the boiling range to limit the number of samples submitted for instrumental analysis. These combinations are indicated by the pairs and triples of sample numbers in brackets in Table 3.

**Analyses** → The set of laboratory measurements listed in Table 1 are being applied to each of the 63 fractions made by vacuum distillation. The list includes two measures of aromatic content, D1319 and the UV method.<sup>8</sup> The fluorescent indicator analysis (ASTM D1319) is widespread in its use and included in emissions regulations. It is regularly applied to diesel fuel samples, although the method is designed for deparaffinized gasoline, and relies on measurements of column length taken up by saturates, olefins, and aromatics made visible by fluorescent dye. The volume percent aromatics determined this way can be affected by cycloparaffins or polar materials.

The UV method compares sample absorbance at selected wavelengths with reference spectra of solutions of aromatics composed of representative compounds in the diesel boiling range. Since the absorbance is proportional to the aromatic rings, weight percent aromatic carbon is reported without regard to substituents. Both methods are indirect; so instrumental analysis by GC/MS and NMR are planned.

The samples will be rated for ignition quality in a constant volume combustion apparatus (CVCA).<sup>9</sup> A single shot of sample is injected into a shaped combustion chamber at controlled temperature and pressure. The temperature, pressure, and stoichiometry of the fuel/air mixture causes the gas mixture to autoignite. When the sample ignites and burns, it results in a pressure rise, which is automatically measured. The ignition delay time from injection to measured pressure rise for various temperatures and reference materials has been correlated with measured cetane numbers for estimating the cetane number of samples. All 72 samples (4 feedstocks, 5 products, & 63 fractions) will be tested in the CVCA.

Engine experiments will be performed with a single cylinder, direct injected, variable compression ratio engine (VCR).<sup>10</sup> The cylinder head can be moved during operation to adjust compression ratio thus allowing knock measurements to be made, which are necessary for measuring cetane number. The piston and intake port are being modified to match contemporary configurations designed to comply with 1991 diesel engine emission standards. Measurements will include cetane number, fuel efficiency, pressures traces, heat release rate, and exhaust emissions of CO, CO<sub>2</sub>, O<sub>2</sub>, NO, NO<sub>2</sub>, C, and unburned hydrocarbons. Selected samples will be tested in the VCR engine.

## Results

The processing, distillation, and laboratory analyses are complete, while the instrumental analyses and CVCA measurements continue. The VCR engine is being modified to reflect contemporary design before the engine experiments take place. Table 3 presents some of the measurements on the 63 fractions to date. Density (specific gravity), abbreviated boiling range, and aromatic composition are given in the table, however, each fraction has received the full analysis listed in Table 1. The number of fractions distilled from each feedstock and product vary in number depending on the boiling range of the starting material.

The results for aromatic composition of the LCO are presented in the series of graphs of Figure 2. This series of graphs is representative of the changes made by hydrogenation. The total aromatic carbon was reduced moderately in concentration as the sulfur was reduced by low severity treatment. The distribution of aromatics decreased most in the highest boiling point fractions, which display the most tricyclic compounds. A similar decrease is noted for dicyclic aromatics, but monocyclics increase across the boiling range. The explanation for this increase will await the ASTM D2425 results to confirm the trend, but in addition to creating corresponding cycloparaffins from the two- and three-ring aromatics, the hydrogenation opened rings in the multicyclics to form alkylbenzenes distributed throughout the lower boiling ranges.

The trend for high severity hydrogenation to limit total aromatics showed the greatest decrease in polycyclics. The overall reduction in monocyclic aromatics was slightly greater for higher boiling ranges. These changes are expected to reduce emissions and are projected to improve ignition delay as shown in Figure 3.

The plot of cetane index versus 50% recovered temperatures (T50) by D86 in Figure 3 was made by two estimating methods; ASTM D976 and D4737. Both correlations use density and T50, but in different ways. D976 uses API gravity and T50 in two terms, while D4737 uses specific gravity and T50 in four terms. Furthermore, the new, four-term correlation used a larger fuel matrix including cracked components and shale oil to develop its correlation. D4737 made lower estimates of cetane number in the front end of the boiling

**TABLE 3. PARTIAL RESULTS FOR DISTILLATION FRACTIONS**

| Property                    |          | Feed      | #1        | #2        | #3        | #4        | #5        | #6       | #7        | #8       |
|-----------------------------|----------|-----------|-----------|-----------|-----------|-----------|-----------|----------|-----------|----------|
| <b>STRAIGHT RUN DIESEL</b>  |          |           |           |           |           |           |           |          |           |          |
| Sp. Gravity                 |          | 0.8458    | 0.8146    | 0.8445    | 0.8483    | 0.848     | 0.845     | 0.847    | 0.859     | 0.863    |
| Dist. T10/T50               |          | 466/551   | 338/404   | 465/480   | 486/498   | 514/523   | 544/550   | 578/584  | 617/622   | 666/673  |
| T90/EP                      |          | 635/672   | 452/475   | 501/515   | 516/529   | 542/556   | 564/576   | 597/610  | 634/643   | 687/698  |
| Arom                        | Tot/Mono | 11.4/4.3  | 12.4/7.9  | 13.6/4.6  | 13.3/4.4  | 12.5/4.3  | 10.9/4.0  | 8.7/3.2  | 9.3/3.1   | 17.1/5.7 |
| C Wt%                       | Di/Tri   | 5.8/1.3   | 4.4/0.1   | 8.6/0.4   | 8.5/0.4   | 7.4/0.8   | 5.7/1.2   | 3.7/1.8  | 3.5/2.7   | 6.2/5.2  |
| <b>LOW A SRD</b>            |          |           |           |           |           |           |           |          |           |          |
| Sp. Gravity                 |          | 0.8280    | 0.7892    | 0.8251    | 0.8373    | 0.8368    | 0.8304    | 0.8203   | 0.8314    | 0.8373   |
| Dist. T10/T50               |          | 442/539   | 241/278   | 386/404   | 440/452   | 482/494   | 530/538   | 567/577  | 615/620   | 673/683  |
| T90/EP                      |          | 622/664   | 323/351   | 438/455   | 474/488   | 510/526   | 552/562   | 587/597  | 631/641   | 699/715  |
| Arom                        | Tot/Mono | 3.3/3.0   | 7.8/7.7   | 5.8/5.6   | 5.0/4.6   | 3.6/3.2   | 2.6/2.2   | 1.5/1.3  | 1.1/0.9   | 0.8/0.6  |
| C Wt%                       | Di/Tri   | 0.3/0.0   | 0.1/0.0   | 0.3/0.0   | 0.4/0.0   | 0.4/0.0   | 0.3/0.0   | 0.2/0.0  | 0.2/0.0   | 0.2/0.0  |
| <b>LIGHT CYCLE OIL</b>      |          |           |           |           |           |           |           |          |           |          |
| Sp. Gravity                 |          | 0.9490    | 0.8849    | 0.9147    | 0.9321    | 0.9440    | 0.9541    | 0.9685   | 0.9979    |          |
| Dist. T10/T50               |          | 476/536   | 384/410   | 447/459   | 483/490   | 515/522   | 548/552   | 583/588  | 643/651   |          |
| T90/EP                      |          | 634/689   | 443/492   | 473/492   | 499/518   | 531/544   | 562/575   | 596/614  | 677/734   |          |
| Arom                        | Tot/Mono | 43.7/6.3  | 42.5/26.7 | 55.3/14.5 | 57.2/6.8  | 60.6/5.1  | 46.1/4.1  | 41.2/3.3 | 46.7/0.1  |          |
| C Wt%                       | Di/Tri   | 28.3/9.1  | 15.0/0.8  | 39.8/1.0  | 49.6/0.8  | 53.9/1.6  | 39.3/2.7  | 28.6/9.3 | 10.4/36.2 |          |
| <b>LOW S LCO</b>            |          |           |           |           |           |           |           |          |           |          |
| Sp. Gravity                 |          | 0.9200    | 0.8849    | 0.9082    | 0.9153    | 0.9230    | 0.9352    | 0.9484   | 0.9497    |          |
| Dist. T10/T50               |          | 462/518   | 370/424   | 444/467   | 472/488   | 503/519   | 543/557   | 595/603  | 650/663   |          |
| T90/EP                      |          | 614/682   | 469/510   | 502/544   | 521/548   | 549/572   | 579/595   | 617/630  | 702/738   |          |
| Arom                        | Tot/Mono | 35.8/16.6 | 29.1/23.3 | 35.4/22.9 | 35.8/20.4 | 36.9/16.7 | 34.1/11.8 | 32.9/6.8 | 32.0/2.4  |          |
| C Wt%                       | Di/Tri   | 15.0/4.2  | 5.8/0.0   | 12.5/0.0  | 15.1/0.3  | 19.0/1.2  | 19.6/2.7  | 17.5/8.6 | 9.5/20.1  |          |
| <b>LOW A LCO</b>            |          |           |           |           |           |           |           |          |           |          |
| Sp. Gravity                 |          | 0.8628    | 0.8479    | 0.8623    | 0.8676    | 0.8708    | 0.8745    | 0.8703   | 0.8448    |          |
| Dist. T10/T50               |          | 419/488   | 362/384   | 412/422   | 446/454   | 477/486   | 514/520   | 547/552  | 606/620   |          |
| T90/EP                      |          | 581/657   | 406/419   | 432/453   | 470/488   | 499/514   | 530/544   | 561/574  | 669/715   |          |
| Arom                        | Tot/Mono | 3.5/3.1   | 5.6/5.4   | 3.6/3.4   | 4.1/3.7   | 3.9/3.4   | 2.9/2.5   | 2.5/2.0  | 1.4/1.0   |          |
| C Wt%                       | Di/Tri   | 0.4/0.0   | 0.2/0.0   | 0.2/0.0   | 0.4/0.0   | 0.5/0.0   | 0.4/0.0   | 0.5/0.0  | 0.4/0.0   |          |
| <b>LIGHT COCKER GAS OIL</b> |          |           |           |           |           |           |           |          |           |          |
| Sp. Gravity                 |          | 0.8676    | 0.8403    | 0.8565    | 0.8740    | 0.8871    | 0.8927    | 0.9094   |           |          |
| Dist. T10/T50               |          | 435/492   | 395/410   | 446/456   | 486/495   | 530/537   | 565/571   | 603/609  |           |          |
| T90/EP                      |          | 574/608   | 429/461   | 473/491   | 508/526   | 547/565   | 580/595   | 624/645  |           |          |
| Arom                        | Tot/Mono | 15.7/8.4  | 10.9/8.5  | 12.6/7.4  | 13.7/6.3  | 14.5/6.0  | 13.8/5.3  | 14.4/4.7 |           |          |
| C Wt%                       | Di/Tri   | 5.9/1.4   | 1.7/0.7   | 4.4/0.8   | 6.4/1.0   | 7.2/1.3   | 6.8/1.7   | 6.1/3.6  |           |          |

**TABLE 3. PARTIAL RESULTS FOR DISTILLATION FRACTIONS  
(Continued)**

| Property               | Feed     | #1       | #2       | #3       | #4       | #5       | #6       | #7       | #8      |
|------------------------|----------|----------|----------|----------|----------|----------|----------|----------|---------|
| <b>LOW S LCGO</b>      |          |          |          |          |          |          |          |          |         |
| Sp. Gravity            | 0.8463   | 0.8184   | 0.8299   | 0.8403   | 0.8524   | 0.8628   | 0.8697   |          |         |
| Dist. T10/T50          | 427/476  | 360/389  | 399/415  | 432/447  | 473/484  | 512/523  | 567/577  |          |         |
| T90/EP                 | 552/599  | 427/457  | 442/467  | 473/492  | 504/526  | 539/550  | 598/624  |          |         |
| Arom                   | Tot/Mono | 10.5/8.2 | 10.0/9.4 | 10.9/9.8 | 10.2/8.4 | 11.0/8.2 | 11.2/7.7 | 11.4/7.2 |         |
| C Wt%                  | Di/Tri   | 2.3/0.0  | 0.6/0.0  | 1.1/0.0  | 1.8/0.0  | 2.8/0.0  | 3.4/0.1  | 3.5/0.7  |         |
| <b>LOW A LCGO</b>      |          |          |          |          |          |          |          |          |         |
| Sp. Gravity            | 0.8393   | 0.8203   | 0.8265   | 0.8324   | 0.8418   | 0.8490   | 0.8498   | 0.8524   |         |
| Dist. T10/T50          | 436/491  | 374/390  | 404/417  | 437/448  | 474/483  | 508/516  | 548/556  | 595/602  |         |
| T90/EP                 | 576/612  | 414/430  | 440/466  | 468/485  | 503/520  | 530/546  | 566/574  | 622/644  |         |
| Arom                   | Tot/Mono | 3.3/3.0  | 4.5/4.3  | 3.9/3.7  | 3.6/3.3  | 3.5/3.1  | 3.3/2.9  | 2.7/2.3  | 2.2/1.8 |
| C Wt%                  | Di/Tri   | 0.3/0.0  | 0.2/0.0  | 0.2/0.0  | 0.3/0.0  | 0.4/0.0  | 0.4/0.0  | 0.4/0.0  | 0.4/0.0 |
| <b>FISCHER-TROPSCH</b> |          |          |          |          |          |          |          |          |         |
| Sp. Gravity            | 0.7770   | 0.7538   | 0.7633   | 0.7710   | 0.7783   | 0.7853   | 0.7913   | 0.7989   |         |
| Dist. T10/T50          | 407/502  | 355/373  | 397/416  | 438/453  | 478/490  | 522/531  | 558/566  | 607/615  |         |
| T90/EP                 | 592/620  | 420/456  | 452/474  | 475/488  | 507/521  | 545/557  | 579/589  | 628/638  |         |
| Arom                   | Tot/Mono | 0.2/0.2  | 0.4/0.4  | 0.3/0.3  | 0.2/0.2  | 0.2/0.2  | 0.1/0.1  | 0.1/0.1  | 0.1/0.1 |
| C Wt%                  | Di/Tri   | 0.0/0.0  | 0.0/0.0  | 0.0/0.0  | 0.0/0.0  | 0.0/0.0  | 0.0/0.0  | 0.0/0.0  | 0.0/0.0 |

range and higher estimates in the back end. These calculations will be compared with the CVCA and VCR results for verification, but the fractions at highest boiling ranges increased the most in cetane index. This is consistent with the results of Weidmann et al, for full-boiling test fuels.

### Conclusions

It has been observed that a consistent set of narrow-boiling samples was unavailable and this work will fill the need, however, this study is in the initial stages permitting few conclusions. The early results obtained to date suggest that the dominant effects for both emissions (by virtue of polycyclic aromatic distribution) and performance (considering the relative increase in cetane index) will be in the higher boiling point fraction. Further instrumental analyses of hydrocarbon type composition and the combustion studies will add to our understanding. The current results offer guidance on where in the boiling range the strongest effects can be found.

The improvement in the high end of the boiling curves is significant for the emissions and performance benefits that were obtained and for resource utilization. It has been suggested generally and implemented in California to reduce the limit for T90 for the D-2 specification. Careful control of upgrading may reduce the necessity to curtail T90 thereby leaving more of each blendstock in the diesel fuel boiling range.

## Acknowledgements

This work has been supported by the U.S. Department of Energy Office of Conservation and Renewable Energy Alternative Fuels Utilization Program (AFUP), John A. Russell, manager, first through its operations at the Oak Ridge National Laboratory, Dr. R.L. Graves, project representative then at the National Renewable Energy Laboratory, Kenneth R. Stamper, program manager representative.

The concept of the study was suggested by Norman R. Sefer the first project manager of the AFUP Alternative Fuel Center at Southwest Research Institute. The able technical staff for the processing included: C.C. Cover, D.L. Hetrick, P.M. Rainwater, and G.R. Segura. The engine combustion studies will be conducted by Dr. T.W. Ryan III. The numerous tables and typescript were prepared by Evangelina S. Martin.

## REFERENCES

1. "Fuel Quality Regulations for Highway Diesel Fuel Sold in 1993 and Later Calendar Years", Federal Register, Vol. 54, No. 163, August 24, 1989.
2. Foster, D.E., Dimplefeld, P.M. Boggs, D.L., Bair, R.E., and Borman, G.L., "The Effects of Fuel Composition on Ignition Delay in Homogeneous Charge and Direct Injection Compression Ignition Engines", Final Report, Contract DE-AC05-84OR21400, U.S. Department of Energy, Alternative Fuels Utilization Program, Report No. ORNL/Sub/84-89677/1, November 1987.
3. Buzza, T.G., and Litzinger, T.A., "A Comparison of Three Coal-Derived, Middle Distillate, Synthetic Fuels in a Single Cylinder DI Diesel Engine", SAE International Fuels & Lubricants Meeting, Toronto, Canada, November 2-5, 1987.
4. Weidmann, K., Menrad, H., Reder, K., and Hutchenson, R.C., "Diesel Fuel Quality Effects on Exhaust Emissions", SAE International Fuels & Lubricants Meeting and Exposition, Portland, Oregon, SAE Paper No. 881649, October 10-13, 1988.

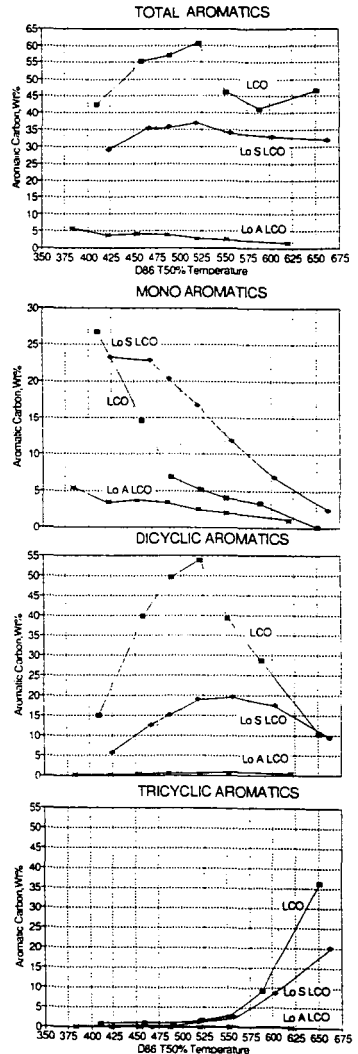


Figure 2. LCO Aromatics Distribution

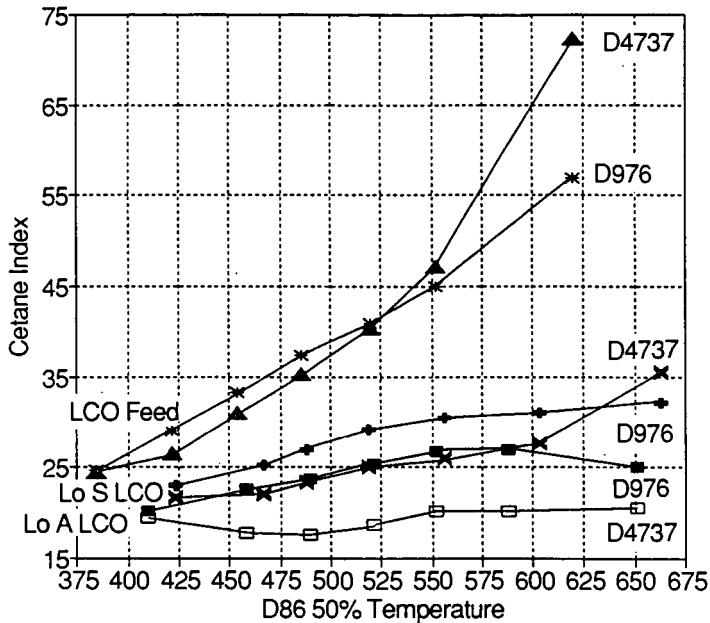


Figure 3. Cetane Index by ASTM D976 & D4737 vs LCO D86 50% Temperature

- Fortnagel, M., Gairing, M., Wagner, W., "Verbesserung des Diesel-Motors-Verschlechterung des Diesel-Kraftsoffs - ein Eiderspruch", VDI Berichte No. 466, 1983.
- Gairing, M., "Anforderungen and Diesel-Kraftsoffqualitat-heute und in Zukunft", VDI Berichte No. 559, Emissionsminderung Automobilabgase - Dieselmotoren - VDI Verlag 1985.
- Cookson, D.J., Lloyd, C.P., and Smith, B.E., "Investigation of the Chemical Basis of Diesel Fuel Properties", Energy and Fuels 2, 854-860, 1988.
- Kohl, K.B., Bailey, B.K., Newman, F.M., and Mason, R.L., "Chemical Analysis of Aromatics in Diesel Fuels", report for California Air Resources Board A932-125, 20 June 1991.
- Ryan, T.W. III, "The Development of New Procedures for Rating the Ignition Quality of Fuels for Diesel Engines", U.S. Army Belvoir RD&E Center, Interim Report 223, BFLRF, Southwest Research Institute, December 1986.
- Ryan, T.W. III, "Ignition Delay as Determined in a Variable Compression Ratio, Direct Injection Diesel Engine", SAE Paper 872036, November 1987.